PROM. NO. 3222

SYNCHRONOUS RECEPTION OF AMPLITUDE MODULATED SUPPRESSED CARRIER SIGNALS

THESIS

PRESENTED TO
THE SWISS FEDERAL INSTITUTE OF TECHNOLOGY ZURICH

FOR THE DEGREE OF DOCTOR OF TECHNICAL SCIENCE

BY
ADEL ABDEL AZIZ AHMED
B. A. (HONS.) CANTAB.
OF EGYPT

ACCEPTED ON THE RECOMMENDATION OF
PROF. DR. F. TANK AND PROF. DR. F. BORGNIS

AKERETS ERBEN AG, DIELSDORF, 1963

TO MY PARENTS AND TO MY WIFE

PREFACE

This work has for an object a study of the radio communication system using double sideband amplitude modulation with the carrier suppressed. This system is distinct from reduced carrier systems in that the carrier is generated at the receiver with correct frequency and phase from information derived solely from the sidebands. The whole of the transmitted power is in the information-carrying sidebands and the transmitter required can be extremely simple, for instance, a balanced modulator.

The advantages of the method include an inherent frequency diversity and homodyne detection which are beneficial in the presence of selective fading and frequency-dependent transmission path lengths. A certain degree of interference cancellation is possible depending on the nature of the interference and adjacent channel selectivity as well as amplification are obtained at audio frequency. Since the superheterodyne principle need not be used, a number of spurious responses can be eliminated.

The receiver is considered with regard to lock range, pull-in range, selective fading and interference cancellation. A method of automatic frequency control is given which operates in addition to the phase-frequency control. An experimental receiver was built for the purpose of investigating these features.

In order to measure the above-mentioned effects, an independent sideband transmitter was constructed and a new wideband phase shifter which was developed for use in conjunction with it is described. It requires bandpass filters with a steep rate of cut-off and the development and construction of suitable mechanical filters is also described here. This phase shifter should have other useful applications.

The work was carried out at the Institute for High Frequency Techniques of the Swiss Federal Institute of Technology in Zurich under the supervision of Professor Dr. F. Tank. The Author wishes to express here his sincere gratitude for the Professor's guidance and constant encouragement during the course of the work.

Thanks are due to the staff of the Institute's workshop and in particular to Herr W. Figel for his precision work on the filters.

Zurich, October 1961

CONTENTS

PREFACE v
CHAPTER
1. General Considerations 1
1.1 Introduction 1
1.2 Comparison of Modulation Systems 2
2. Receiver 10
2.1 General 10
2.2 Method of Operation 11
2.3 Synchronization 17
2.4 Fading and Signal Phase Variation 30
2.5 Interference 33
2.6 Detector 34
2.7 Frequency Control 35
2.8 Interference Cancellation 35
3. Test Apparatus 39
3.1 Transmitter 39
3.2 Phase Shifter 43
4. Practical Work and Measurements 56
4.1 Transmitter 56
4.1.1 Phase Shifters 59
1. Mechanical Filters 62
4.2 Receiver 86
5. Conclusions 103
5.1 Transmitter 103
5.1.1 Phase Shifters 103
1. Mechanical Filters 104
5.2 Receiver 104
5.3 Complete System 105
APPENDIX 1 107
APPENDIX 2 111
REFERENCES 117
ZUSAMMENFASSUNG (SUMMARY IN GERMAN) . . 121
CURRICULUM VITAE 123

CHAPTER 1

GENERAL CONSIDERATIONS

1.1. Introduction

In this work a study is made of suppressed carrier amplitude modulated radio systems. In the normal amplitude modulation system (AM) only one third of the transmitted power carries indispensable information. Although it is true that single sideband (SSB), and wideband frequency modulation (FM) make good use of the power, yet certain advantages have been claimed for double sideband suppressed carrier systems (DSB) (1)*. It should be noted that wideband FM and pulsed systems are not in direct competition with DSB for terrestrial long-distance ionospheric communication as the large bandwidth required precludes their use on short waves (2—30 Mc/s). SSB theoretically requires half the bandwidth of DSB, though this condition is not always fully realized in practice, and the operating frequency must be known and maintained to within less than 10 c/s or so. In addition SSB transmitters are fairly complicated and usually require repeated critical adjustments. The DSB transmitter is very simple, equally efficient in the use of power as SSB but requires twice the bandwidth. The receiver is based on quite different principles from those usual in practice. It bears a certain similarity to the homodyne receiver, but derives carrier frequency and phase information from the sidebands. Certain possibilities of interference cancellation exist, while selectivity and gain are obtained at audio frequency. Distortion normally caused by selective fading and frequency-dependent transmission path lengths can be greatly reduced. Although SSB and DSB are equally good as regards power utilization and signal to noise ratio, the DSB transmitter is far simpler than that for SSB.

* Numbers in brackets refer to the References on Pages 117—119.

In certain circumstances where bandwidth is not the prime consideration, DSB would appear to have some clear advantages. As an example, let us consider communication with a space vehicle. In general, such a vehicle would have a high velocity relative to the other station with which it is communicating. The Doppler shift would have to be known for a SSB system, whereas with DSB the derived carrier would by contrast be a source of information for the relative velocity, as the transmitting frequency would be known in advance. Further, the best possible use must be made of the available space, permissible weight and the power supply. With regard to space and weight the DSB system has the advantage while the power efficiency is the same as with SSB. In the interests of reliability the simpler DSB would also appear to have an advantage.

Phase-locked systems are being used for the detection of weak AM and FM signals in noise in a near-optimum manner. In the case of the AM signal the loop synchronizes with the carrier and no use whatever is made of the sidebands in controlling the local oscillator. The DSB system achieves the same result and dispenses with the carrier and its associated power consumption altogether.

A synchronous receiver which incorporates automatic frequency control and interference cancellation is studied here. This latter permits it to be used synchronously or asynchronously as a single sideband receiver. An independent sideband transmitter for investigating the receiver is also studied in connection with a new type of wideband phase shifter and associated mechanical bandpass filters.

1.2. Comparison of Modulation Systems

The merits and demerits of the various types of modulation have been extensively treated in the literature. We shall therefore only briefly review the main points involved before going on to a more detailed discussion of double sideband (suppressed carrier) modulation.

Pulse modulation is extensively used for multi-channel telephony. The noise performance can be said to be in between that of amplitude modulation and frequency modulation. Pulse-code modulation permits unlimited relaying of a quantized signal without any cumu-

lative effect of noise provided the signal to noise ratio is greater than about 20 dB. The large bandwidth required by pulse systems limits their use to UHF and microwaves.

Frequency modulation is extensively used for broadcasting and mobile communications of all types. A large proportion of the total radiated energy is in the information-carrying sidebands as compared to amplitude modulation. The method possesses an important interference suppressing property. Since amplitude limiting is used, noise appears through its effect on the signal phase. If the noise amplitude is smaller than the signal, then the noise modulation index will always be less than one. As the signal modulation index can be 100 or more, then the phase deviation produced by noise of half the signal amplitude is, for example, 0·005 of the signal deviation. Since modulation index decreases with increasing modulation frequency, pre-emphasis and de-emphasis are used to increase the modulation index at higher modulation frequencies, or sometimes a phase-modulated transmitter is used, where frequency deviation is proportional to modulating frequency. This suppression will be more effective the greater the frequency deviation. The bandwidth required is given approximately by $2(f_d + f_m)$ where f_d is the deviation and f_m the highest modulation frequency, being of the order 180 Kc/s for high-fidelity broadcasting and 40 Kc/s for voice communication. The interference amplitude caused by an adjacent transmitter is proportional to carrier separation but the audible interference effect falls off again as the interfering frequency rises. The use of frequency modulation is in practice limited to VHF as the bandwidth required is prohibitive at lower frequencies while indirect ray short wave transmission is not possible due to the much greater distortion that would result as compared with amplitude modulation.

Amplitude modulation, simple to produce and detect is used for medium and short wave broadcasting and to some extent for other services. The simplicity of the system is an advantage but it is wasteful of power and compared to single sideband, of bandwidth, which is equal to twice the highest modulation frequency required. Only one third of the transmitted power carries indispensable information. For example, in an anode-modulated Class-C amplifier, the DC supply provides the carrier power continuously while the modulator supplies

the whole power required to generate sidebands. Amplitude limiting can be used to suppress pulse-type interference but there is no noise suppression as in frequency modulated systems; where intelligibility only is required and a higher background noise can be tolerated, there is not so much difference between the two types.

In high-frequency long distance circuits selective fading may occur, with frequencies only 100 c/s apart fading independently. If the carrier fades, severe distortion occurs while if its phase shifts relative to its original position with respect to the sidebands, envelope distortion occurs. In this case, we may write for the wave

$$v = A_0 \sin(\omega_0 t + \varphi_0) + A_m \sin \omega_m t \sin \omega_0 t$$

where
A_0 = carrier amplitude
$\frac{1}{2} A_m$ = sideband amplitude
$\omega_0 / 2\pi$ = carrier frequency
$\omega_m / 2\pi$ = modulation frequency
φ_0 = carrier phase displacement.

We obtain

$$v = (A_0^2 + 2 A_0 A_m \sin \omega_m t \cos \varphi_0 + A_m^2 \sin^2 \omega_m t)^{\frac{1}{2}} \cos(\omega_0 t - \varphi_m)$$

$$\text{where } \tan^{-1} \varphi_m = \frac{A_0 \cos \varphi_0 + A_m \sin \omega_m t}{A_0 \sin \varphi_0}$$

There are two effects present here. The phase of $\cos \omega_0 t$ is modulated by φ_m and the amplitude of the wave differs from the original when $\cos \varphi_0$ is less than one. If we let $\varphi_0 = \pi/2$ we obtain

$$v = (A_0^2 + A_m^2 \sin^2 \omega_m t)^{\frac{1}{2}} \cos(\omega_0 t - \varphi_m)$$

$$= \left[A_0^2 + \frac{1}{2} A_m^2 (1 - \cos 2\omega_m t) \right]^{\frac{1}{2}} \cos(\omega_0 t - \varphi_m)$$

$$= \left[\left(A_0^2 + \frac{1}{2} A_m^2 \right) - \frac{1}{2} A_m^2 \cos 2\omega_m t \right]^{\frac{1}{2}} \cos(\omega_0 t - \varphi_m)$$

There is thus a double frequency component in the envelope. If the carrier is made very large, this becomes negligible and the case is like that of the suppressed carrier system where the modulation output

amplitude is proportional to $\cos\varphi_o$. Such phase differences can arise very easily owing to different transmission path lengths for different frequencies. Amplitude modulation systems using an amplified or reconditioned carrier go some way to reducing this effect but amplitude reduction can still occur if $\cos\varphi_o < 1$. The synchrodyne receiver uses an oscillator which is injection locked to the incoming carrier and a synchronous detector.

Single sideband communication, essentially the translation of the modulation band, erect or inverted to another frequency band, is used extensively for point to point communication. The frequency band is half that required for amplitude modulation. For fixed services, the crystal-controlled carrier frequencies are agreed upon and have to be generated correctly to within about 10 c/s. It is in fact possible to adjust the carrier frequency approximately aurally as is done by amateurs. In speech, for example, most of the higher frequency components are harmonically related to the lower ones and the ear permits an adjustment probably by a similar mechanism to that which enables it to recognize harmony. It is not possible to perform this adjustment automatically at the present state of the art and single sideband is only used commercially when operation at a number of prearranged frequencies is envisaged. This is one of the drawbacks of the system and sometimes a pilot carrier at reduced power is transmitted. Other disadvantages are disappearance of the signal during fading (unless diversity reception is used) and complicated terminal equipment which includes linear amplifiers and requires skilled adjustment. The suppression of the undesired sideband is often incomplete so that it is not always possible to use a channel which is theoretically free, in the neighbourhood of another transmitter. Also, most existing single sideband equipment is incapable of transmitting phase information, that is, the transient response is poor. The advantages include full use of the transmitted power, small bandwidth and relative freedom from the distortion associated with selective fading and multipath transmission.

Single sideband transmissions with carrier cannot be satisfactorily received on a normal AM receiver utilizing envelope detection. When the sideband is of comparable magnitude with the carrier severe distortion results. The relative energy content of the higher audio frequencies is small and this fact has led to various attempts at devising a

SSB system compatible with AM, or more correctly, a system by means of which only half the normal bandwidth of AM would be needed and which could be used with no changes to existing AM receivers and with little alteration to transmitters in use. Systems using AM for the lower audio frequencies and SSB with carrier for the higher audio components have been proposed but have many drawbacks.

At the time this work was closing an ingenious system of compatible single sideband (CSSB) was described by Kahn (2). As has been mentioned above, a two-component wave (carrier and sideband) is not satisfactory for AM receivers. It is shown in the article by Kahn that a three-component wave can be used to provide a low distortion signal in an AM receiver (apart from the obvious case of a normal AM wave). The carrier is to one side of the spectrum and there are first-order and second-order sidebands. By suitably selecting the relative amplitudes of the components a compromise is arrived at between envelope distortion and undesired sideband radiation. The amplitude relationship between *carrier/first sideband/second sideband* at full modulation is 0·7/1/0·3.

This three-element mathematical model of the wave may be written as:

$$e = E\left[(1 - 0{\cdot}3\, m^2)\cos \omega_0 t + m \cos (\omega_0 + \omega_m) t + 0{\cdot}3\, m^2 \cos (\omega_0 + 2\,\omega_m) t\right]$$

where E = carrier voltage in absence of modulation
m = envelope modulation factor
ω_0 = carrier angular frequency
ω_m = modulation angular frequency

Since the second-order component needed follows a squared function of the percentage modulation it becomes negligibly small at low modulation percentages. This occurs in practice at the highest modulation frequencies. Thus the bandwidth required is practically equal to the highest modulation frequency to be transmitted. By studying the phase modulation occuring in the CSSB wave it is shown that the same phase modulation may be produced by an appropriate combination of a pair of two-element waves in conjunction with special non-linear

circuits. If the resulting wave is amplitude modulated by the modulation signal a CSSB wave results.

In practice the audio signal is first used to produce a SSB wave which is then passed through two signal paths each containing a nonlinear network providing lower attenuation for higher amplitude levels. In one signal path a carrier is added of amplitude equal to the sideband amplitude at 100 percent modulation. In the other path a carrier of twice the sideband level also at 100 percent modulation is added and the resulting signal is heterodyned to a higher frequency. The two signals are then mixed and the output limited. After any necessary frequency translation this is then fed to the low-level RF stages of the transmitter, where normal amplitude modulation by the audio signal then takes place. Instead of using the audio input signal itself for this purpose, a signal derived from the intermediate SSB wave is used so as to compensate for the phase shift inevitable in the SSB generation. The CSSB output from the transmitter contains no inherent envelope distortion, its spectrum is practically confined to one sideband and it can be received on a normal AM receiver.

It should be noted that SSB is a concise term defining the use of the modulation band erect or inverted after frequency translation. A full or pilot carrier is not strictly a part of a SSB signal. The correctness of the CSSB nomenclature could be questioned on these grounds. The CSSB wave is not compatible in one sense as it cannot satisfactorily be received by a normal SSB receiver with a product detector. Nevertheless it does resemble a SSB wave with carrier and other components added. This is however only a matter of definition and of how much differentiation may be implied by the adjective *compatible.*

A CSSB signal would be unsatisfactory for the synchronous receiver which is studied in this work. At high percentages of modulation operation may be correct, but at low percentages the receiver would synchronize between carrier and first order sideband causing the output to be at half the modulation frequency.

The generation of two sidebands with carrier suppressed is very simple and is usually the first step in the generation of a single sideband. Ring or Cowan modulators are often used, but any balanced modulator will do. Reception can be obtained by the use of a phase-locked local oscillator and a synchronous detector. Since there is no

carrier transmitted, the types of distortion which occur with carrier fading or phase shift in the case of normal amplitude modulation are absent. As in the case of single sideband there is maximum use of the transmitted power. Its division between two sidebands conveys the additional information of the exact carrier frequency and phase.

As a disadvantage, the required bandwidth is twice as great, though the advantages of the narrower single sideband bandwidth are not always fully realizable in practice, due to incomplete cancellation of the undesired sideband. The suppressed carrier system offers the possibility of cancellation in the output of discrete interfering frequencies, completely when these are confined to one sideband and to a certain extent in other cases. Also, the absent carrier frequency need not be known and the presence of a carrier only alters the synchronization characteristic if DC components are carried through in the receiver and are allowed to contribute a part of the control voltage. There is however, a tendency for faulty synchronization to occur between the carrier and one sideband, though in this case the other sideband acts as a strong interference signal tending to make the condition unstable. The use of an automatic frequency control system described in Sec. 2.7 permits the synchronizing loop bandwidth to be made narrower, with certain advantages. The system has an inherent frequency diversity and even total fading of one sideband should not interrupt reception completely if it is for a short period, though synchronization would be lost. In the experimental receiver described in Sec. 4.2, synchronization was maintained until one sideband had faded to 34 dB below normal strength. In practice it would be possible to ensure that synchronization be maintained down to a level where the signals are too weak to be otherwise useful. An important additional advantage is the extreme simplicity of the transmitter compared to single sideband. There is, of course, no ideal system, but the suppressed carrier system appears to possess certain useful characteristics which could find practical application (1).

As will be shown in Sec. 2.2, the receiver output from both sidebands (with ideal operation) gives four times the power output recovered from one sideband alone. If the noise contributions from both sidebands are equal, it is easily shown that the signal to noise ratio for double sideband is equal to that for single sideband. For equal trans-

mitted powers, amplitude modulation with carrier gives a signal to noise ratio of one third of that obtained with either of the above systems. Sometimes it is the peak power that poses a limitation (4). Under such conditions single sideband is capable of twice the signal to noise ratio of double sideband, since upper and lower sidebands can add to give four times the power amplitude of one sideband. With ordinary amplitude modulation, the signal to noise ratio is only one-eighth of that with single sideband of the same peak power.

CHAPTER 2

RECEIVER

2.1. General

Under this heading, we may logically include a study of synchronization, the effects of noise and interference, selective fading, and frequency-dependent transmission path lengths. These factors are all of importance at the receiver where any measures for improvement would have to be made. The normal transmitter for suppressed carrier communication is very straightforward, this being indeed one of the advantages of the system.

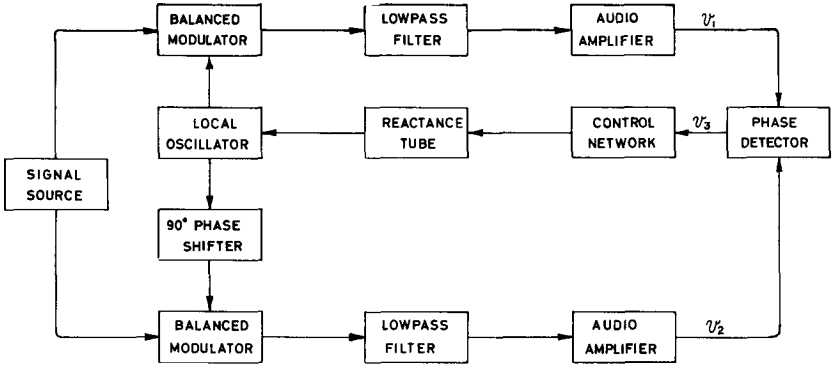

FIG. 2.1. Showing basic diagram of receiver.

We shall first treat the receiver generally, assuming that the sidebands are of different amplitudes due to fading and that they have undergone different delays along the transmission path. We shall then consider some possible improvements that could be made, and lastly, a method will be discussed whereby certain interfering signals may be cancelled.

The basic receiver is shown in Fig. 2.1. The signal is applied to two detectors where it is demodulated in one detector by using a voltage of correct carrier frequency and in the other by a voltage of this frequency shifted through 90°. The resulting outputs are filtered and applied to a modulator stage whose output is shown to contain a term proportional to the sine of twice the phase error of the local oscillator. This voltage may then be used to synchronize the local oscillator. When the phase is correct, one output has its maximum value and the other will be zero, if the signal consists of two sidebands of equal amplitude.

2.2. Method of Operation

It is helpful in understanding the mode of operation of the receiver to consider it as a servomechanism or regulating system. A general block diagram for a servomechanism is shown in Fig. 2.2, (3). For comparison the receiver is shown as a regulating system in Fig. 2.3. It may be thought of as a Type 1 servo system. From a comparison of the diagrams it can be seen that the actual "output" of the receiver is the regulated local oscillator frequency. In fact the modulation signal output which is what we would normally wish to obtain from the receiver is a by-product of the comparator system. In what directly follows, "output" will be taken to mean the regulated oscillator output, while the frequency and phase information of the original carrier used in obtaining the sidebands is the input quantity. That the carrier itself is absent and that the information is only available indirectly in the coded form of the sidebands is irrelevant to the principle of operation.

Let the (absent) carrier frequency be identical with the local oscillator frequency and let there be zero phase error. Then the output from the phase comparator to the reactance control unit will also be zero and the oscillator frequency will remain equal to the input frequency. Now assume a step change to take place in the carrier phase used for generating the sidebands in the transmitted signal. An error voltage will be applied to the reactance control altering the frequency which will then cause the oscillator phase to advance or retard until it is again identical with the input. Due to the integrating action the system will

continue regulating until identity of phase is re-established. If we now allow the input frequency to rise somewhat, then the input phase will be continually advancing. Again an error signal will be produced causing the output phase also to advance. The system will settle to a constant phase error with the output frequency identical with the input frequency. The higher the system gain the smaller will the fixed error be for a given deviation of the input frequency.

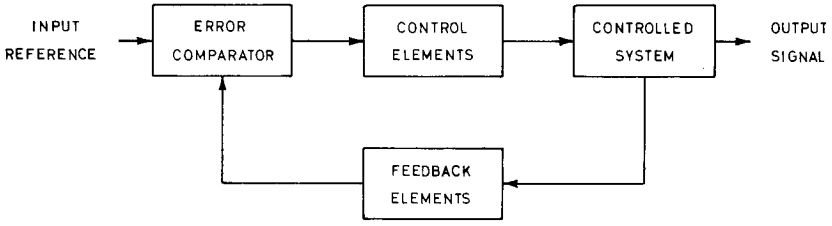

FIG. 2.2. Showing a block diagram of a servomechanism or regulating system.

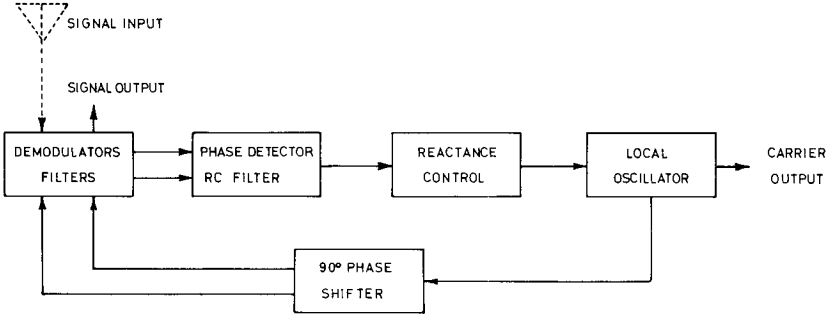

FIG. 2.3. Showing a block diagram of the receiver with its elements in the configuration of a servo system. (Compare with Fig. 2.2.)

If now the input phase were to undergo rapid perturbations though the average input frequency were to remain constant then the output phase would be more stable than the input phase. This is due partly to the RC filter and partly to the integrating action of the oscillator. If the phase variations are too great, there will be loss of synchronism. For

some critical frequency of phase variation the feedback may become positive, in which case the variations may be magnified and instability may result. Very slow variations of phase will be followed by the system. The properties of the system are such that it can be locked onto a coherent signal in the presence of strong wideband noise provided the approximate frequency is known. Thus in the present application the noise may be so strong that the demodulated output signal becomes useless, yet the oscillator may be made to remain synchronized in the presence of even stronger noise.

With given circuit constants there will be a certain range over which the system will be able to maintain the correction, holding the local oscillator frequency to the desired value. This is termed the lock range. If the mistuning be increased further the system will fall out of synchronism (in much the same way as a synchronous machine falls out of step when the load torque becomes too great). A steady state then exists in which the oscillator frequency undergoes non-linear perturbations (see Appendix 1). If the error is again decreased, these perturbations will become slower and slower until at a certain value of mistuning (pull-in range) the system will again lock to the signal. Even within the pull-in range, this process requires a certain time for its completion.

We shall now proceed to consider these points in more detail. In order to simplify the algebra, we shall at first assume that the input consists of two single side-frequencies. We shall show later that the results thus derived are equally applicable to signals consisting of sidebands.

We shall first consider the general case where the receiver local oscillator is at a different frequency to that of the absent carrier. For this part of the analysis, a phase φ is assumed and as the frequency is initially different, φ will be varying. The frequency difference δ which is included in the oscillator frequency term will be required later and can for the time being be regarded as equal to zero.

Let $\omega_0/2\pi =$ correct carrier frequency

$\omega_m/2\pi =$ modulation frequency

$\theta =$ equal phase shift undergone by sidebands in opposite directions

$\delta/2\pi$ = frequency error of local oscillator
φ = phase error of local oscillator
A, B = amplitude of sidebands
E = amplitude of local oscillator output
K_1 = constant of the modulators.

Higher products removed by the filters are left out for simplicity.

Input $= A\cos(\omega_0 t + \omega_m t + \theta) + B\cos(\omega_0 t - \omega_m t - \theta)$ then

$$v_1 = \frac{1}{2}K_1 AE\cos(\delta t + \varphi - \theta - \omega_m t) + \frac{1}{2}K_1 BE\cos(\delta t + \varphi + \theta + \omega_m t)$$

$$= \frac{1}{2}K_1 AE\cos(\delta t + \varphi)\cos(\omega_m t + \theta) + \frac{1}{2}K_1 AE\sin(\delta t + \varphi)\sin(\omega_m t + \theta)$$

$$+ \frac{1}{2}K_1 BE\cos(\delta t + \varphi)\cos(\omega_m t + \theta) - \frac{1}{2}K_1 BE\sin(\delta t + \varphi)\sin(\omega_m t + \theta)$$

$$= \frac{1}{2}K_1 E[A^2 + B^2 + 2AB\cos 2(\delta t + \varphi)]^{1/2}\cos$$

$$\left\{\omega_m t + \theta - \tan^{-1}\left[\left(\frac{A - B}{A + B}\right)\tan(\delta t + \varphi)\right]\right\}.$$

When $\delta = 0$ and φ is constant, this represents the modulation signal output.

Similarly,

$$v_2 = \frac{1}{2}K_1 E[A^2 + B^2 - 2AB\cos 2(\delta t + \varphi)]^{1/2}\cos$$

$$\left\{\omega_m t - \theta - \tan^{-1}\left[\left(\frac{B - A}{B + A}\right)\tan(\delta t + \varphi)\right]\right\}.$$

It is seen that this output disappears when $\delta = \varphi = 0$ and $A = B$.

Further, multiplying v_1 by v_2, we obtain

$$v_3 = K_1^2 K_2 E^2 \left[\frac{1}{4} AB \sin 2(\delta t + \varphi) + \frac{1}{8}(A^2 + B^2) \sin 2(\delta t + \varphi) \cos(\omega_m t + \theta) + \frac{1}{8}(B^2 - A^2) \cos 2(\delta t + \varphi) \sin(\omega_m t + \theta) \right]$$

where K_2 is a phase detector constant.

The second and third terms contain frequencies of the order of the modulation frequencies. The first term, considered with $\delta = 0$, represents a voltage

$$\tfrac{1}{4} K_1^2 K_2 E^2 AB \sin 2\varphi$$

and is used to obtain synchronization. When the frequency error varies, this regulation is a dynamic process, with typical *pull-in* and *lock range* characteristics.

When several modulation frequency components are present simultaneously, that is when the signal input to the receiver is of the general form

$$\sum_{\eta=1,2,3,\ldots}^{n} A_\eta \cos[(\omega_o + \omega_\eta) t + \theta_\eta] + B_\eta \cos[(\omega_o - \omega_\eta) t - \theta_\eta]$$

then it can be seen from the foregoing that the signal output will be

$$v'_1 = \sum_{\eta=1,2,3,\ldots}^{n} \frac{1}{2} K_1 E [A_\eta^2 + B_\eta^2 + 2 A_\eta B_\eta \cos 2(\delta t + \varphi)]^{1/2} \cos \left\{ \omega_\eta t + \theta_\eta - \tan^{-1} \left[\left(\frac{A_\eta - B_\eta}{A_\eta + B_\eta} \right) \tan(\delta t + \varphi) \right] \right\}$$

The phase detector is assumed to be an ideal multiplicative mixer and we shall represent its two input voltages resulting from the multiple sidebands (following the low-pass filters) as

$$v'_1 = \sum_{\nu=1,2,3,\ldots}^{n} \frac{1}{2} K_1 E [A_\nu \cos(\delta t + \varphi - \theta_\nu - \omega_\nu t) + B_\nu \cos(\delta t + \varphi + \theta_\nu + \omega_\nu t)]$$

$$v'_2 = \sum_{\mu=1,2,3,\ldots}^{n} \frac{1}{2} K_1 E [A_\mu \sin(\delta t + \varphi - \theta_\mu - \omega_\mu t) + B_\mu \sin(\delta t + \varphi + \theta_\mu + \omega_\mu t)]$$

The phase detector output voltage will then be

$$\begin{aligned} v'_3 = \frac{1}{8} K_1^2 K_2 E^2 \sum_{\mu}^{n} \sum_{\nu}^{n} & A_\mu A_\nu \{\sin[2(\delta t+\varphi) - (\omega_\mu + \omega_\nu) t - \theta_\mu - \theta_\nu] \\ & - \sin[(\omega_\mu - \omega_\nu) t + \theta_\mu - \theta_\nu]\} \\ + A_\mu B_\nu & \{\sin[2(\delta t + \varphi) + (\omega_\nu - \omega_\mu) t - \theta_\mu + \theta_\nu] \\ & - \sin[(\omega_\mu + \omega_\nu) t + \theta_\mu + \theta_\nu]\} \\ + A_\nu B_\mu & \{\sin[2(\delta t + \varphi) + (\omega_\mu - \omega_\nu) t + \theta_\mu - \theta_\nu] \\ & + \sin[(\omega_\mu + \omega_\nu) t + \theta_\mu + \theta_\nu]\} \\ + B_\mu B_\nu & \{\sin[2(\delta t + \varphi) + (\omega_\mu + \omega_\nu) t + \theta_\mu + \theta_\nu] \\ & + \sin[(\omega_\mu - \omega_\nu) t + \theta_\mu - \theta_\nu]\}. \end{aligned}$$

Clearly, all terms with coefficients having suffixes $\mu \neq \nu$ must represent alternating components. These are attenuated by the RC filter between the phase detector and the reactance control. Their main effect is to act as interference in the phase control loop. In addition if a particular fading condition were to arise such that

$$A_\nu \gg B_\nu$$
$$\text{and } B_\mu \gg A_\mu \quad \text{where } \mu \neq \nu,$$

then faulty synchronization of the local oscillator to the arithmetic mean frequency of the components represented by A_ν and B_μ could momentarily occur. This would cause the output signal voltage to contain a component of angular frequency $\frac{1}{2}(\omega_\mu + \omega_\nu)$, a value not present in the original signal. Considering the case when $\mu = \nu = \eta$, we find that the phase control voltage is

$$\sum_{\eta=1,2,3,\ldots}^{n} \frac{1}{4} K_1^2 K_2 E^2 A_\eta B_\eta \sin 2\varphi \text{ volts.}$$

Thus a DC component in the output is only produced by equal modulation frequency components in the signal and quadrature channels, both derived from the same sideband pair. It can thus be seen that the operation is basically the same with sidebands as with two discrete side-frequencies.

2.3. Synchronization

The treatment of the phenomenon of synchronization is similar to that used for the synchronization of oscillators and the same approach will be used.

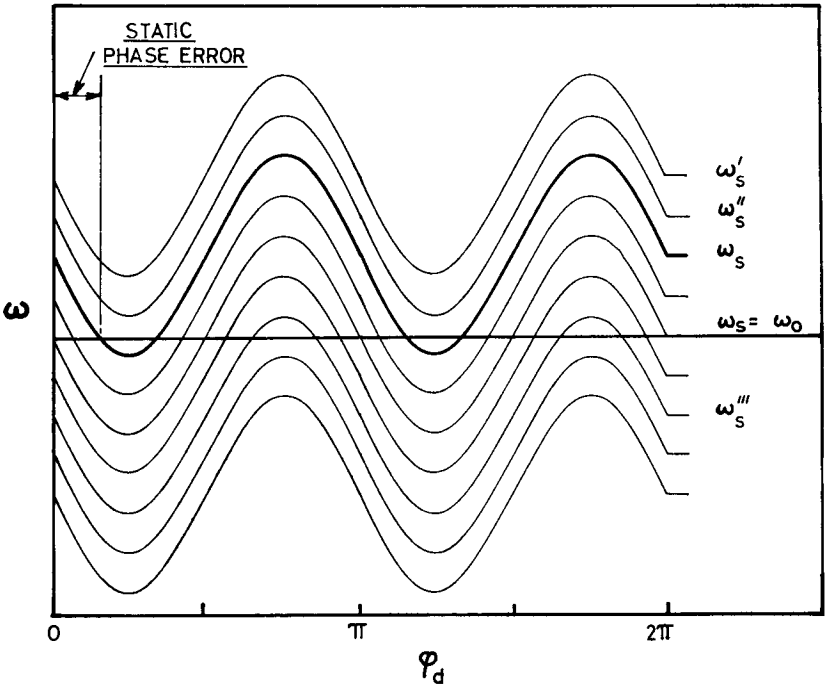

FIG. 2.4. Graphical representation of steady-state phase error. Local oscillator frequency is plotted as a function of (reference phase) — (oscillator phase) = φ_d for various free-running frequencies ω_s, ω'_s, . . .

Let the reactance tube modulator have a control constant S radians/sec per volt. In general we shall follow the notation used in the extensive literature on synchronized oscillators. The voltage range of the phase demodulator is

$$\pm \tfrac{1}{4} K_1^2 K_2 E^2 AB \text{ or a total change of } \tfrac{1}{2} K_1^2 K_2 E^2 AB \text{ volts.}$$

The lock range is then $\frac{1}{2} K_1^2 K_2 E^2 ABS$ radians/sec.
A physical idea of the steady state phase error can be obtained from the diagrams in Figs. 2.4 and 2.5. It can be seen that in contrast to the case of normal synchronization of oscillators with a single reference

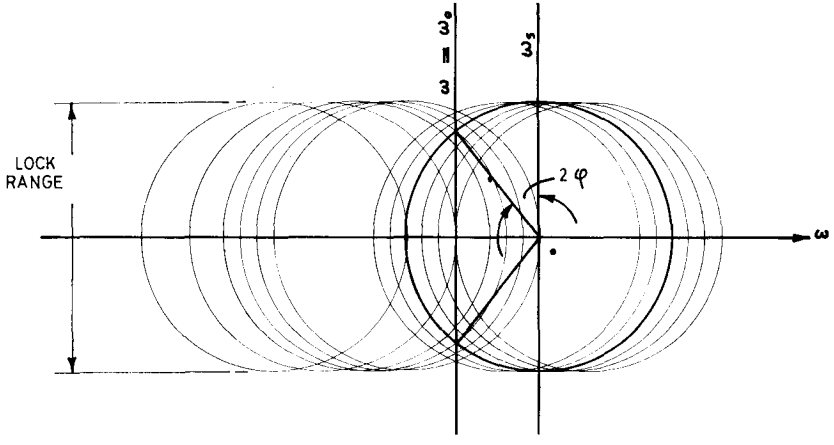

FIG. 2.5. Showing the steady-state phase error of the receiver local oscillator. The diameter of a circle represents the lock range while the position of its centre is at the free-running frequency. The intersection of a radius with the line $\omega = \omega_0$ is a possible locking condition when it occurs in a stable area of negative feed-back.

frequency, the local oscillator may synchronize in phase or at 180° out of phase. This does not affect the receiver output. The pull-in range cannot be greater than the lock range but it may be smaller. The pull-in range required will depend on the frequency stability of the transmitter and receiver. It is not desirable to make the lock range greater than necessary, since if it is too large, and if the receiver were to be synchronized to a strong signal it may become impossible to tune to a weaker signal on an adjacent channel. The receiver would have to be tuned so far away from the strong signal that the weaker signal would be passed

over. The performance in the presence of fading will also be better when the *pull-in/lock range* ratio is greater. When it is locked to a strong, slightly mistuned signal, the receiver may be operating satisfactorily even if the pull-in range is small, but when the signal fades, however, it may fall out of synchronism and remain in that condition. When operation is at a fixed frequency with a stable local oscillator this condition may not be so important and other advantages may be gained while allowing the pull-in range to become small. These will be discussed later. The conditions necessary to ensure a pull-in range bearing a certain proportion to the lock range will now be discussed for various control networks between the phase detector and the reactance control element. We shall neglect the effects of time delays introduced by the modulator circuits and the low-pass filters.

Case of Direct Connection

This case has been treated for a synchronized oscillator by Labin (5) and

Pull-in range = *Lock range.*

In contrast to the usual case of a phase-locked oscillator, a direct connection is not very practicable with the receiver. Sideband asymmetry or mistuning give rise to AC components in the control loop and therefore a filter should be used.

Case of RC Filter (6), (Fig. 2.6a).

We have $E_2 (1 + j\omega CR) = E_1$

or more generally, $$\frac{dE_2}{dt} + \frac{E_2}{RC} = \frac{E_1}{RC} \tag{2.1}$$

where E_1 represents the phase discriminator output and E_2 is the input voltage to the reactance control element.

Let $\omega_o/2\pi$ = correct carrier frequency

$\omega_s/2\pi$ = controlled local oscillator frequency

$\omega_d/2\pi$ = difference between local oscillator free-running frequency and carrier frequency.

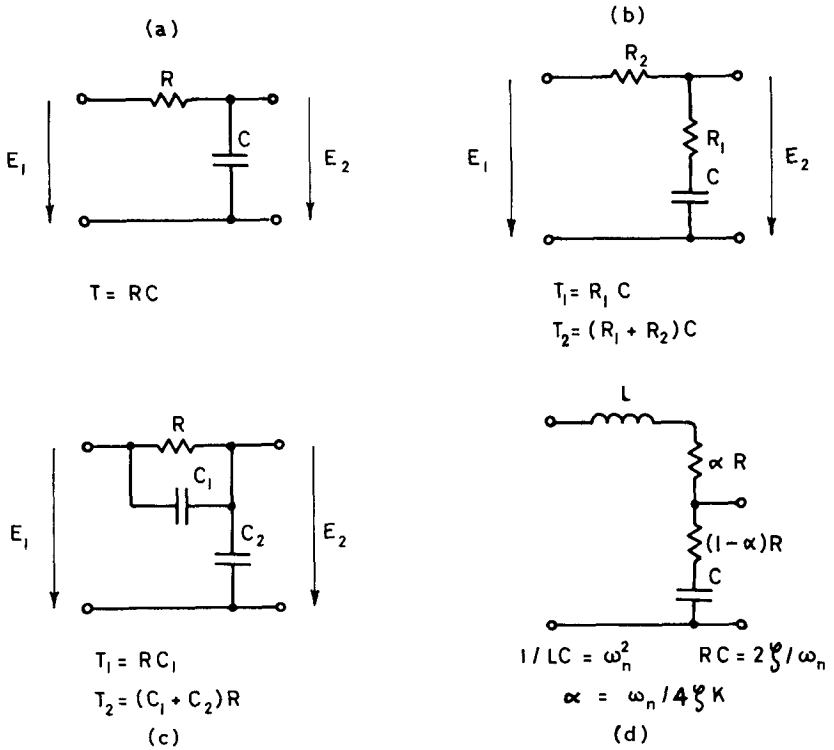

FIG. 2.6. (a), (b) and (c) showing control networks for the phase-lock servo loop. The transfer function is

$$\frac{E_2}{E_1} = \frac{1 + p\,T_1}{1 + p\,T_2}.$$

The equivalent circuit for the system is shown in (d).

$$\varphi \equiv \int^{t} (\omega_o - \omega_s)\,dt$$

and $\varrho = 1/RC$

We then have $\dfrac{d\varphi}{dt} = \omega_o - \omega_s$

and $\dfrac{d^2\varphi}{dt^2} = -\dfrac{d\omega_s}{dt}$ since ω_o is a constant.

Remembering that the reactance control constant is S, we can write

$$\frac{d^2\varphi}{dt^2} = -\frac{d\omega_s}{dt} = -S\frac{dE_2}{dt}$$

or $$\frac{d\varphi}{dt} = -SE_2 + C_1, \text{ where } C_1 \text{ is a constant.}$$

Since at $E_2 = 0$, $C_1 = \omega_d$, then $SE_2 = \omega_d - \frac{d\varphi}{dt}$.

Substituting in Equation (2.1),

$$\frac{d^2\varphi}{dt^2} + \varrho\frac{d\varphi}{dt} - \varrho\omega_d + \frac{1}{4}K_1^2 K_2 E^2 ABS\varrho \sin 2\varphi = 0.$$

Letting $$\xi = 2\varphi$$

$$\tau = \left(\frac{1}{2}K_1^2 K_2 E^2 ABS\varrho\right)^{\frac{1}{2}} t$$

$$\alpha = \sqrt{\frac{2\varrho}{K_1^2 K_2 E^2 ABS}}$$

$$\beta = \frac{4\omega_d}{K_1^2 K_2 E^2 ABS}$$

we obtain $$\frac{d^2\xi}{d\tau^2} + \alpha\frac{d\xi}{d\tau} + \sin\xi = \beta \qquad (2.2)$$

The apparent inconsistency of dimensions is due to the fact that τ is a dimensionless relative time, defined in terms of the network time constant. This differential equation has been solved by Giger (7),* who gives a curve relating the minimum value of α which will ensure synchronization for a given value of β (which in this case represents frequency off-set) regardless of the initial conditions (Fig. 2.7). At the edge of the lock range, that is $\beta < 1$, synchronization is assured for $\alpha = 1{\cdot}1931 \approx 1{\cdot}2$. This result is valid for β plus or minus.

Using the published solution for the equation, we can so dimension the RC network as to ensure a certain desired ratio of pull-in to lock range, provided of course, that other disturbing effects are negli-

* see Appendix 1.

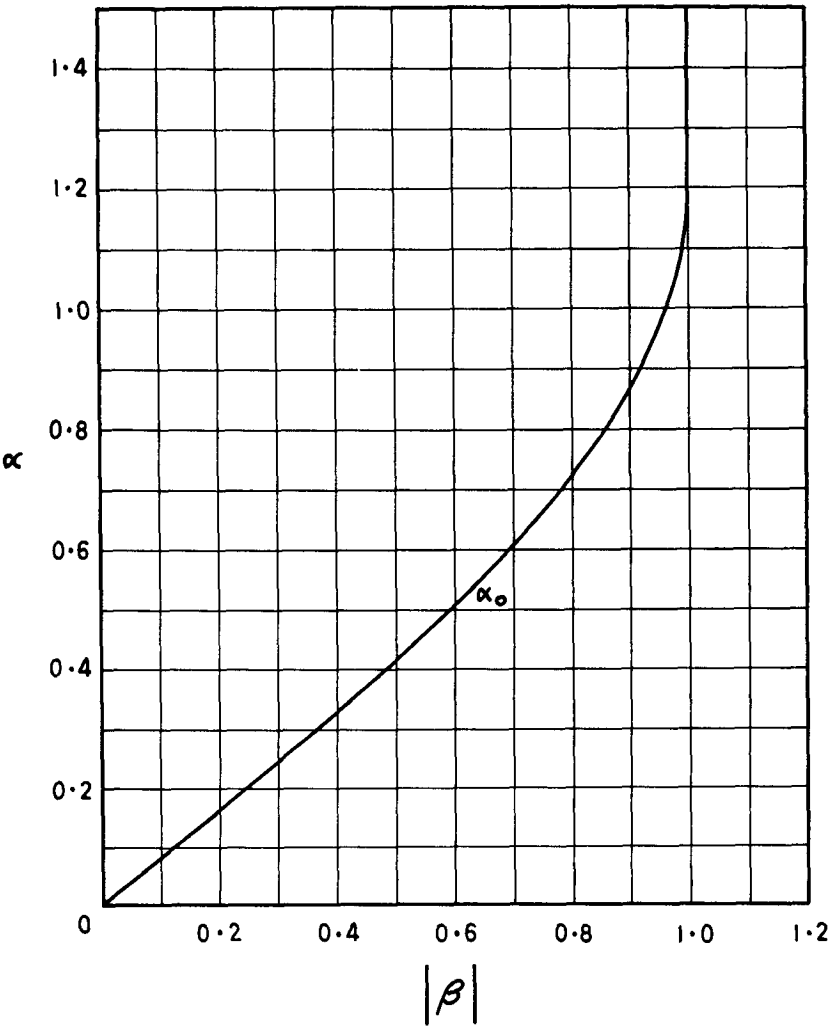

FIG. 2.7. Curve for the system described by the equation

$$\frac{d^2\xi}{d\tau^2} + \alpha\frac{d\xi}{d\tau} + \sin\xi = \beta$$

giving α_0, the value of α which will ensure synchronization for a given $|\beta|$. The area between the curve and the α-axis represents certain synchronization regardless of initial conditions, (7).

gible. For the synchronization of oscillators to a single frequency (as in colour television) the phase detector output is (ideally) DC when synchronization has occurred and it has been shown that outside the locking range, the phase detector output consists of a series of exponential waves (9). In the case of the receiver, we have in addition a term of modulation frequency in the phase detector output when synchronized (except for the condition of zero mis-tuning and symmetrical sidebands), and of approximately modulation frequency when outside the lock range. In the experimental receiver used the interference caused by this term was the main factor in determining the RC filter cut-off frequency.

Case of Lag Networks

In the case of the control networks shown in Fig. 2.6b and c, we have

$$\frac{E_2}{E_1} = \frac{1 + p\,T_1}{1 + p\,T_2}.$$

Using the same reasoning as that used in the derivation of the case of the RC filter, the resulting differential equation is found to be

$$\frac{d^2\varphi}{dt^2} + \frac{1}{T_2}\left(1 - \frac{T_1 K_1^2 K_2 EABS}{2} \cdot \cos 2\varphi\right)\frac{d\varphi}{dt} + \frac{K_1^2 K_2 EABS}{4\,T_2} \cdot \sin 2\varphi - \frac{\omega_d}{T_2} = 0.$$

It is seen that this leads to Equation (2.2) when $T_1 = 0$.

As the coefficient of $\frac{d\varphi}{dt}$ contains a function of φ, this equation cannot be brought to the form of (2.2). There is at present no known analytic solution to it.

Approximate results for a phase-controlled oscillator with such a control network have been derived by Gruen (8). According to his measurements

$$\frac{\textit{pull-in range}}{\textit{lock range}} \approx \sqrt{\frac{\omega_n}{K}},$$

and

$$\frac{\textit{pull-in range}}{\textit{lock range}} \approx \frac{\omega_n}{K}$$

for an RC filter control network, where K is the lock range and

$$\omega_n = \sqrt{\frac{2K}{T_2}}.$$

This last result is equivalent to an approximation of the curve of α as a function of $|\beta|$ by a straight line from the origin up to the point where

$$\alpha \approx \beta \approx \frac{1}{2}.$$

From a comparison of the expressions it can be seen that a reduction of ω_n causes a smaller reduction of the pull-in range with the lag network. Useful results were obtained by Gruen (8) for the phase-controlled oscillator in the synchronized state by using the approximation $\sin x \approx x$ for small x. The receiver is exactly analogous.

If $\varphi_1 =$ phase of reference (though absent) carrier
$\varphi_2 =$ phase of local oscillation
$\varphi = \varphi_1 - \varphi_2$
$F(p) =$ transfer function of control network between phase detector and reactance tube

and

$$K = \sum_{\eta=1,2,3,\ldots}^{n} \frac{1}{4} K_1^2 K_2 E^2 A_\eta B_\eta S$$

then $\frac{d\varphi}{dt}$ is the instantaneous frequency difference between the controlled oscillator and the reference, while $\frac{d\varphi_1}{dt}$ is the instantaneous frequency difference between the synchronizing signal and the free-running oscillator, where the phases are measured with respect to a coordinate system rotating at the free-running angular speed of the local oscillator.

In operational notation the differential equation for the control loop is then

$$p\varphi + KF(p)\sin 2\varphi = p\varphi_1 \tag{2.3}$$

If we let $\sin 2\varphi \approx 2\varphi$, we have

$$p\varphi_2 + 2KF(p)\varphi_2 = 2KF(p)\varphi_1 \tag{2.4}$$

First considering the case of a direct connection for which $F(p) = 1$, we obtain for the system response to a unit step change of the input phase

$$\mathscr{L}\varphi_2(t) = \frac{2K}{p(p+2K)}$$

where $\mathscr{L}$ denotes the Laplace transform.
Resolving into partial fractions we have

$$\mathscr{L}\varphi_2(t) = \frac{1}{p} - \frac{1}{p+2K} \qquad \text{and therefore}$$

$$\varphi_2(t) = 1 - e^{-2Kt}, \qquad \text{assuming that}$$

the initial detuning is zero.

If now the input phase is varied sinusoidally the system response is

$$\frac{\varphi_2}{\varphi_1}(j\omega) = \frac{1}{1 + j\omega/2K}$$

Now the response of an RC filter is given by

$$\frac{V_{out}}{V_{in}}(j\omega) = \frac{1}{1 + j\omega CR}$$

where $1/CR$ is the cut-off frequency. It can thus be seen that the control system behaves as an RC filter with respect to variations of the input phase reference and has a cut-off frequency of

$$\omega_c = 2K \text{ radians/second.}$$

It has been shown that in such systems the mean square phase error

caused by random interference is proportional to the noise bandwidth which is defined as

$$B = \int_{-\infty}^{+\infty} \left| \frac{\varphi_2}{\varphi_1}(j\omega) \right|^2 d\omega \tag{2.5}$$

This is the bandwidth of an ideal filter with a rectangular bandpass characteristic which would pass the same mean square noise. Substituting the $j\omega$ response obtained above, the integration is performed to yield

$$B = 2\pi K \text{ radians/second.}$$

For the networks shown in Fig. 2.6b and c

$$F(p) = \frac{1 + pT_1}{1 + pT_2}$$

where T_1 and T_2 are as defined in Fig. 2.6. The transient response is then

$$\frac{\varphi_2}{|\varphi_1|}(t) = 1 - e^{-\zeta\omega_n t}\left(\cos\sqrt{1-\zeta^2}\,\omega_n t - \frac{\zeta - \frac{\omega_n}{2K}}{\sqrt{1-\zeta^2}} \cdot \sin\sqrt{1-\zeta^2}\,\omega_n t\right)$$

where $\omega_n^2 \equiv 2K/T_2$ and $\zeta\omega_n \equiv \frac{1}{2T_2} + K \cdot \frac{T_1}{T_2}$.

The time constants are then $T_1 = \frac{2\zeta}{\omega_n} - \frac{1}{2K}$ and $T_2 = \frac{2K}{\omega_n^2}$.

The parameter ζ determines the damping. $\zeta < 1$ represents underdamping (oscillatory), $\zeta = 1$ is critical damping and $\zeta > 1$ represents over-damping. A rule of thumb is to make $4 > \zeta > 1$ in order to avoid sluggishness in the system response.

Since $\frac{\omega_n}{2K} = \frac{2\zeta}{1 + 2KT_1}$ and $T_1 \geq 0$,

we have the maximum value for $\frac{\omega_n}{2K}$ when $T_1 = 0$ (single time-constant RC network)

$$\left.\frac{\omega_n}{2K}\right|_{\max} = 2\zeta.$$

For a fixed value of ω_n as the system gain increases to infinity we have

$$\left.\frac{\omega_n}{2K}\right|_{\min} = 0$$

The transient response for these two limits is shown in Fig. 2.8(a)(8) for $\zeta = 0{\cdot}5$.

The frequency response of the system with these control networks obtained by substituting the transfer function $F(p)$ into Equation (2.4) is found to be

$$\frac{\varphi_2}{\varphi_1}(j\omega) = \frac{1 + 2j\zeta\frac{\omega}{\omega_n}\left(1 - \frac{\omega_n}{4\zeta K}\right)}{1 + 2j\zeta\frac{\omega}{\omega_n} - \left(\frac{\omega}{\omega_n}\right)^2} \tag{2.6}$$

This is shown in Fig. 2.8 (b) (8) for the limiting values of $\frac{\omega_n}{2K}$ for $\zeta = 0{\cdot}5$. For $\zeta = 1/2$, $\omega_c \approx \omega_n$ radians/second.

Substituting from Equation (2.6) into the expression for the noise bandwidth (2.5), we have

$$B = \int_{-\infty}^{+\infty} \frac{1 + 4\zeta^2\left(\frac{\omega}{\omega_n}\right)^2\left(1 - \frac{\omega_n}{4\zeta K}\right)^2}{1 - (2 - 4\zeta^2)\left(\frac{\omega}{\omega_n}\right)^2 + \left(\frac{\omega}{\omega_n}\right)^4} \cdot d\left(\frac{\omega}{\omega_n}\right)$$

from which

$$B = \frac{4\zeta^2 - 4\zeta\left(\frac{\omega_n}{2K}\right) + \left(\frac{\omega_n}{2K}\right)^2 + 1}{2\zeta} \cdot \pi\,\omega_n$$

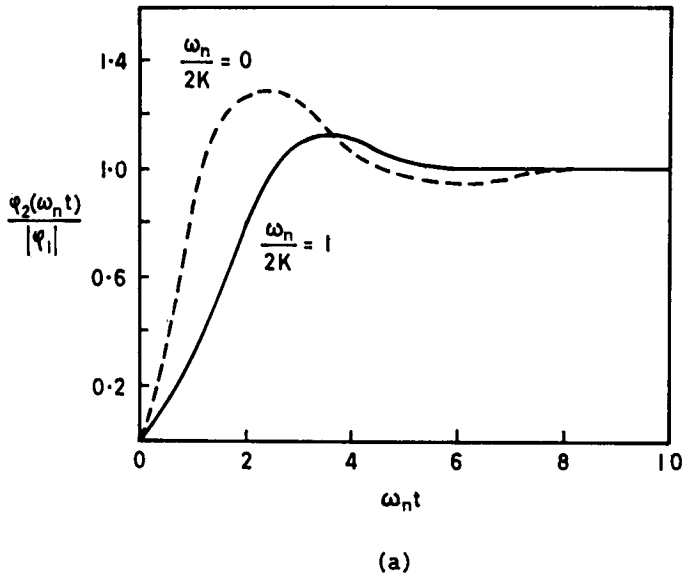

(a)

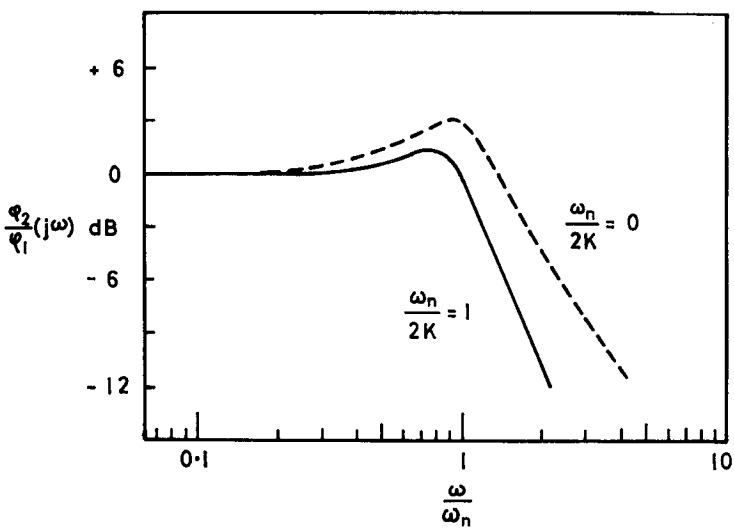

(b)

FIG. 2.8. a) Transient response for $\zeta = 0{\cdot}5$
b) Frequency response for $\zeta = 0{\cdot}5$

Now if $\omega_n/2K \ll 1$, then

$$\frac{dB}{d\zeta} = 2\pi\omega_n - \frac{\pi\omega_n}{2\zeta^2} = 0 \text{ for minimum, whence } \zeta = \frac{1}{2}.$$

With this value, the noise bandwidths for two limiting cases are

$$B\Big|_{\frac{\omega_n}{2K}\to 0} = 2\pi\omega_n \text{ and}$$

$$B\Big|_{\frac{\omega_n}{2K}\to 1} = 2\pi K.$$

The bandwidth and gain constant of the system can thus be adjusted independently using the lag networks (Fig. 2.8), (8). The equivalent network exhibiting the same characteristics is shown in Fig. 2.6d (8). If the oscillator drift, static phase error and noise bandwidth requirements are known, then T_1, T_2 and K can be determined for the system design. For an RC network, the results are obtained by setting $T_1 = 0$ in the above expressions. When the receiver is compared with the case of a phase-controlled oscillator synchronized to a single frequency, it is seen that for a given K the receiver has twice the bandwidth. This is due to the phase comparator output being proportional to $\sin 2\varphi$ instead of to $\sin\varphi$.

Useful results are given by McAleer (9) who has treated phase-locked oscillators from the servomechanism point of view. The pull-in time has been given by Richman (10) as being

$$t_{pull\text{-}in} \approx \frac{4\ (\textit{Initial frequency off-set})^2}{(\textit{Noise bandwidth})^3}$$

This expression is obtained by assuming that the filter capacitor voltage does not change appreciably during each period of the pull-in cycles. It is not valid right up to the limits of the pull-in range where the pull-in time becomes infinite.

It would be possible to make the phase comparator output become a linear function of the phase error, though the nature of the signals does not permit the use of flip-flop circuits or other techniques used in the phase control of pulse circuits. A wave-shaping circuit which

could operate even with small variations of the input amplitude would be required. Such a triangular characteristic could be realized using an arrangement of diodes or non-linear resistances.

It is interesting to note that the method of deriving a phase control voltage from (FM) sidebands has been used for another purpose, namely, to regulate the centre frequency of a FM transmitter (11).

2.4. Fading and Frequency-dependent Transmission-Path Length

The main effects of fading are a reduction of the sensitivity of the synchronizing loop, reducing the lock range and the pull-in range. Fig. 2.9 shows the influence of the fading of one sideband on the lock range and on various initial values of pull-in range. The different curves for the pull-in range correspond to different filter time-constants. The ratio *pull-in range / lock range* increases with fading. This must clearly be so since a which determines the fractional pull-in range varies as $1/\sqrt{K}$ while the lock range varies directly as the loop gain factor K (Sec. 2.3). As synchronization is lost between signals, operation must

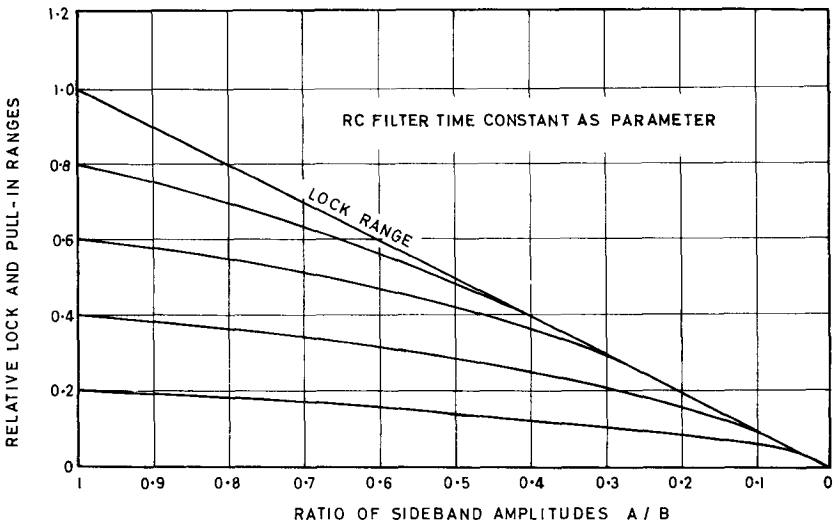

FIG. 2.9. Showing the effect of selective fading of one sideband on the lock range and various initial values of pull-in range. The curves are normalized with *lock range* = 1 for symmetrical sidebands. A family of curves is obtained by varying the phase-lock filter time-constant as parameter.

always be within the pull-in range. It is therefore particularly useful that the pull-in range is less drastically affected by fading. The curves, normalized with *lock range* = 1, were calculated using the published solution curve (Fig. 2.7) for Equation (2.2), (7).

Further, it can be seen that the noise bandwidth decreases with fading in the case of no filter between phase detector and reactance control. In the case of the lag network with the damping factor $\zeta = \frac{1}{2}$ it will be seen that at large signal strengths, the noise bandwidth B will be reduced in proportion to $\sqrt{K}$ whereas at smaller signal levels B varies directly as K. The control loop cut-off frequency also drops with

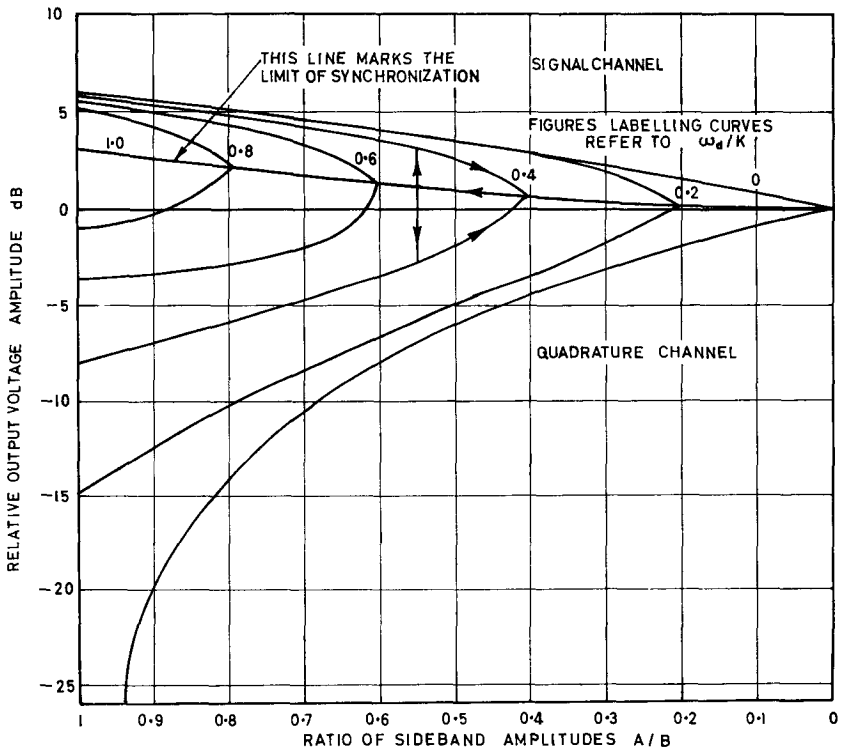

FIG. 2.10. Showing the effect of one sideband fading on the signal and quadrature channels for several values of frequency off-set. The hysteresis effect indicated by the arrows on one of the curves occurs when the *pull-in range* is smaller than the *lock range*.

fading. It should be noted that it does not matter whether the sidebands fade asymmetrically for these changes: only the product of their amplitudes is relevant.

With fading, the detected output is also reduced, firstly owing to the reduction of input signal and secondly since the reduction of lock range is equivalent to a greater frequency off-set, the phase error will be increased, reducing the output still further. This leads to a rapid loss of synchronization after a certain point. Fig. 2.10 shows calculated curves for the signal and quadrature channels with fading of one sideband, with the curves labelled in terms of mistuning. The graph is valid only when traversed from left to right unless *pull-in range* = *lock range*. This condition cannot always be realized here since sideband asymmetry causes the phase detector output to contain an AC component of modulation frequency, thus necessitating the use of a low-pass filter which will reduce the pull-in range. When the curves join the line marking loss of synchronization the signal thereafter becomes a complicated mixture since the local oscillator frequency is no longer constant but "hesitates" periodically near the correct value and then undergoes a rapid excursion away to return again at a repetition rate of about twice the difference between the free-running frequency and the desired frequency. This is exactly analogous to the process which occurs in the case of phase-controlled synchronized oscillators.

As the receiver parameters are so dependent on signal strength it would clearly be an advantage to have an efficient AGC system. There are also other practical advantages to be gained by using AGC, (Sec. 4.2).

Another effect is caused by variation of the virtual height of ionospheric layers with frequency. For two different frequencies representing a given modulation component in the two sidebands the difference in transmission path length may vary from zero to many kilometers, being very large near the critical frequency (28). If these delay differences are small compared with the rise and decay times of the modulation then a phase shift only will result. In the previous calculations for the receiver we have assumed that the phase difference is divided equally into $+\theta$ and $-\theta$ between the sidebands. We shall now justify this assumption. If we have two side frequencies ω_1, and ω_2 where $\omega_1 > \omega_2$, and if the higher frequency wave be delayed by a

time t_1, we have a phase lag of $\omega_1 t_1$. If we choose a new point in time as our reference lagging the reference point in the lower side frequency by t_2 we can make the lead of the lower side frequency equal to the lag of the upper side frequency, or

$$t_2 = \frac{\omega_1}{\omega_1 + \omega_2} \cdot t_1$$

If the frequencies are high as is usually the case we may write

$$t_2 \approx \tfrac{1}{2} t_1$$

The results obtained with this substitution will only be correct for changes which are slow compared with the loop transient phase response, a condition which will usually be fulfilled in practice.

Typical rise times for the lower frequency components of speech are of the order of 10 milliseconds with decay times of about 100 msec. The upper components have rise times of the order of less than 1 msec. Delay time differences are therefore unlikely in practice to do more than alter the phase of sideband components. With other types of modulation signal though, the delay difference could become comparable with rise times. Thus if the modulation is a sine wave of frequency f_{m1} and a rapid change to f_{m2} were to occur, then if the time delay difference between the sidebands is sufficiently long, the receiver will synchronize between the two. In that case the output will change from f_{m1} to $\tfrac{1}{2}(f_{m1} + f_{m2})$ and finally to f_{m2}. If at the start of a signal the sidebands arrive with a time delay then the start of the synchronization process will be delayed until both sidebands arrive.

2.5. Interference

There are two ways in which an interfering signal may make its presence felt. It may appear directly in the output, or it may interfere with proper synchronization. The behaviour of the receiver with regard to interference which can be represented as a phase change in the input reference is indicated by the transient and sine-wave responses derived earlier, (Sec. 2.3). An interfering signal $P \cos(\omega_o t + \omega_i t)$ appears in the output as $\tfrac{1}{2} K_1 PE \cos \omega_i t$ and as $\tfrac{1}{2} K_1 PE \sin \omega_i t$ in

the quadrature output. It produces a term $\frac{1}{4} K_1^2 K_2 E^2 P \sin 2\omega_i t$ in the phase control voltage.

The choice of system bandwidth is a matter of compromise. A narrower bandwidth causes greater susceptibility to interference introduced at the reactance tube input, of which the above is an example. It confers an advantage, however, in another respect. If a carrier is present, the receiver may synchronize wrongly between the carrier and one sideband. In this case, however, the derived reference frequency is not constant but is situated midway between the lowest sideband component of sufficient amplitude and the carrier, and will vary as the modulation varies. A narrower system bandwidth reduces the ability of the receiver to follow such changes. It may in practice be preferable to provide a choice of bandwidths according to which type of interference is more objectionable, bearing in mind, however, the reduction in pull-in range consequent on the use of narrow bandwidths. An addition to the circuit will later be described, which would permit the use of narrower lock ranges.

2.6. Detector

The detector used here is the homodyne or coherent detector. This type has been fully treated by Tucker (12) and has been used in the synchrodyne receiver, where a local oscillator is synchronized by the incoming carrier by frequency pulling. It is assumed that the operation of the detector is not influenced by the signal, but is determined by the local oscillator voltage, which performs a switching action. For optimum operation of the detector with respect to signal to noise ratio φ (Sec. 2.2) should be zero. The use of the automatic frequency control described in the next Section (2.7) would tend to reduce the static phase error φ by reducing the mistuning. The signal detector in the receiver under discussion can take the form of a multi-grid mixer tube, since the output of interest is at audio frequencies. In other cases where a DC component in the output is of interest other forms have to be used. The phase and frequency control detectors used in the receiver are examples. Tucker (12) has shown that when the output required is DC, the signal to noise ratio at the output of the detector is improved over that existing at the input by a factor of $\sqrt{2}$.

2.7. Frequency Control

If the system bandwidth is narrowed to reduce the faulty carrier-sideband synchronization mentioned earlier, the lock range is reduced, raising the stability requirements for the local oscillator. It is possible however to introduce a frequency control which operates similarly to the well-known Automatic Frequency Control (AFC) except that the control voltage is derived differently. If in Fig. 2.11 output v_2 is differentiated, we obtain

$$v_4 = \frac{dv_2}{dt} = \frac{1}{2} K_1 AE(\delta - \omega_m) \cos(\delta t + \varphi - \theta - \omega_m t) + \frac{1}{2} K_1 BE(\delta + \omega_m) \cos(\delta t + \varphi + \theta + \omega_m t)$$

If this is multiplied with v_1 in a modulator, we get

$$\frac{1}{8} K_1^2 K_3 A^2 E^2 (\delta - \omega_m) + \frac{1}{8} K_1^2 K_3 B^2 E^2 (\delta + \omega_m) + \text{AC components of higher frequency} = \frac{1}{8} K_1^2 K_3 E^2 [\delta (A^2 + B^2) + \omega_m (B^2 - A^2)].$$

When the sideband amplitudes are equal, we thus have a DC control voltage varying linearly with the frequency error which may be used to control frequency by means of the same reactance-tube stage as is used for phase control. If the sidebands are of unequal amplitude, the component $\omega_m (B^2 - A^2)$ may cause some mistuning. If an interfering signal $P \cos(\omega_o + \omega_i) t$ is present, it produces an error voltage in the frequency control of $\frac{1}{4} P^2 E^2 K_1 K_3$.

2.8. Interference Cancellation

Refering to Fig. 2.11 we have already shown in Sec. 2.2 that

$$v_1 = \frac{1}{2} K_1 AE \cos(\delta t + \varphi - \theta - \omega_m t) + \frac{1}{2} K_1 BE \cos(\delta t + \varphi + \theta + \omega_m t)$$

$$v_2 = \frac{1}{2} K_1 AE \sin(\delta t + \varphi - \theta - \omega_m t)$$

$$+ \frac{1}{2} K_1 BE \sin(\delta t + \varphi + \theta + \omega_m t)$$

v_2 is to be shifted by 90° relative to v_1. We must ensure that the terms in brackets are of positive quantities, and if we assume $\omega_m > \delta$, we should preferably write

$$v_1 = \frac{1}{2} K_1 BE \cos(\omega_m t + \theta + \delta t + \varphi)$$

$$+ \frac{1}{2} K_1 AE \cos(\omega_m t + \theta - \delta t - \varphi)$$

$$v_2 = \frac{1}{2} K_1 BE \sin(\omega_m t + \theta + \delta t + \varphi)$$

$$- \frac{1}{2} K_1 AE \sin(\omega_m t + \theta - \delta t - \varphi).$$

We can now represent a 90° phase shift by adding 90° to the terms in brackets and obtain

$$v_6 = (v_2 + 90°) = \frac{1}{2} K_1 BE \cos(\omega_m t + \theta + \delta t + \varphi)$$

$$- \frac{1}{2} K_1 AE \cos(\omega_m t + \theta - \delta t - \varphi).$$

When this is added to v_1 we obtain

$$v_8 = K_1 BE \cos(\omega_m t + \theta + \delta t + \varphi).$$

This result has been known in other connections for a long time (13). Its significance here is due to the possibility of complete suppression of any interference on the A sideband. The process can be reversed and interference on the other sideband can be suppressed by shifting v_1 or v_2 by 180° and adding as before. If interference on one sideband is so severe that synchronization is lost, reception could continue if the

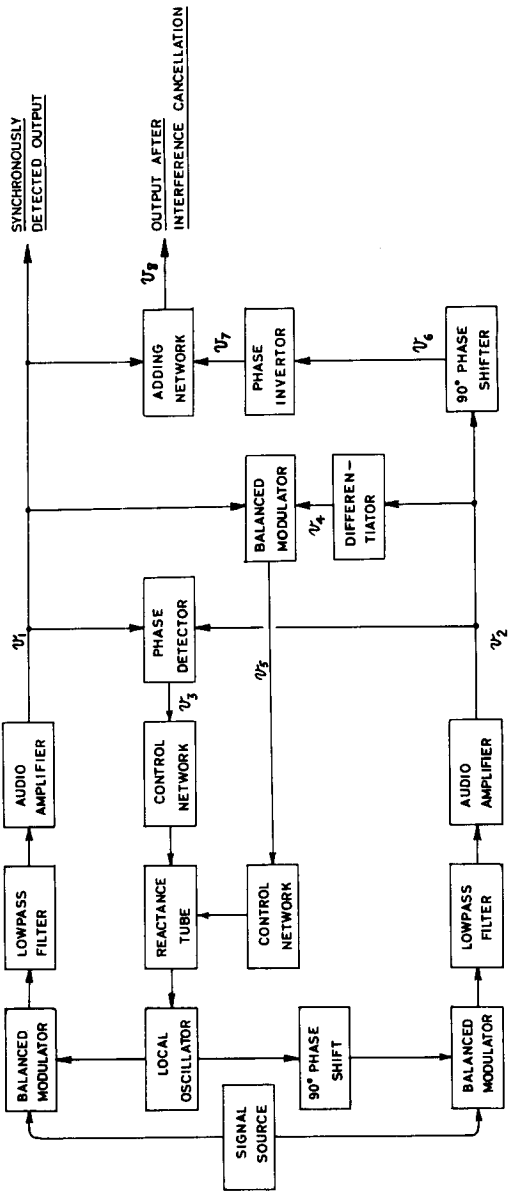

FIG. 2.11. Receiver with separate frequency control and interference cancellation.

frequency off-set is maintained by some other means to within about 10 c/s, as is usual in single sideband practice.When this sideband cancellation is employed, the signal output is of course reduced, but the signal to interference ratio may be improved.

Time did not permit an investigation to be completed of other cases where the interference is divided in some other manner between both sidebands.

CHAPTER 3

TEST APPARATUS

3.1. Transmitter

The transmitter needed to produce the required double sideband signal with suppressed carrier is a balanced modulator, with associated amplifiers. In the experimental set-up, however, we would like to investigate the system performance with sidebands fading independently and undergoing different phase shifts and transmission delays. It is true that in the case of sine wave modulation the signal could be simulated by two oscillators with a frequency separation equal to twice the modulation frequency. This representation would only be valid for the simplest type of modulation and the side frequencies would not have a fixed relationship between them. Although one cannot speak of a fixed phase relationship between two different frequencies a change of phase in the detected output could not be related to a change of phase in one of the sidebands unless they were to be derived from a common source. In consequence, it was decided to build an independent sideband transmitter covering a typical audio frequency bandwith. We could have employed balanced modulators with sharp filters to separate the sidebands and thus obtained independently modulated sidebands. This method has the disadvantage that the filters would have had to be made for different frequency bands with their attenuation curves intersecting precisely at the carrier frequency. In addition, the relative time delay undergone by the sidebands would vary with the exact position of the carrier relative to the filter response curves which may, for instance, vary with temperature. It would be somewhat difficult to attempt the construction of mechanical filters with attenuation curves crossing at a predetermined point. Instead, two filters are produced for the most convenient range for

their construction and the sidebands are derived in another way using the phase shifter described elsewhere (Sec. 3.2). The filters do not have to be similar, though it is more convenient if they are, since a common local oscillator for both phase shifters can then be employed.

The arrangement used is a double single sideband transmitter (Fig. 3.1). The balanced modulators suppress the carrier and it can easily be shown that for exact phase shifts and equal voltage inputs to the modulators, each signal appears on only one sideband. The phase shift at the carrier frequency can be produced very exactly, but the wideband audio phase shifter presents some problems. We shall consider the more general case when the phase shifter has phase and amplitude errors.

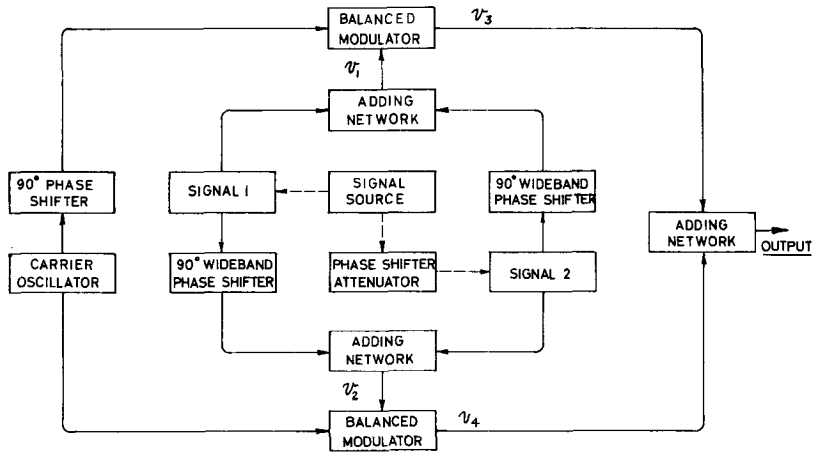

FIG. 3.1. Basic diagram of the independent sideband transmitter used. One signal source is used as shown dotted. The attenuator thus reads the attenuation of one sideband directly.

Let the local oscillator voltage be proportional to $\cos \omega_0 t$ and let the modulation signal voltage be proportional to $\cos \omega_m t$. We obviously need consider only one modulation signal. Let us assume that after passage through the phase shifter, the signal becomes

$$v_1 = C \cos (\omega_m t + \psi)$$
$$v_2 = D \sin (\omega_m t - \psi)$$

where 2ψ is the phase shifter phase error and D/C is its output amplitude ratio $= R$.

We obtain $v_3 = \frac{1}{2} K_1 C \{\cos[(\omega_o - \omega_m)t - \psi] + \cos[(\omega_o + \omega_m)t + \psi]\}$

and $v_4 = \frac{1}{2} K_1 D \{\cos[(\omega_o - \omega_m)t + \psi] + \cos[(\omega_o + \omega_m)t - \psi]\}$

Letting $\omega_1 = \omega_o - \omega_m$ and $\omega_2 = \omega_o + \omega_m$

we get $$v_5 = \frac{1}{2} K_1 (C^2 + D^2 + 2CD\cos 2\psi)^{1/2} \cos \left\{\omega_1 t - \tan^{-1}\left[\left(\frac{C-D}{C+D}\right)\tan\psi\right]\right\}$$

$$+ \frac{1}{2} K_1 (C^2 + D^2 - 2CD\cos 2\psi)^{1/2} \cos \left\{\omega_2 t - \tan^{-1}\left[\left(\frac{C+D}{D-C}\right)\tan\psi\right]\right\}$$

Thus ideally, with no phase and amplitude errors, one sideband cancels out.

In this case, the desired to undesired sideband output voltage ratio S is given by

$$S^2 = \frac{1 + R^2 + 2R\cos 2\psi}{1 + R^2 - 2R\cos 2\psi} \tag{3.1}$$

Ideally of course R should be equal to one, but if

$R = (1 + \gamma)$ where $\gamma \ll 1$, then for $\psi \ll 1$

we have $S^2 \approx \dfrac{4}{(2\psi)^2 + \gamma^2}$.

For the phase shifter used here,

$$R^2 = \frac{1 + F^2 + 2F\cos 2\varphi_3}{1 + F^2 - 2F\cos 2\varphi_3} \text{ and } \tan 2\psi = \frac{2F\sin 2\varphi_3}{1 - F^2}$$

where F = filter attenuation in the phase shifter, and φ_3 = an unrestricted parameter in the phase shifter.

For small φ_3, we can derive the relation

$$\cos 2\psi \approx (1 - 8F^2\varphi_3^2).$$

If we expand the expression for R^2 with the above value for $\cos 2\psi$ and substitute into equation (3.1), we obtain

$$S^2 = \frac{1 + 2F + 3F^2 - 2F^3 - 4F\varphi_3^2 - 14F^2\varphi_3^2 - \cdots}{F^2 + 4F^3 + 6F^4 - 2F^2\varphi_3^2 - \cdots}$$

$$\text{for } F \ll 1 \text{ and } \varphi_3 \ll 1.$$

This result shows what a small influence the choice of φ_3 has on the suppression of the undesired sideband, causing at most a very slight deterioration when it is larger. For small F and φ_3 this reduces to the interesting result:

$$S \approx \frac{1}{F}$$

This indicates that if a given filter is used directly to remove one sideband substantially the same suppression ratio is obtained as when using the same filter in this phase shifter in the phasing method of single sideband generation. Thus the compromise choices available in the phase shifter between phase and amplitude error by variation of φ_3 may be useful in other applications but are not important here.

The advantages in using the arrangement described may be summarized as follows:

- The sidebands are modulated independently, permitting the introduction of different time delays and amplitudes.
- The phase shifts undergone by the sidebands are identical in so far as the phase shifters as units are identical.
- The sharp bandpass filters may be made for the most convenient frequency for construction, with the same undesired sideband rejection as if they were used directly at the working frequency. Also, they need not bear any precise relationship to one another.

For the introduction of a time delay or phase shift in one sideband, it may be more convenient to do this at a frequency higher than audio. A very convenient point is just before or after the bandpass filter in the phase shifter (Fig. 3.6) where the signal appears as a low radio frequency.

3.2. Phase Shifter

The system described here to generate independently modulated sidebands requires the use of networks giving a 90° phase shift over the band of modulation frequencies. Passive networks have been devised which approximately fulfill this requirement over restricted frequency ranges (14, 15, 16).

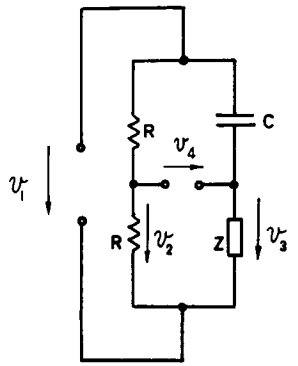

FIG. 3.2. Phase-shift network.

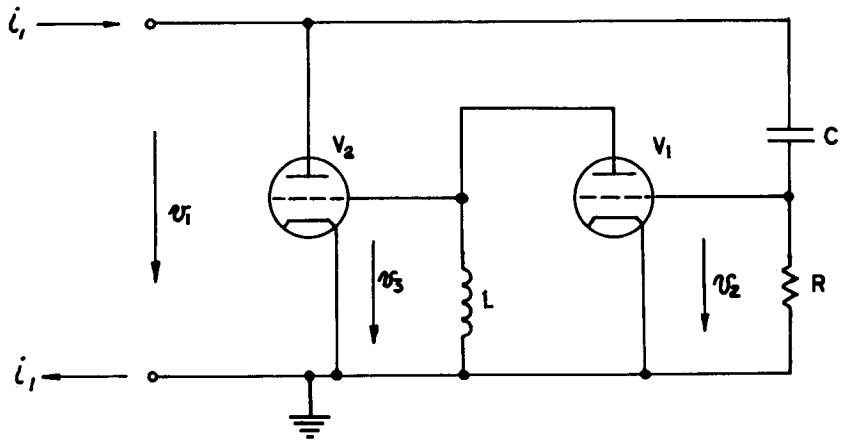

FIG. 3.3. Circuit for obtaining a frequency-dependent resistance.

It was decided to experiment with various other possible arrangements for obtaining the phase shift and two new methods are described here. The first method, although rather limited in scope is of some interest. Some experiments were performed, but it was not developed further. The second phase shifter described is the one that was developed for the present work and presents interesting possibilities.

First Phase Shifter

The network shown in Fig. 3.2 with a resistor in the position Z is used to provide a variable phase shift with a constant output voltage. The phase shift is not constant with frequency. With any impedance Z, it follows from elementary considerations that

$$2v_4 = \frac{1 - j\omega CZ}{1 + j\omega CZ} v_1$$

the phase shift being $\tan^{-1} 2\omega CZ / (1 - \omega^2 C^2 Z^2)$.
Thus we have a 90° phase shift when Z is a resistance of magnitude $1/\omega C$ and in order to provide a phase shift constant with frequency Z would have to vary. The output voltage is in any case constant for all values of resistive Z.

One way of approximating this requirement is shown in Fig. 3.3 which represents the circuit for AC only. The admittance at the left-hand terminal pair is a conductance of value $G = g_{m1} g_{m2} \omega^2 LCR$ where g_{m1}, g_{m2} are the mutual conductances of $\mathbf{V}_1$ and $\mathbf{V}_2$. There is a susceptance as well but this can be neglected if $j\omega CR \ll 1$.
Thus we have a conductance of the form

$$G = K \times (\textit{frequency})^2 \text{ where } K \text{ is a constant.}$$

Referring to Fig. 3.4, let

$$Y_2 = Kf^2, \text{where } f \text{ is the applied frequency.}$$

We have for the characteristic admittance

$$Y_0 = \sqrt{Y_1 Y_2 + Y_2^2/4} = \sqrt{Y_1 Y_2}\sqrt{1 + Y_2/4 Y_1}$$

If we let $Y_2/4\ Y_1 \ll 1$
then $Y_0 \approx \sqrt{Y_1\ Y_2}$
and as $Y_2 = Kf^2$
therefore $Y_0 \approx \sqrt{K\ Y_1} \cdot f$

Of course, in practice it may be rather difficult to achieve this. A simple approximation is to add just one conductance in series with the frequency-dependent element and one in parallel. Fig. 3.5 shows graphs for the function $G = 10^{-3} f^2\ \mu$ mhos with different values of series conductance. It can be seen that a good degree of linearity may be achieved even with this simple arrangement. For instance, with $G_{series} = 1500\ \mu$ mhos, the error from linearity in the range of 300 c/s to 1200 c/s is 1·5 in 1000. The intersept of the extended straight line approximation with the zero ordinate gives the value of parallel conductance to be added, in this case 150 μ mhos. If the required value of K cannot be achieved by the circuit of Fig. 3.3, amplification may be introduced to increase the conductance, but this must be accomplished without phase change.

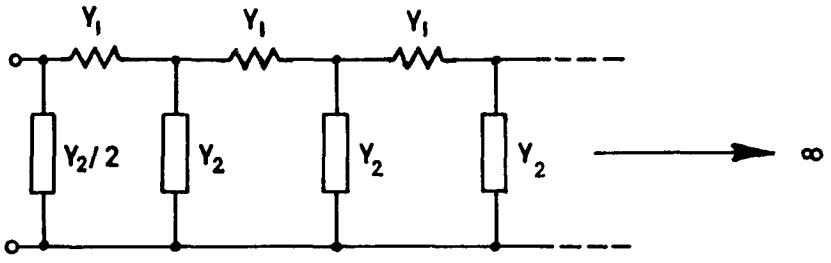

FIG. 3.4. Frequency-dependent resistance approximation.

In order to check the stability of the circuit we shall calculate the loop gain. Let the anode slope resistance of both valves be R_a and the mutual conductance g_m. Since $\mathbf{V}_2$ must also be supplied with HT we shall assume an anode load resistor R_l to be in shunt with the input terminals. The anode slope resistance of $\mathbf{V}_1$ may be taken to include the equivalent loss resistance of the coil L. Assuming that the series

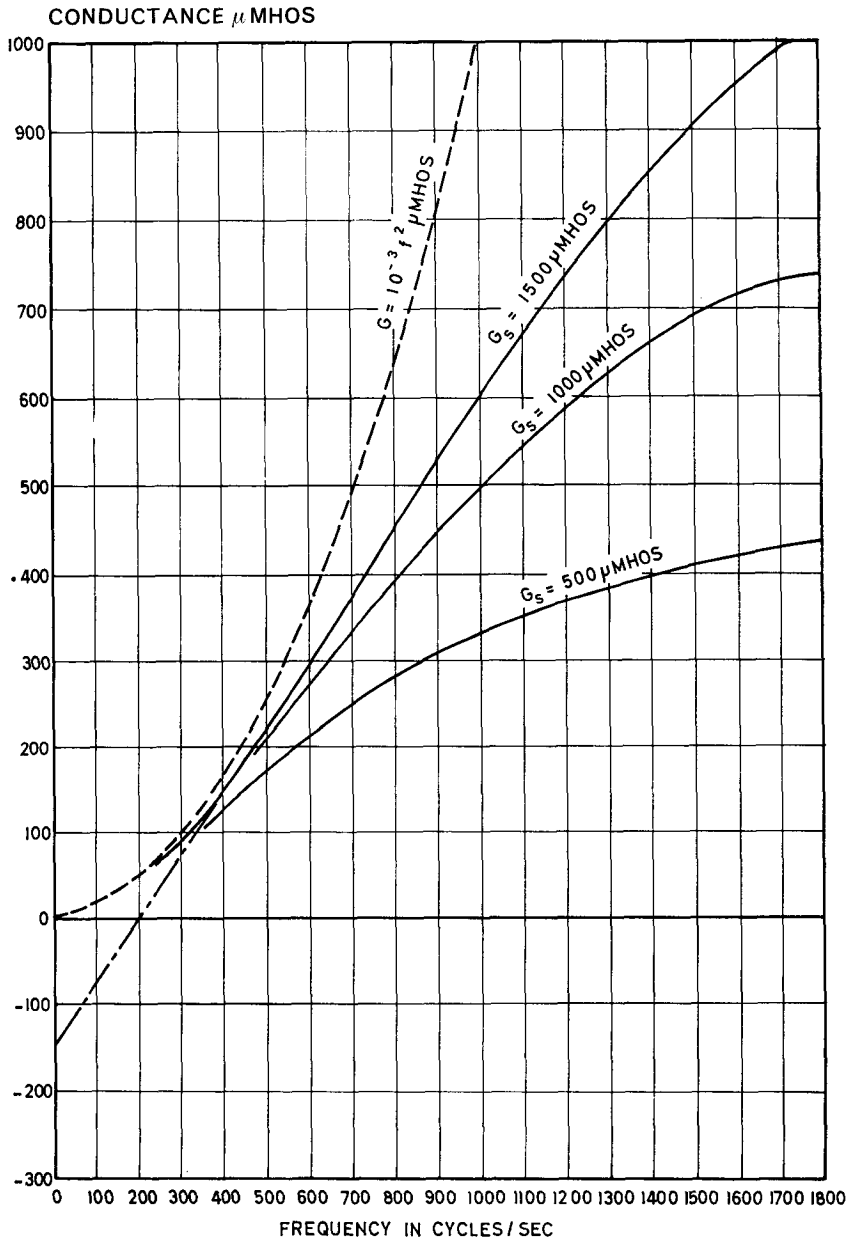

FIG. 3.5. Showing conductance characteristics of the frequency-dependent resistance.

combination of R and C places a negligible load on $\mathbf{V}_2$, the complex loop gain is found to be

$$G = -\frac{g_m^2 R_a^2 R_l R \omega C \omega L}{(R_a + R_l)(j\omega L + R_a)(1 + j\omega CR)}$$

$$= \frac{g_m^2 R_a^2 R_l R \omega C \omega L [(\omega L \omega CR - R_a) + j(\omega CRR_a + \omega L)]}{(R_a + R_l)[(R_a - \omega L \omega CR)^2 + (\omega CRR_a + \omega L)^2]}.$$

The phase angle is therefore given by

$$\cos\varphi = \frac{\omega L \omega CR - R_a}{[(\omega^2 L^2 + R_a^2)\omega^2 C^2 R^2 + R_a^2 + \omega^2 L^2]^{1/2}}$$

Noting that $\omega CR \ll 1$, we obtain

$$\lim_{\frac{\omega_L}{R_a} \to 0} \cos\varphi \approx -1 \text{ or } \varphi \approx \pi$$

This represents the case of high Q which would be aimed at in practice. The admittance consists of an almost pure conductance with practically no susceptance component.
The phase shift with very low Q is given by

$$\lim_{\frac{\omega_L}{R_a} \to 1} \cos\varphi \approx -\frac{1}{\sqrt{2}} \text{ or } \varphi \approx \left(\pi \pm \frac{\pi}{4}\right)$$

The ambiguity can be resolved by considering $\sin\varphi$. For $0 < Q < \infty$ the phase conditions for oscillation cannot be fulfilled since

$$\pi/2 < \varphi < \pi.$$

The circuit will therefore be stable even with lossy elements. Parasitic elements not shown in the circuit diagram may however cause spurious oscillations to occur.

Instead of a frequency-dependent resistance a frequency-independent reactance could also be used for C (Fig. 3.2). Dielectrics with frequency-dependent dielectric constant, however, only exhibit this behaviour at much higher frequencies.

Second Phase Shifter

This phase shifter uses a different principle to the present methods, and is theoretically capable of providing any desired phase difference between any number of outputs to a degree of accuracy depending on the characteristics of the filters used in it (17).

Fig. 3.6 shows a schematic block diagram of this arrangement for the particular case of a 90° phase shifter.

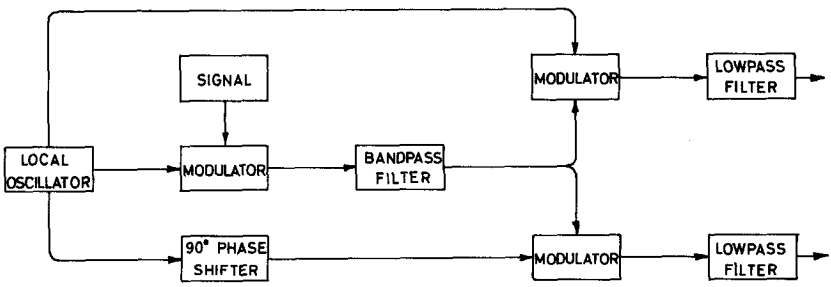

FIG. 3.6. Basic diagram of the new 90° phase shifter.

The signal is used to amplitude modulate a local oscillator frequency, the carrier being suppressed. Of the two resulting sidebands, one is selected by a filter. If the local oscillator frequency is sufficiently high, the upper or lower sideband could be used; if the local oscillator frequency is just above the highest signal frequency, however, then use of the upper sideband would be preferable to attenuate residual signal through the modulator. This single sideband is then demodulated using the same local oscillator frequency. From the resulting components, the modulation signal is then recovered by a lowpass filter. The phase of this output is found to vary as the phase of the local oscillator voltage used for demodulation, in the same direction or with opposite sign depending as to whether the upper or lower sideband is used. This is the reason why one sideband alone must be used since in the combined output from the two sidebands, the phases cancel leaving a signal whose phase is constant and whose amplitude depends on the phase of the demodulating carrier.

The phase shifter is shown in a more general form in Fig. 3.7 where we assume that the detecting signal has some phase φ with respect to the carrier used in obtaining the sidebands.

Let $\cos \omega_m t$ represent the signal input voltage, $\cos \omega_0 t$ represent the local oscillator voltage and K_4 be a modulator constant.

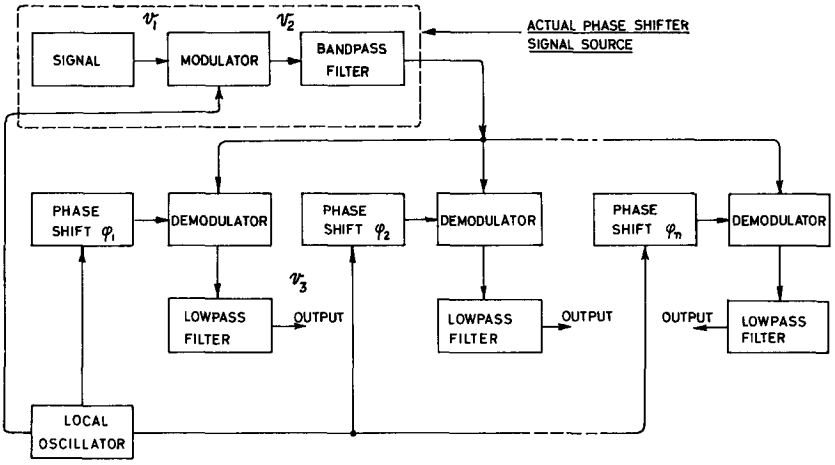

FIG. 3.7. *More general form of the phase shifter or single-phase to poly-phase converter.*

Then $$v_2 = K_4 \cos(\omega_0 + \omega_m) t + K_4 \cos(\omega_0 - \omega_m) t$$

Assume that the bandpass filter alters this to

$$PK_4 \cos(\omega_0 - \omega_m) t + QK_4 \cos(\omega_0 + \omega_m) t$$

After demodulation and the low pass filter, this gives

$$v_3 = \frac{1}{2} PK_4 \cos(\omega_m t + \varphi) + \frac{1}{2} QK_4 \cos(\omega_m t - \varphi)$$

$$= \frac{1}{2} K_4 (P + Q) \cos \omega_m t \cos \varphi + \frac{1}{2} K_4 (Q - P) \sin \omega_m t \sin \varphi$$

$$= \frac{1}{4} K_4 (P^2 + Q^2 + 2PQ \cos 2\varphi)^{1/2} \cos \left[\omega_m t - \tan^{-1} \left(\frac{Q - P}{Q + P} \right) \tan \varphi \right]$$

Letting the phase shift $\tan^{-1}\left(\frac{Q-P}{Q+P}\right)\tan\varphi=\theta$

we have in the case of two detectors using voltages proportional to $\cos(\omega_0 t+\varphi_3)$ and $\cos(\omega_0 t+\varphi_4)$ a phase difference $(\theta_1-\theta_2)$,

where $$\tan(\theta_1-\theta_2)=\frac{(\tan\varphi_3-\tan\varphi_4)\left(\frac{Q-P}{Q+P}\right)}{1+\left(\frac{Q-P}{Q+P}\right)^2\tan\varphi_3\tan\varphi_4}$$

The amplitude ratio of the two output voltages is given by

$$R=\left(\frac{P^2+Q^2+2PQ\cos 2\varphi_3}{P^2+Q^2+2PQ\cos 2\varphi_4}\right)^{1/2}$$

In the particular case of a 90° phase shifter we have, say

$$\varphi_4=\varphi_3+\pi/2$$

giving $$\tan(\theta_1-\theta_2)=\frac{Q^2-P^2}{2PQ\sin 2\varphi_3}$$

and $$R=\left(\frac{P^2+Q^2+2PQ\cos 2\varphi_3}{P^2+Q^2-2PQ\cos 2\varphi_3}\right)^{1/2}$$

If we let $\beta=$ phase error from 90°,

we obtain $$\tan\beta=\frac{2PQ\sin 2\varphi_3}{Q^2-P^2}$$

If we designate the attenuation produced by the filter $F=P/Q$, we may write for a 90° phase shifter

$$R=\left(\frac{1+F^2+2F\cos 2\varphi_3}{1+F^2-2F\cos 2\varphi_3}\right)^{1/2}$$

and $$\beta=\tan^{-1}\frac{2F\sin 2\varphi_3}{1-F^2}$$

By expanding these expressions in a series it can be shown that for $\varphi_3\ll 1$ and $F\ll 1$ then

$$R = 1 + 2F + 2F^2 - 6F^3 - 4F\varphi_3^2 - 14F^4 - 8F^2\varphi_3^2 - \cdots$$
$$\approx 1 + 2F + 2F^2$$

and the phase error is given by

$$\beta \approx 4F\varphi_3 \text{ radians.}$$

No notice has been taken of phase shifts occuring in the modulators, intermediate amplifiers, bandpass or lowpass filters. If the phase shifts in both channels are identical after the demodulators, they have no influence on the relative phase of the two outputs. The phase shift occuring in the bandpass filter does however have an effect when the attenuation of the undesired sideband is small, that is, for the lowest signal frequencies. Since the carrier frequency should be positioned on the flank of the bandpass curve, where the relative attenuation for a given small excursion of frequency on either side is largest, the phase shift will be substantially the same for both sidebands. The different delays undergone by the two sidebands when one is located in the passband are of small importance since the attenuation should then be sufficient to make the errors given above negligible.

Curves of the above functions are shown in Figs. 3.8 and 3.9. Ideally the phase shifter should give two voltages of equal amplitude differing by 90° in phase. It is seen that for a non-ideal filter, the output amplitude ratio can be made to remain constant, as the phase error assumes its largest value, while the phase is always 90° for the condition of greatest disparity in output voltages. Any combination in between is possible, depending on the relative importance of phase and amplitude errors in the particular application. It is assumed that the filter produces a constant phase shift.

The value of ripple in the filter pass-band is the same as that of the whole system, while the system bandwidth equals the filter bandwidth. This is excluding the lowpass filters which do not have to fulfil any stringent requirements and can be made maximally flat and as wideband as desired, as well as neglecting the reduction in amplitude at very low modulation frequencies.

The position of the local oscillator frequency with respect to the filter attenuation curve alters the type of frequency characteristic obtained. This is a matter of compromise. Figs. 3.10 and 3.11 show

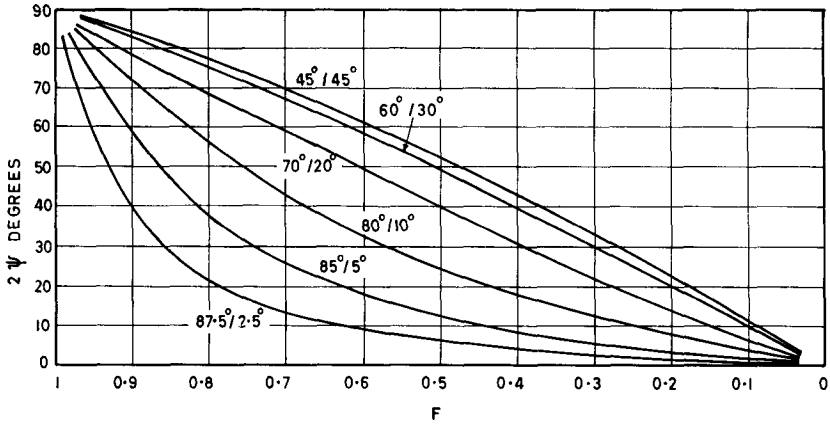

FIG. 3.8. Showing the phase shifter output phase error as a function of the filter attenuation F, for various values of the parameter φ_3.

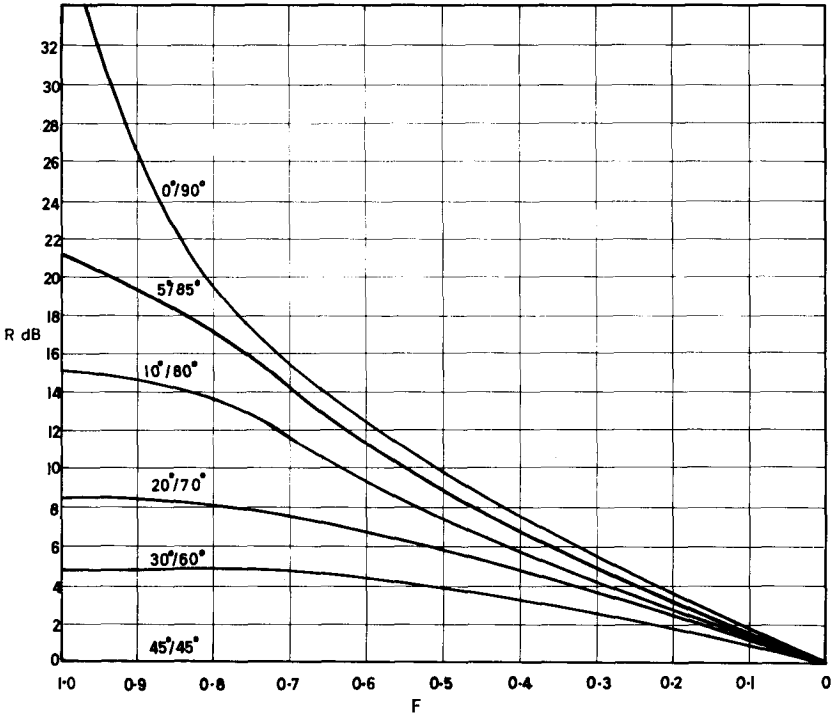

FIG. 3.9. Showing the phase shifter output voltage ratio R in dB as a function of the filter attenuation F, for various values of the parameter φ_3.

curves for the cases of maximum phase error and maximum amplitude error, that is $\varphi_3 = 0$ and $\varphi_3 = \pi/4$ respectively. The filter is assumed to be a single ideal section of attenuation $\alpha_{nepers} = 2\cosh^{-1}\Omega$ where Ω is the normalized frequency, the filter bandwidth being equal to 1. The errors are plotted against normalized modulation frequency Ω_m, for various values of normalized carrier frequency Ω_o. It can be seen that in both cases, if the error at a given frequency is to be reduced, then a larger error will have to be tolerated outside the range. Of course different filter characteristics produce different curves, but generally the character is similar since the slope of the attenuation

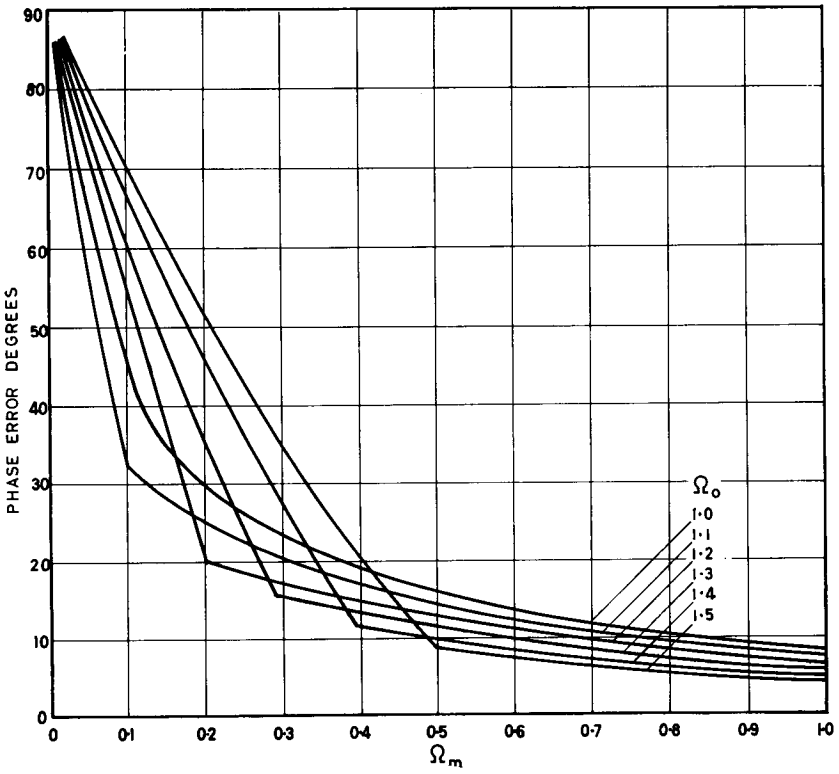

FIG. 3.10. Showing the phase shifter phase error from 90° as a function of normalized signal frequency Ω_m with filter bandwidth = 1, for various values of normalized carrier frequency Ω_o. The filter attenuation characteristic is assumed to be α (nepers) $= 2\cosh^{-1}\Omega$. These are maximum errors for $\varphi_3 = \pi/4$, the output amplitudes being equal.

characteristic usually drops off as the frequency moves away from the edge of the pass-band unless a rejection frequency is included. In practice, the performance of the phase shifter would be far better than that suggested by the curves where a simple single-section filter has been assumed in the calculation.

Positioning the carrier frequency on the flank of the filter curve although increasing the relative attenuation between the sidebands also decreases the absolute value of the desired sideband for small modulation frequencies. An equalizer network may be introduced before the phase shifter, without affecting its performance otherwise, provided it does not become overloaded. The use of balanced modulators is preferable since although the carrier should only contribute

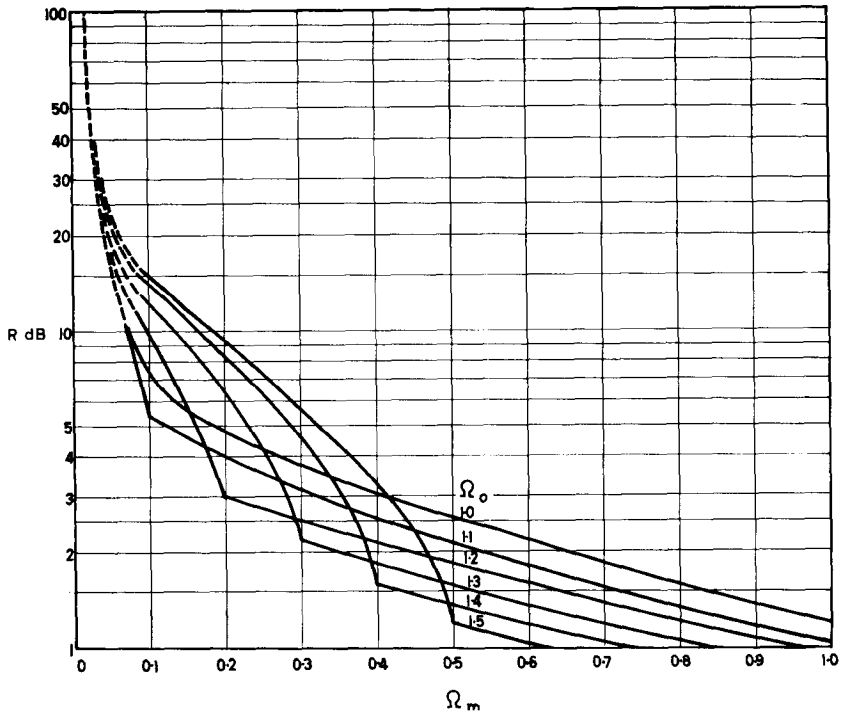

FIG. 3.11. Showing the phase shifter output voltage ratio R as a function of normalized signal frequency Ω_m with filter bandwidth = 1, for various values of normalized carrier frequency Ω_o. The filter attenuation characteristic is assumed to be α (nepers) = 2 $\cosh^{-1} \Omega$. These are maximum values for R with $\varphi_3 = 0$, the phase shift being exactly $\pi/2$.

DC in the output it may also affect the signal output phase if its amplitude is large.

In addition to the use to which this phase shifter is put to in this work, it should find numerous other applications, particularly as it can be made to produce any number of outputs at any desired phase. One case would be that of a wideband single-phase to poly-phase converter. Here, φ_3 could be so chosen that the phases are always correct, down to the lowest frequencies, while the amplitude variation could be eliminated by sufficient amplification followed by limiting. Controlled rectifiers could thus be driven to produce power. In the case of an almost constant frequency no bandpass filter need be used, as a null network could be employed to reject the single side-frequency. Such a single-phase to poly-phase converter would be extremely simple.

It should be noted that the principle of demodulating a voltage by using two phases of another voltage is not new and has been used, for instance, in a well-known method for regulating the centre frequency of a frequency-modulated transmitter using a motor with a two-phase stator to rotate the tuning capacitor (28). This arrangement does not shift the phase of a given signal but provides an output at the difference frequency of two inputs. In the phase shifter described here, the output frequency is always equal to the input frequency exactly.

CHAPTER 4

PRACTICAL WORK AND MEASUREMENTS

4.1. Transmitter

The transmitter circuit is shown in Fig. 4.1. As described in Section 3.1 it consists of two balanced modulators whose outputs are added together. The audio signal and RF voltages are applied to the modulators with 90° phase shifts. The audio signals to each sideband are combined in adding circuits preceding the modulators.

Ring or Cowan modulators are often used as balanced modulators, but use has been made here of the new deflection tube Type 7360. This possesses the advantages of not requiring symmetrical signal sources and of providing some gain. The manufacturer's figure for carrier suppression is 60 dB. The RF voltage is applied to the first grid while the audio signal voltage is between one deflecting electrode and earth. The tube is balanced by altering the DC voltage of one electrode relative to the other. The voltage dividers from which these potentials are derived should have approximately the same internal resistance since this reduces the effect of supply voltage variations. The 12 KΩ resistor common to both circuits is also helpful in this respect. Such a balanced modulator would normally work into either a filter selecting one sideband or into a tuned RF transformer for double sideband suppressed carrier generation. In that form it represents a very simple and effective transmitter for the communication system forming the subject of this work. Since currents to both anodes are derived from a common electron beam, the arrangement possesses inherent symmetry. In the experimental transmitter the outputs of two such modulators must be added together and an asymmetrical output is required. The transformer used for this purpose must be quite

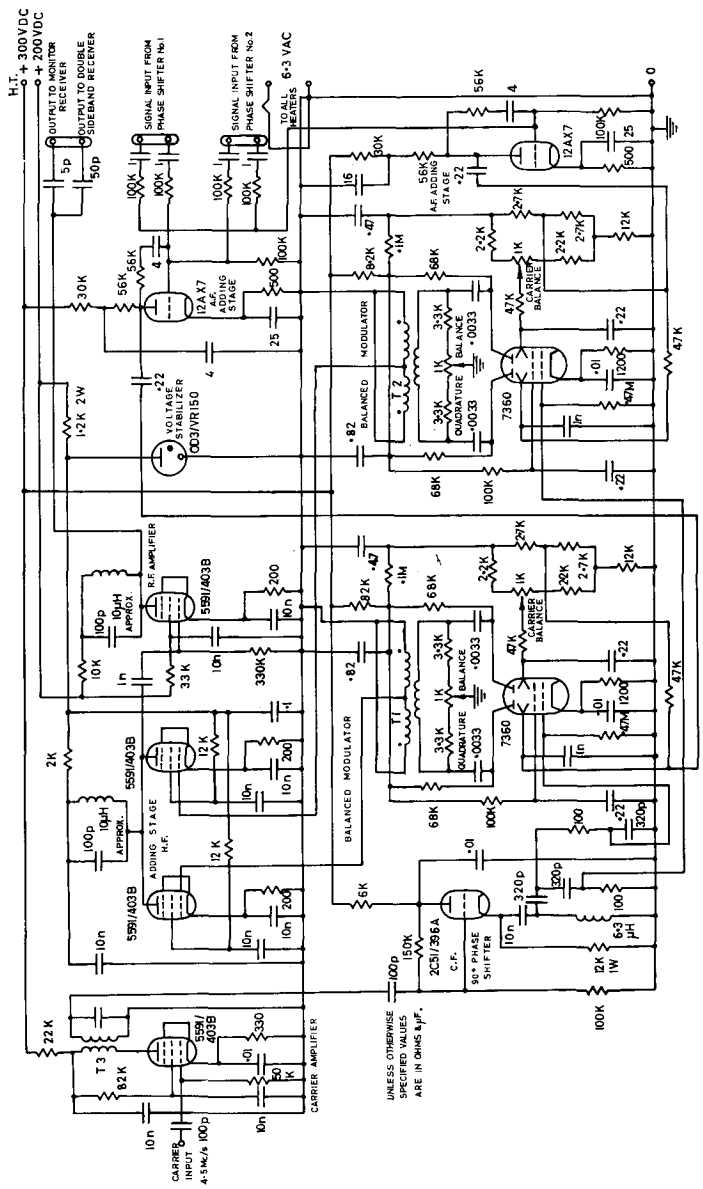

FIG. 4.1. Circuit diagram of the independent sideband transmitter.

symmetrical with respect to stray capacitive coupling. Suitable toroidally-wound transformers were made using ferrite rings. An excellent material is available in the form of tubes for antennas. Rings were sliced off and polished to form cores about 10 mm across. The secondary is in two oppositely wound halves with the outsides earthed (since these are closest to the symmetrical primary). Using such a transformer it was just possible to attain 60 dB carrier suppression, although the balance point is dependent on the audio input level and about 40 dB is nearer the figure that can be expected in practice. The sideband and carrier levels were measured using a *Collins* communications receiver with S-meter previously calibrated in terms of input voltage.

The outputs from the modulators are then applied to the adding stage. This consists of two pentodes with a common load, consisting of a broadly tuned circuit. The combined signal is then amplified and coupled to the receiver. A loose coupling is provided to the monitoring receiver. Correct cancellation naturally depends on the gains of the two halves of the adding stage remaining equal, and in order to help ensure this the high tension supply is stabilized. This section of the transmitter is very carefully screened.

The RF voltage from the *General Radio* signal generator is first amplified and then applied to a cathode follower stage with a phase shifting network as a load. The accuracy of the phase shift depends on the elements having pure reactances and resistances. It is therefore an advantage to work at a low impedance level. This is done here and the impedance at the network terminals is 100 ohms.

This is not a suitable value for the cathode follower load and is hence transformed to 400 ohms resistive by a resonance impedance transformation. At first, another type of phase shifter was used, consisting of a 20 μH inductance in parallel with a 5 K Ω variable resistor, both in series with a 100 pF capacitor. This is perfectly effective but requires careful adjustment every time the frequency is altered. The present arrangement is more broad-band.

The audio inputs to the two sidebands must be added together and a feedback adding arrangement is used. It can be shown easily that this causes the input resistance to become very low and at the same time, the gain is stabilized. This is particularly important here, since

sideband cancellation depends on the levels being accurately maintained.

The voltage input to the modulator is of the order of a few volts, and considerable trouble was experienced with shielding. Eventually the transmitter was dismantled and rebuilt on two separate screened chassis. The smaller chassis contains the adding stage, amplifier and voltage stabilizer. Even so, the 60 dB carrier suppression quoted was not achieved with both modulators and 40 dB is the approximate value. The procedure is to turn each modulator on in turn and adjust the carrier to minimum. The value of the adjustment potentiometers was progressively reduced and fixed resistors were added until a fine adjustment control resulted. With both modulators on, the voltages change a little and the minimum must be re-adjusted, using all four controls. Modulating signal is then supplied from one phase shifter and using the amplitude and phase controls on the phase shifter, one sideband is cancelled out. As monitored on the *Collins* receiver, unwanted sideband cancellation was 30 dB below the desired sideband. The procedure is then repeated with the other phase shifter. One phase shifter is then supplied directly from the signal source, the other through a calibrated attenuator, which then reads the attenuation of one sideband directly.

The deflection tubes were fairly stable after a warm-up period of an hour or so, though trouble was experienced due to stray magnetic fields from the mechanical filter biasing magnets. This also occurred with the phase shifter modulators and was eliminated by the use of *mu-metal* tube shields.

4.1.1. Phase Shifters

The diagram of Fig. 4.2 shows the circuit of the phase shifters. Two such identical units were made. The signal is applied to the deflecting electrode of a Type 7360 beam deflection tube, the same type as that used in the transmitter. The auxiliary carrier of about 100 Kc/s is suppressed and the two resulting sidebands appear at the secondary of the symmetric to asymmetric transformer. As in the case of the transmitter, this is also toroidally wound on a ring core of *Ferroxcube*. Although direct coupling is no problem at 100 Kc/s, capacitive cou-

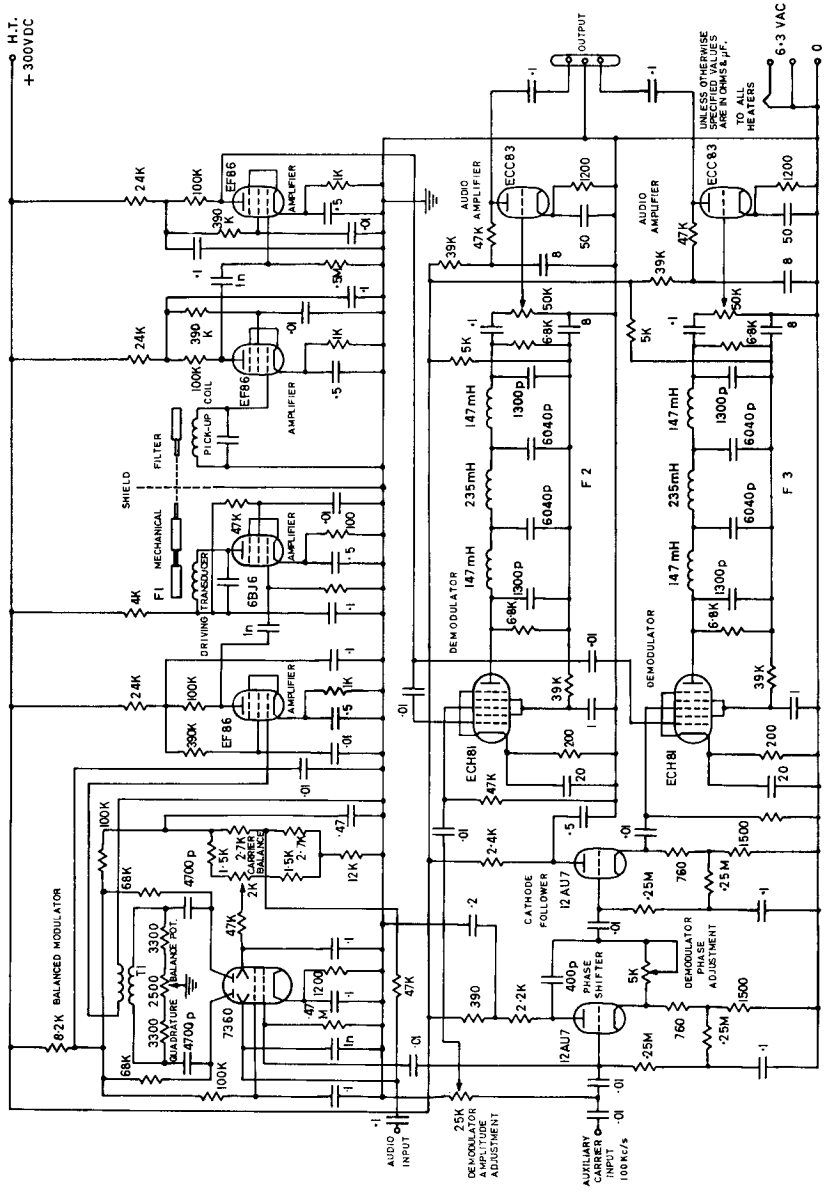

FIG. 4.2. Circuit diagram of one of the two identical phase shifters.

pling with the core was sufficient to make balance impossible. Earthing the core and the use of a carefully designed shield remedied this. Although the two controls provide a carrier balance and a gain balance, it is not possible to match the higher derivatives of the characteristic curves of the two halves of the system. There is thus a small harmonic component in the output.
Considering the modulator output, if

$$v_1 \cos \omega_0 t + v_2 \cos (\omega_0 \pm \omega_m) t + v_3 \cos (\omega_0 \pm 2\,\omega_m) t$$

represents the (small) carrier and the two sidebands with their harmonic components, and if the filter selects the upper sideband we get

$$v'_1 \cos \omega_0 t + v'_2 \cos (\omega_0 + \omega_m) t + v'_3 \cos (\omega_0 + 2\,\omega_m) t$$

This consists of a carrier of angular frequency $(\omega_0 + \omega_m)$ and two sidebands. Since the carrier balance point varies somewhat with the modulating voltage, unbalance occurs during the modulation cycle and some carrier is always present. As a result of this effect, the upper sideband selected by the mechanical filter consists of the desired wave modulated to a small depth by the sidebands mentioned. The effect of this is that the second harmonic distortion is carried through to the output while the carrier contributes a DC component.

After suitable amplification the signal is applied to the mechanical filter, with the carrier frequency positioned on a flank of the attenuation curve. The amplitude of the input to the filter must be restricted so that the transducer is not driven into a curved part of the characteristic and so produce further harmonic distortion. Further amplification is required after the filter and the signal is thereafter applied to the first grids of two heptode mixers. These are used as demodulators and are supplied with the carrier frequency in quadrature to each other. Of the resulting combinations, the signals are selected by maximally flat low-pass filters and after amplification represent the output. Apart from the small errors due to non-ideal band-pass filters (Figs. 3.10, 3.11) any other variations can only occur from dissimilarity after the demodulators. Care must be taken to make the circuits and low-pass filters as nearly identical as possible.

The carrier voltages for the demodulators are derived from the input in one case and through a phase shifter in the other. This consists of a phase splitter with equal anode and cathode resistors feeding an RC circuit. It can easily be seen that this arrangement provides a voltage of constant magnitude and variable phase.

The phase shifters have a useful frequency range of from about 300 c/s to 7 Kc/s which could be extended by using other filters.

4.1.1.1. Mechanical Filters

The phase shifter used here requires a bandpass filter with similar characteristics to the filters used for single sideband selection. As shown in the section on the transmitter, the rejection of the undesired sideband will be approximately proportional to the filter attenuation. By positioning the phase shifter carrier on the flank of the filter curve, just far enough from the edge of the passband so that the lowest desired frequency is just in the passband, we obtain a flat response for the desired range. It was decided to design for a passband of from 300 c/s to 7 Kc/s in this particular case, and to aim for a rejection of at least 30 dB unwanted sideband rejection at 300 c/s. There would then be about 20 dB rejection at 200 c/s. Naturally, the rejection at higher frequencies would be better. As has been mentioned already, filters used for single sideband afford some guidance as to what can be done. Formerly, crystal filters were used almost exclusively, while more recently mechanical filters and inductor-capacitor filters of improved Q have been used. If we arbitrarily specify the permissible ripple in the passband at 1 dB for a bandwidth of 7 Kc/s at 100 Kc/s, we obtain using the procedure of Dishal * (18) a filter of 8 stages and a minimum required Q of about 1000 for sufficient steepness. This is somewhat beyond the limit of inductor-capacitor filters.

There remains the choice between mechanical and crystal filters. While satisfactory crystal filters could no doubt have been designed, the quartz crystals would have had to be ground to specification by a specialist concern. Since only two filters were to be made, this would not have been a practical solution. It was felt instead that the work

* see Appendix 2

should be capable of being carried out by the Institute's workshop, especially since there was bound to be a certain amount of experimenting. For these reasons and for the interest afforded by the subject, it was decided to construct mechanical filters.

We shall therefore first review and summarize some of the available literature on the subject here for convenience. The basic types of mechanical filter sections have been treated extensively in the literature. Since electrical filters and circuits have been analysed in great detail, it is natural that the subject of mechanical filters should mainly have been considered in terms of electrical equivalents. The basic filter section shown in Fig. 4.3 has been considered by Mason (19) and Roberts and Burns (20). We shall outline these results. A cylindrical rod transmitting waves in torsion or a thin cylindrical rod carrying compression waves is equivalent to a section of transmission line. Consider the sections of line shown in Fig. 4.3, of electrical lengths θ_1, θ_2 and impedances Z_1 and Z_2.

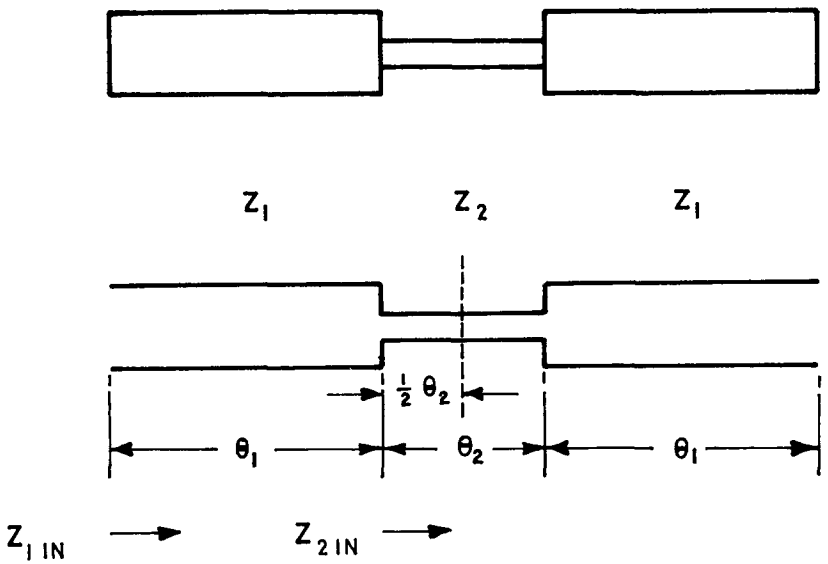

FIG. 4.3. Showing basic mechanical filter section and electrical transmission line equivalent (20).

If we open the section at its centre, we have

$$Z_{2in} = \frac{Z_2}{j \tan \frac{\theta_2}{2}}$$

therefore, $$Z_{1in} = Z_1 \cdot \frac{Z_2 - Z_1 \tan \theta_1 \tan \frac{\theta_2}{2}}{j\left(Z_1 \tan \frac{\theta_2}{2} + Z_2 \tan \theta_1\right)}$$

For a short-circuit at the centre, we have similarly,

$$Z'_{1in} = j Z_1^2 \cdot \frac{Z_2 \tan \frac{\theta_2}{2} + Z_1 \tan \theta_1}{Z_1 - Z_2 \tan \frac{\theta_2}{2} \tan \theta_1}$$

The product of these expressions is the iterative impedance squared,

$$Z_0^2 = Z_1^2 \cdot \frac{\varphi^2 \tan \frac{\theta_2}{2} - \varphi \tan^2 \frac{\theta_2}{2} \tan \theta_1 + \varphi \tan \theta_1 - \tan^2 \theta_1 \tan \frac{\theta_2}{2}}{\tan \frac{\theta_2}{2} + \varphi \tan \theta_1 - \varphi \tan^2 \frac{\theta_2}{2} \tan \theta_1 - \varphi^2 \tan^2 \theta_1 \tan \frac{\theta_2}{2}}$$

$$= \frac{Z_1^2}{\varphi^2} \cdot \frac{\varphi^2 + 2\varphi \tan \theta_1 \cot \theta_2 - \tan^2 \theta_1}{\frac{1}{\varphi^2} + \frac{2}{\varphi} \cdot \tan \theta_1 \cot \theta_2 - \tan^2 \theta_1}$$

where $$\varphi = \frac{Z_2}{Z_1}$$

When Z_0 has a real component, power can be accepted from the source, that is, there is a passband. The limits of the ranges of θ_1 which make Z_0^2 positive are given by numerator and denominator roots, which occur in closely-spaced pairs when φ is very small or very large.

For instance, for $\theta_2 = \theta_1$ and large φ

we have $\tan^2 \theta_1 = 2\varphi + \varphi^2$

from which $\tan \theta \approx \pm (\varphi + 1)$

and $$\tan(\theta' - \theta'') = \frac{2}{\varphi} \cdot \frac{(\varphi + 1)}{(\varphi + 2)}$$
$$\approx \frac{2}{\varphi}\left(1 - \frac{1}{\varphi}\right)$$

Similarly, Roberts and Burns have tabulated a useful list of bandwidths for various practical combinations. They also discuss expedients for producing very narrow bands, which do not, however, concern this work. Another approach, based on the impedance transforming properties of quarter-wave lines, was used for one experimental filter. This has already been treated extensively in the literature on microwave filters, and Struszynski (21) has treated the case of torsional filters.We shall outline these results here for convenience, with reference to longitudinal filters. A factor must be introduced relating change of length to electrical charge in order to take care of the dimensions at the transducer. Since the electromechanical coupling is very small and the terminations are wholly mechanical resistances, we do not need to know the magnitude of this coupling coefficient. The mechanical resonators can again be considered as equivalent to lengths of electrical transmission line. We shall consider a filter composed of halfwave resonators (or slugs) connected by quarter-wave necks.

The slugs can be considered as a four-terminal equivalent as shown in Fig. 4.4. To a first approximation, however, the parallel resonant circuits can be omitted since they present an open circuit at resonance, and off-resonance are shunted by the high capacitance (compliance) of the thin necks. Thus the filter appears as shown in Fig. 4.5.

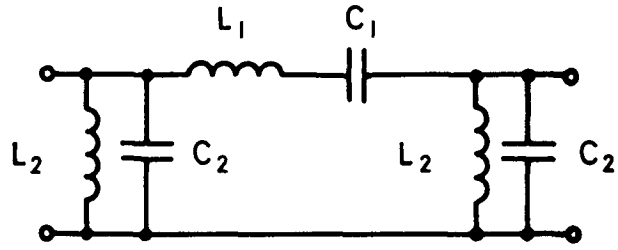

FIG. 4.4. Showing lumped-element equivalent circuit for mechanical resonator.

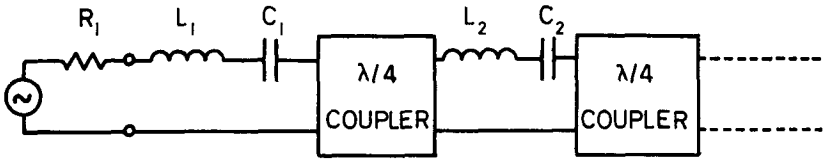

FIG. 4.5. Filter equivalent circuit.

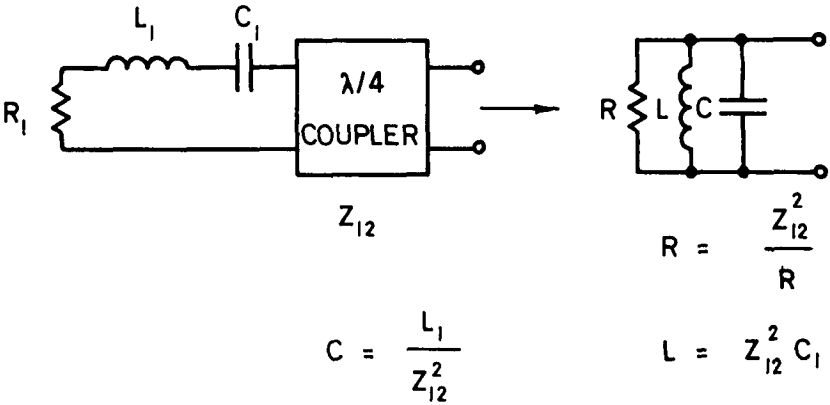

FIG. 4.6. First step in the transformation by the quarter-wave inverter.

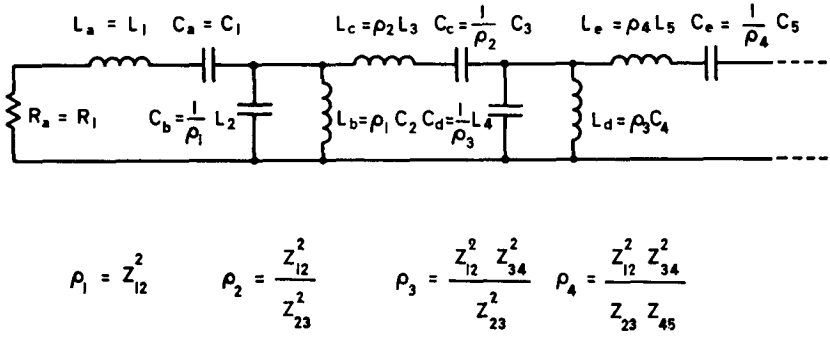

FIG. 4.7. Equivalent bandpass circuit. In practice since all resonators were made alike $L_1 = L_2 =$ etc. and $C_1 = C_2 =$ etc.

The quarter-wave lines have well-known inverter properties

$$Z_{in} = Z_0^2 \, Y_{load}$$

and $$Y_{in} = Z_{load} / Z_0^2$$

where Z_0 is the characteristic impedance.

Thus a shunt capacitance appears through the quarter-wave inverter as a series inductance of value $L = Z_0^2 C$ and a series inductance appears as a shunt capacitance $C = L/Z_0^2$.
Fig. 4.6 shows the first step in the transformation. When seen through the next inverter, the new parallel resonant circuit becomes again a series circuit and the series circuit L_2 C_2 is transformed to a parallel one. Carrying through this transformation step by step, the whole filter can then be represented as a bandpass equivalent circuit (Fig. 4.7) where the first circuit elements R_1, C_1, L_1 are again obtained by dividing inductance and resistance values and multiplying capacitance values by the transformation coefficient of R_1. This bandpass filter can be derived from a lowpass prototype, whose elements may be obtained from known formulae in the literature (22, 23). For an odd number of elements (symmetrical filter) this low-pass prototype is for unity cut-off frequency and terminating resistances.

Thus each inductance in the prototype low-pass filter must be multiplied by

$$\frac{R_1}{\omega_2 - \omega_1}$$

and each capacitance must be divided by $R_1 (\omega_2 - \omega_1)$, where R_1 is the actual terminating resistance and ω_2, ω_1 the pass-band limits. The inductances are then series-resonated with capacitances to the centre frequency $\omega_0 = \sqrt{\omega_1 \omega_2}$ and the capacitances are likewise parallel-resonated to ω_0 to give the band-pass circuit of Fig. 4.7. The values can then be expressed as

$$L_a = L_1 = \frac{R_1 f_1}{\omega_2 - \omega_1} \qquad C_a = C_1 = \frac{\omega_2 - \omega_1}{R_1 \omega_0^2 f_1}$$

$$L_b = \varrho_1 C_2 = \frac{R_1 (\omega_2 - \omega_1)}{\omega_0^2 f_2} \qquad C_b = \frac{1}{\varrho_1} \cdot L_2 = \frac{f_2}{R_1 (\omega_2 - \omega_1)}$$

$$L_c = \varrho_2 L_3 = \frac{R_1 f_3}{\omega_2 - \omega_1} \qquad C_c = \frac{1}{\varrho_2} \cdot C_3 = \frac{\omega_2 - \omega_1}{R_1 \omega_o^2 f_3}$$

where $f_1, f_2,$ refer to the prototype elements, and C_1, L_1 refer to the resonator equivalent circuit, Fig. 4.4. For ϱ_1, ϱ_2, etc., see Fig. 4.7.
It is more convenient for construction to make all the resonators alike, thus

$$L_1 = L_2 = \ldots\ldots = L$$
$$C_1 = C_2 = \ldots\ldots = C$$

Since $$LC = \frac{1}{\omega_o^2}$$

$$\varrho_1 = R_1^2 \frac{f_1}{f_2}$$

$$\varrho_2 = \frac{f_3}{f_1}, \text{ etc.}$$

Since ϱ_1, ϱ_2, are defined in terms of the coupler impedances (Fig. 4.7),

$$Z_{12} = \frac{f_1}{\sqrt{f_1 f_2}} \cdot R_1$$

$$Z_{23} = \frac{f_1}{\sqrt{f_2 f_3}} \cdot R_1, \text{ etc.}$$

As the characteristic impedance of the resonators is

$$Z_o = \frac{2}{\pi} \sqrt{\frac{L}{C}} = \frac{2}{\pi} \cdot \frac{\omega_o R_1 f_1}{(\omega_2 - \omega_1)}$$

we can relate the coupler impedances to the resonator impedance, or since the impedance varies as the square of the diameter, we have the coupler diameters in terms of the resonator diameters.

If
Z_{IC} = Intrinsic Impedance of coupler material
Z_{IR} = Intrinsic Impedance of resonator material
D_{cnm} = Coupler diameter between resonators m and n
D_R = Resonator diameter,

then $$D_{c12} = \left(\frac{Z_{IR}}{Z_{IC}} \cdot \frac{\pi}{2} \cdot \frac{\omega_2 - \omega_1}{\omega_0} \cdot \frac{1}{\sqrt{f_1 f_2}}\right)^{1/2} \cdot D_R$$

$$D_{c23} = \left(\frac{Z_{IR}}{Z_{IC}} \cdot \frac{\pi}{2} \cdot \frac{\omega_2 - \omega_1}{\omega_0} \cdot \frac{1}{\sqrt{f_2 f_3}}\right)^{1/2} \cdot D_R \quad \text{etc.}$$

The choice of the longitudinal mode to the torsional is based on various reasons. Where narrow bands are desired, the ratio of resonator to coupler diameters becomes large. (For longitudinal filters, the percentage bandwidth is roughly equal to the ratio of coupler to resonator cross-sectional areas.) There is an upper limit to resonator diameter before undesired modes become disturbing. As there is also a lower practical limit to the coupler diameter the torsional mode is the more advantageous since the characteristic impedance varies as the fourth power of the diameter, compared with the square in the case of longitudinal vibrations. In this case, however, we are concerned with a fairly broad band and in any case, the operating frequency given by the phase shifter auxiliary carrier can be freely chosen, permitting the percentage bandwidth to be increased by lowering the frequency to the limit where the filter becomes too flimsy. As the velocity of propagation for the torsional mode is about $^2/_3$ that for the longitudinal mode, the torsional filter is the shorter. This length is not a drawback in an experimental set-up. The electro-mechanical transducer is also simpler in the longitudinal filter. It is more difficult to achieve the required symmetry in order that undesired modes (e.g. transverse shear) should not be excited in torsional transducers. A further important point is the question of tolerances, which are twice as small in torsional as in longitudinal filters.

Using certain ferrites, it is possible to obtain a sufficiently tight electro-mechanical coupling so that the filter may be terminated in an electrical resistance. Since only two filters were required, a simpler direct magneto-strictive excitation was used in conjunction with a mechanical termination.

In order to undertake measurements of the resonant frequencies of resonators and couplers, a bridge was constructed as shown in Fig. 4.8. The absolute accuracy of resonance determination was within about 50 c/s. When comparing resonators, however, the comparative accuracy was within a few cycles. The bridge is first balanced at the

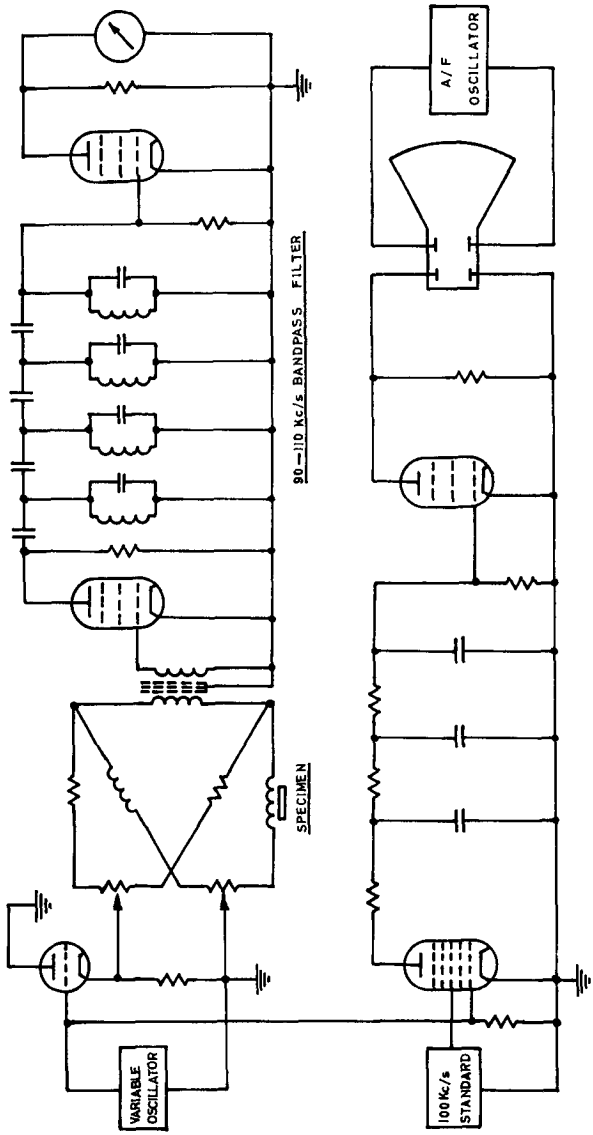

FIG. 4.8. Basic circuit diagram of the bridge constructed for determining the resonant frequencies of mechanical resonators. When the specimen resonates, more energy is absorbed and the impedance of the corresponding bridge arm is altered. The maximally-flat bandpass filter removes harmonics which otherwise make balance difficult.

approximate frequency of resonance. A slight unbalance is then caused by introducing additional resistance in the arm containing the test coil. At the resonant frequency, the increased loss in this arm increases the unbalance output voltage. A smaller coil is used for the thinner couplers. In order to measure the resonant frequency of the individual resonators in a complete filter, the two adjacent resonators must be firmly clamped, corresponding to an electrical open circuit. This is best thought of in this way: if the two adjacent resonators are perfectly clamped, then at the resonant frequency, the two quarter-wave couplers will transform this condition so that the test resonator will be free to oscillate. The design of suitable clamps was only achieved after some experiments. The clamp should apply a large force symmetrically on as much of the resonator face as possible while not in any way touching the quarter-wave couplers. It should preferably be non-magnetic and must be capable of being fitted to the completed filter without damaging the finely finished surfaces. To obtain good contact with the filter surfaces, lead washers were at first used. These, with a Q of 40, and deforming readily to form close contact would be very suitable if the lead did not flow out from under the washers and touch the couplers. Washers of a suitable plastic material were finally used, with a force of about 250 Kg (550 lb.).Great care must be excercised in fitting and removing clamps (Figs. 4.9 and 4.10).

A jig was constructed on which the terminations were fitted as straight lengths of wire. This method permits a more rapid interchanging of wires of different diameters. The rubber latex coatings necessary for damping were then applied with a brush.

The first filter made consisted of separate resonators and couplers. It was found that the resonant frequency of a resonator depends on the diameter. This is probably due to a departure of the propagation from purely longitudinal and to the coupling of energy to other modes as their frequencies approach the longitudinal resonance. Fig. 4.11 shows the variation of length required to resonate at a certain frequency as a function of diameter. The couplers were a push fit in the resonators, to which they were silver soldered in a high-frequency induction furnace. This filter was not a success owing to the bandwidth being too large for the termination to be correct over a sufficient portion of the band and probably also due to changes in the properties of the *Invar*

steel (36% Ni 64% Fe) used. Several other filters for the same bandwidth (10 Kc/s at 104 Kc/s) were made in one piece. The resonators were individually tuned using the clamps, but there was no way of checking the couplers. The precise resonant frequency of these should

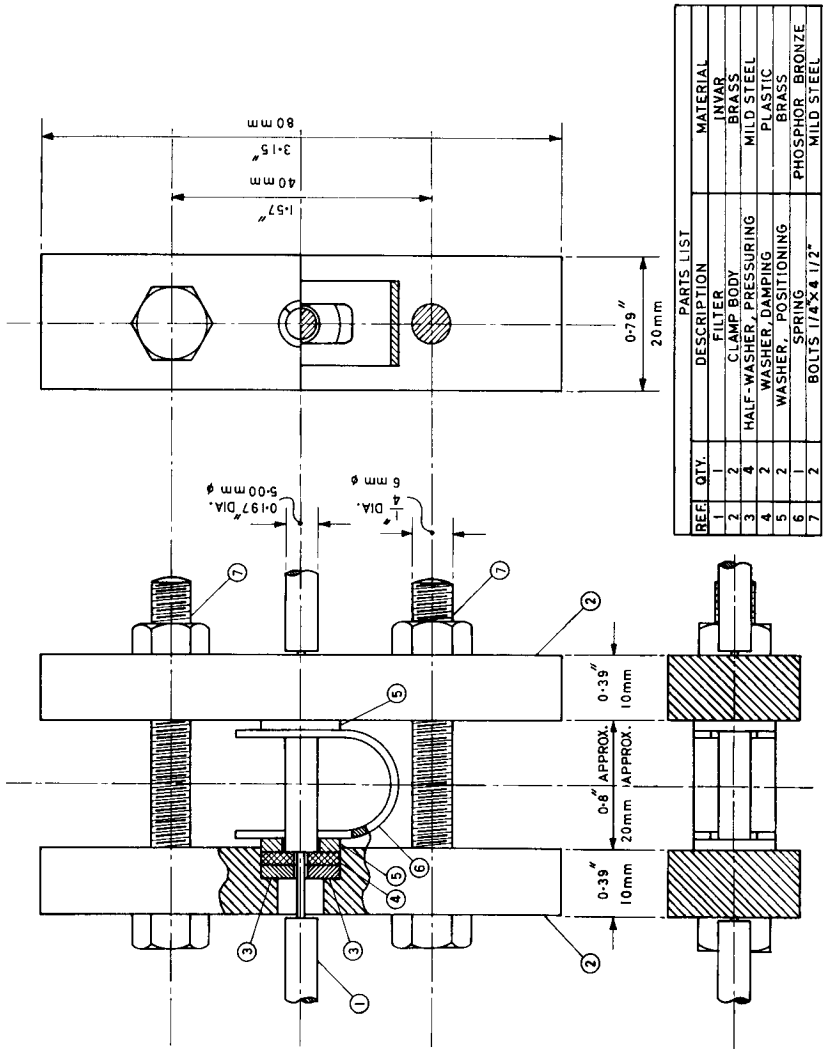

FIG. 4.9. Showing the clamp developed for use in measuring assembled filter elements. Two such clamps were used simultaneously.

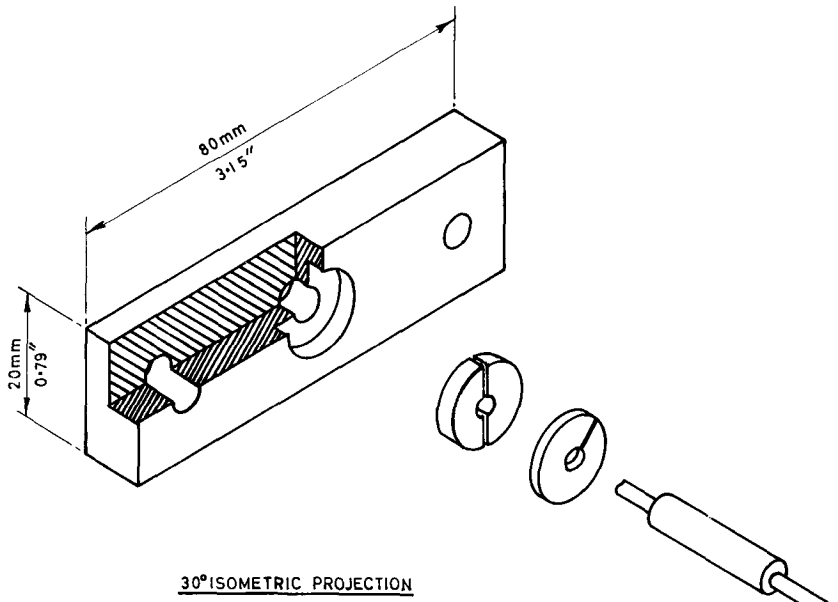

FIG. 4.10. Isometric sketch of the clamp depicted in Fig. 4.9.

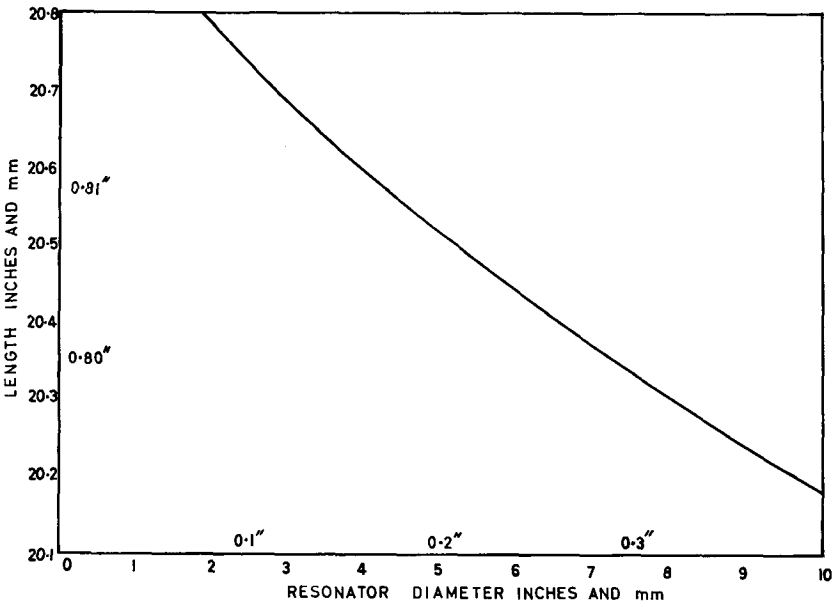

FIG. 4.11. Showing measured length of *Invar* cylinder which was required for resonance at 105 Kc/s as a function of the diameter.

not have been very critical, however. The terminations used consisted of about 2 meters of copper wire wound as a spiral with three coats of latex rubber. Coils at each end provided coupling and small permanent magnets were used to provide bias to bring the operating point to a steeper part of the magnetostriction characteristic (Fig. 4.12). Two magnets symmetrically placed were used so as to minimize the resultant force tending to press the resonator against the coil former, which

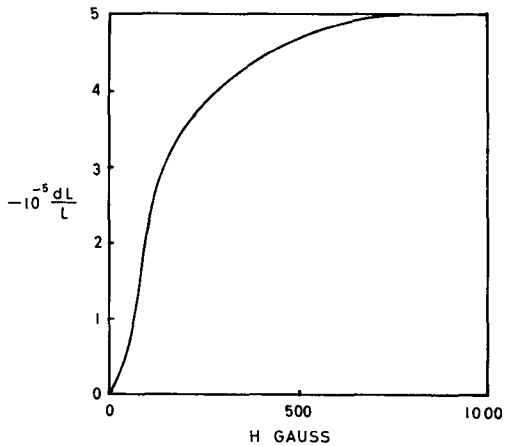

FIG. 4.12. Showing change in length due to magnetostriction (nickel).

was made of *Teflon* for low friction. A typical unsatisfactory curve for the fourth filter made is shown in Fig. 4.13 giving magnitude of the characteristic. Note that the dotted part of the curve was the original which included the masking effect of direct magnetic coupling with the filter acting as a common core to the end coils. A small coil, connected in opposition in series with the driving coil was then fitted round the filter and its position adjusted for the greatest cancellation outside the band. An improvement of about 7 dB may be noted.

The next filter, No. 5, also in one piece and of eight sections was designed for 6·5 Kc/s bandwith at 104 Kc/s. Though the results (Fig. 4.14) were in many respects better, the two sharp dips in the pass-band are too deep to be acceptable. Small sharp pips on the upper frequency flank were got rid of by very careful re-tuning of the resonators. It was found that the two pass-band dips could be made to

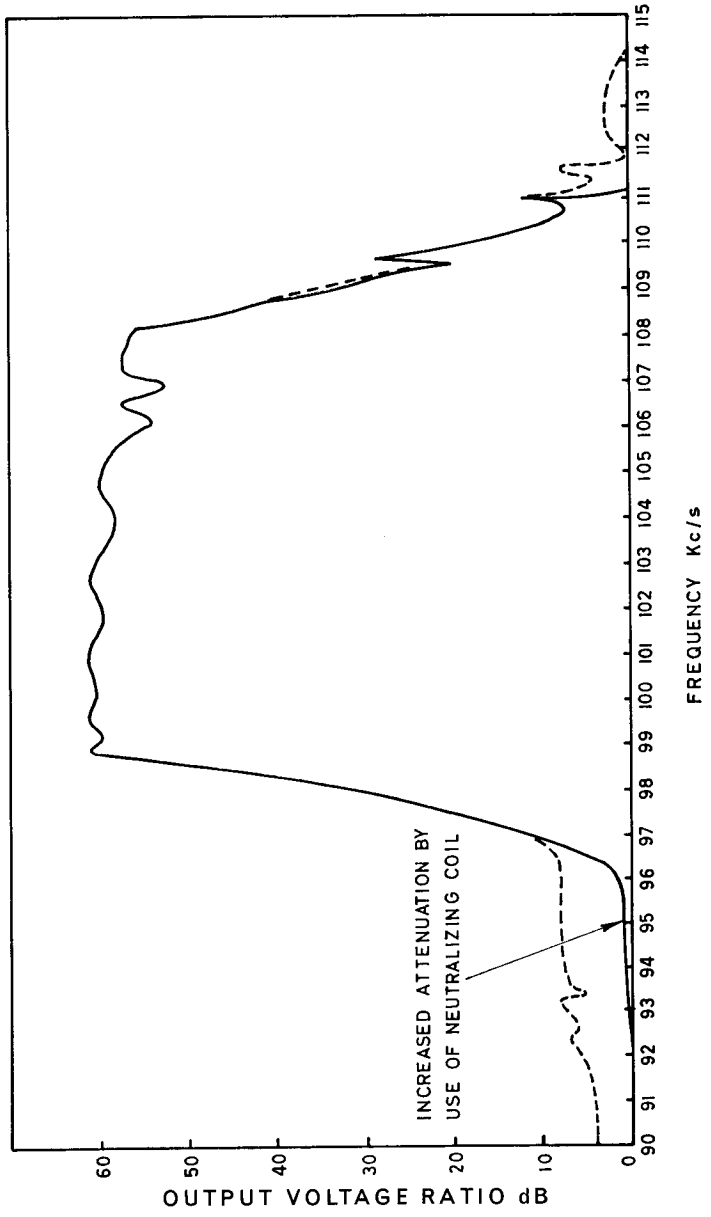

FIG. 4.13. Showing response curve for Filter No. 4.

disappear if a small amount of rubber was painted onto resonators 2, 3, 6 and 7.

This was not regarded as a suitable result and as a further try, the length to diameter ratio was altered. Experiment indicated, as may be expected, that this ratio should be greater. A new filter with the same pass-band was dimensioned for thinner resonators and couplers. Attempts to turn this in one piece were altogether unsuccessful, the filter always fracturing after some resonators had been completed. It was then decided to try a new method of construction. The filter would be made in separate parts as for the very first case, but the couplers would be made to fit very precisely into holes reamed in the resonators. In order to check the coupling provided by the method, two test resonators were made to the highest accuracy available. One was turned in one piece together with two half-wave rods on either side, of the same

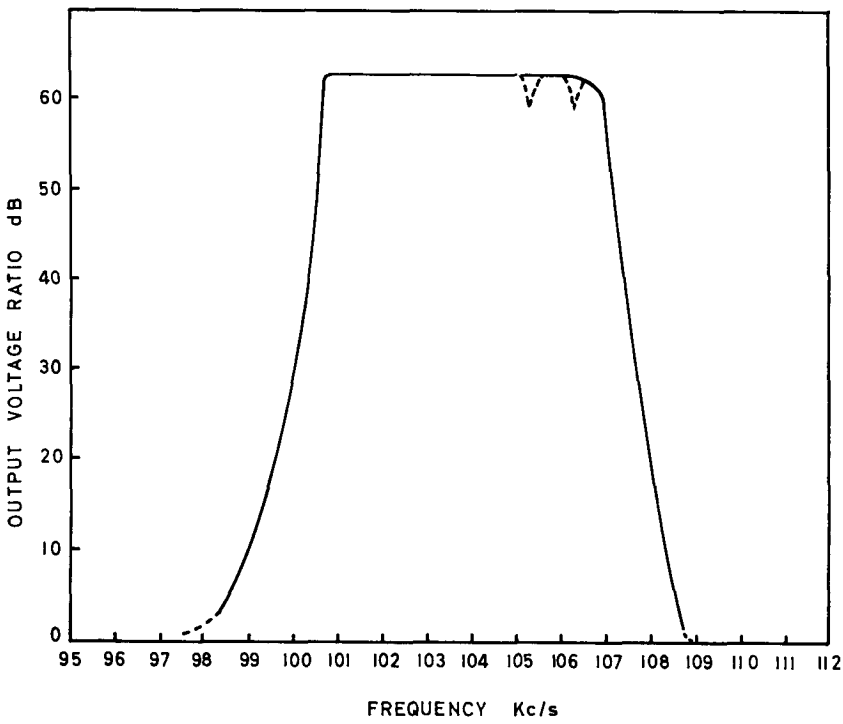

FIG. 4.14. Showing response curve for Filter No. 5.

diameter as the couplers to be used. The other resonator had holes, into which were pressed similar rods of coupler diameter. These were then accurately trimmed off to be a half wavelength long. Thus the same free condition existed at the resonator face as at the ends of the half-wave rods. When measured, the element with the pressed-in parts resonated at 100 c/s higher than the other. This is logical since there is bound to be a small air-gap with material missing at motional loops and there are no rounded fillets. Then the lengths of coupler were turned off in both cases, flush with the resonator face. When measured the resonators exhibited almost the same resonant frequency difference, providing a check in case the half-wave elements had been dissimilar. A repetition of this experiment was performed and gave almost identical results. With respect to the end resonators, a check was made between a solid part and another with two holes, one filled with *Invar* and one with copper, both turned flush with the resonator face. Again, an increase of 100 c/s was noted. Bearing this expected difference in mind, 9 resonators were accurately machined and tuned to 100 c/s lower than desired. The filter was then concentrically assembled. The terminations used were particularly neat and compact, consisting of copper wire spirals encapsulated in rubber in flat aluminium dishes. The filter did not give satisfactory results until the copper wire terminations were soft-soldered on. It would appear that a suitable dry fit cannot be achieved with copper, which is too soft. The response curve of this 9-element filter is shown in Fig. 4.15 while Fig. 4.16 shows the effect of variation of the termination impedance. Since the limitations imposed by turning a long thin structure were removed, it was possible to add another section. A great advantage of this method (apart from the fact that turning was not possible anyway) is that if a mistake were to occur in turning, the whole filter is not rendered useless. Also, it results in a precisely known profile at the junction surface of coupler and resonator. When turning in one piece, a fillet however small is bound to occur and it is not possible to guarantee uniformity in this respect. It was found to be important that the bottom of the hole in the coupler should correspond closely to the shape at the end of the coupler.

All the filters up to and including No. 6 had identical elements, with end half sections. One filter, No. 7 was dimensioned to give a

Chebyshev response (22, 23) with 0·5 dB ripple in the pass-band. The coupler diameters are given in Table 1. In fact, the ripple varied from 1 to 2 dB. Consideration of the machining tolerances attainable on the lathe available shows this to be the most probable cause of the failure to realize the design values. The design did not give any better results than the simpler equal-element method and the production is more complicated particularly in obtaining very exact press fits for various odd diameters of couplers instead of for one size which can be chosen (within limits) to match available tools. For these reasons the filter type used for No. 6 was adopted as the final one. Two filters, as identical as possible were made, measured and assembled, Nos. 8 and 9. They were as identical as could be ascertained and have similar pass-band ripple to that of No. 6.

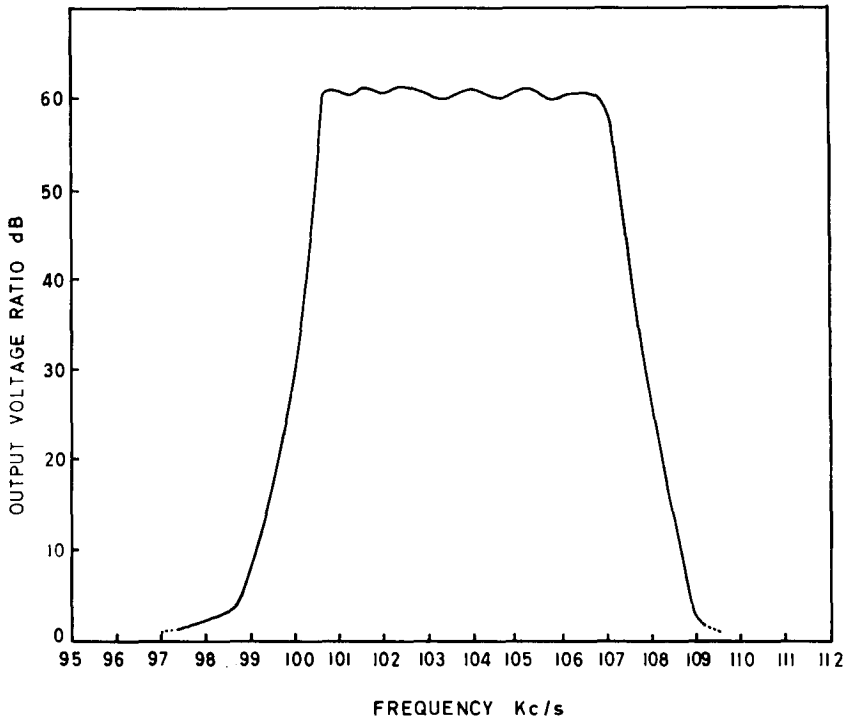

FIG. 4.15. Showing response curve for Filter No. 6.

Excessive ripple may be due to a variety of causes. Reflections from the ends of the lossy lines are unlikely to be one. For the lengths of line used, the frequencies for which an integral number of half waves occurs are spaced very closely to each other. In any case, the lines were extended to over 3 meters (10′) as a check and clamped progressively closer to the filter. Reflection effects appear for lines shorter than about 1·5 meters. The spiral form used is particularly suitable since it is very compact and the radius of curvature is greatest at the start, where reflections would be most objectionable. Other reasons for the ripples are probably insufficient tolerances on the neck diameters, and the possibility of mismatch, since the terminating lines were available in diameter steps of 0·05 mm (2 mils) or about 10% impedance steps. The tolerances on the larger diameter of the resonator are not so critical. The likelihood of this being so can be seen from the following figures

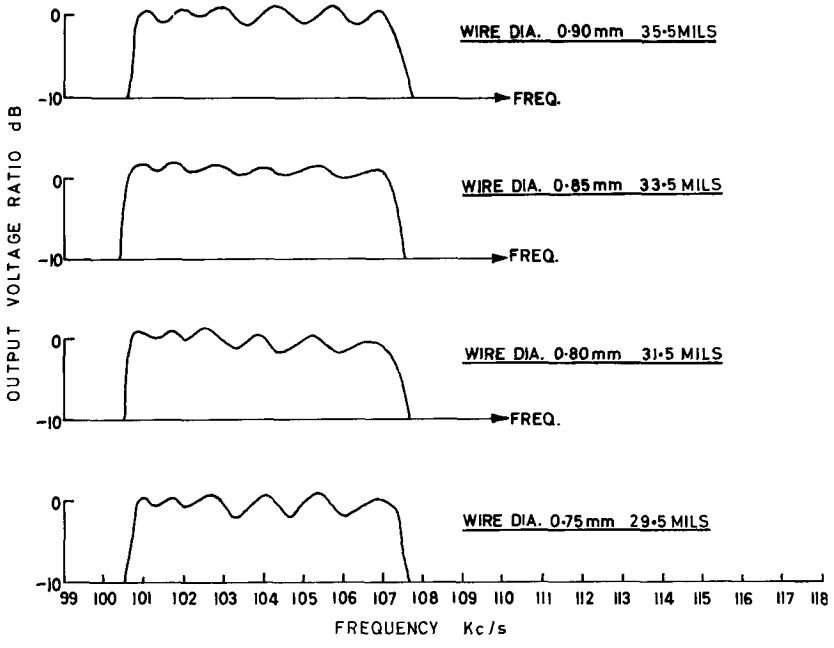

FIG. 4.16. Response curves for the pass-band of Filter No. 6 showing the effects of changing the diameter of the copper wire used in the terminations.

in Table 1. Both sets refer to otherwise identical filters, one with 0·5 dB ripples in the pass-band, the other with 2 dB ripples in the pass-band. The latter figure was the one obtained when a 0·5 dB design was constructed (Fig. 4.17).

D_{mn} denotes the diameter of the coupler between resonators m and n, in millimeters.

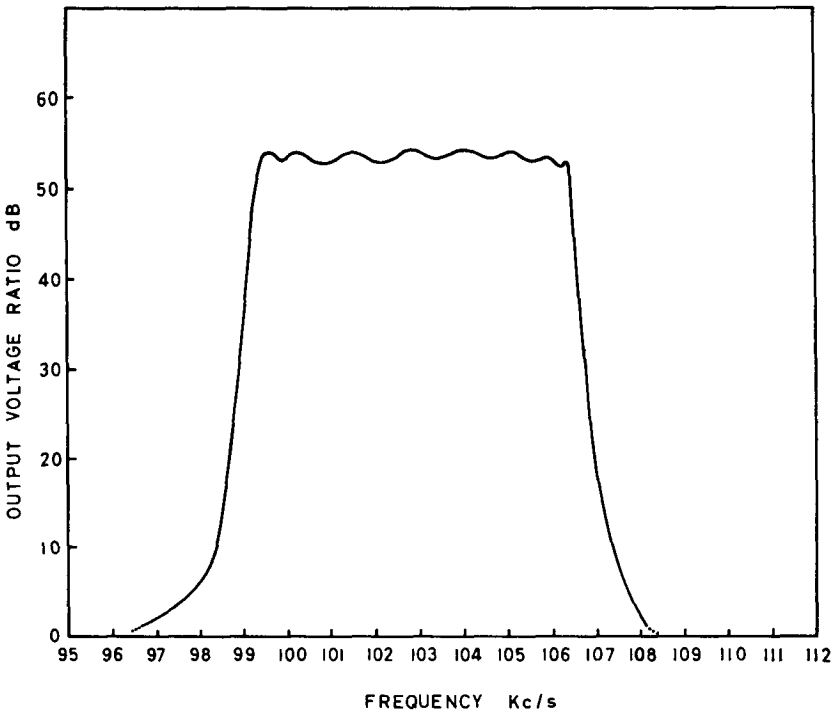

FIG. 4.17. Showing response curve for Filter No. 7.

TABLE 1

Coupler	for Ripple dB		Difference mm
	0·5	2·0	
D_{12}	1·295 mm	1·239 mm	0·056
D_{23}	1·166 mm	1·148 mm	0·018
D_{34}	1·143 mm	1·134 mm	0·009
D_{45}	1·137 mm	1·130 mm	0·007
⋮	⋮	⋮	⋮
D_{89}	1·295 mm	1·239 mm	0·056

Apart from the end couplers, the difference is of the order of a hundredth of a mm (0·0004″). The machining tolerances for the resonators are $\pm$ 0·005 mm, while tolerances on the couplers are not quite as good. The difference in coupler impedance between the two filters is about 10% for the end couplers and 1%– 2% for the remainder. This could also very easily have been caused by a variation in the properties of the material used, perhaps by irregular warming during turning, or by lack of homogeneity in the stock. In conclusion, we may summarize by saying that two mechanical filters with a satisfactory performance for the purpose were finally made. One design for 0·5 dB equal ripple in the pass-band resulted in a filter of 2 dB ripple, the difference being shown to be probably due to machining tolerances. A more satisfactory process would have been centreless grinding.

Attempts at heat treatment which aimed at obtaining a small thermoelastic coefficient together with a small expansion coefficient were not very successful, and the final filters have a frequency variation of about 40 c/s per °C, due almost entirely to variation of Young's modulus. This was not considered a serious drawback for a laboratory model. It was thought better not to mount any electron tubes on the same chassis as the filter (as in the test jig), to avoid large temperature

variations. Figs. 4.20, 4.21, and 4.22 show some examples of the filters made and their terminations. Fig. 4.23 shows the set-up for filter measurements. It may be added that great care must be taken with the shielding owing to the high attenuation. A diagram of the constructional layout used is shown in Fig. 4.19.

When the two final filters were measured again following a lapse of three months after their construction, the curves had somewhat improved (Fig. 4.18). The only apparent change was in the consistency of the rubber encasing the terminating spirals. This had apparently absorbed moisture and had become much more sticky and soft. It had lost its rubber-like springiness and underwent plastic deformation on being stressed. The other possibility is that of ageing of the *Invar* material after machining, leading to a better homogeneity of the structure.

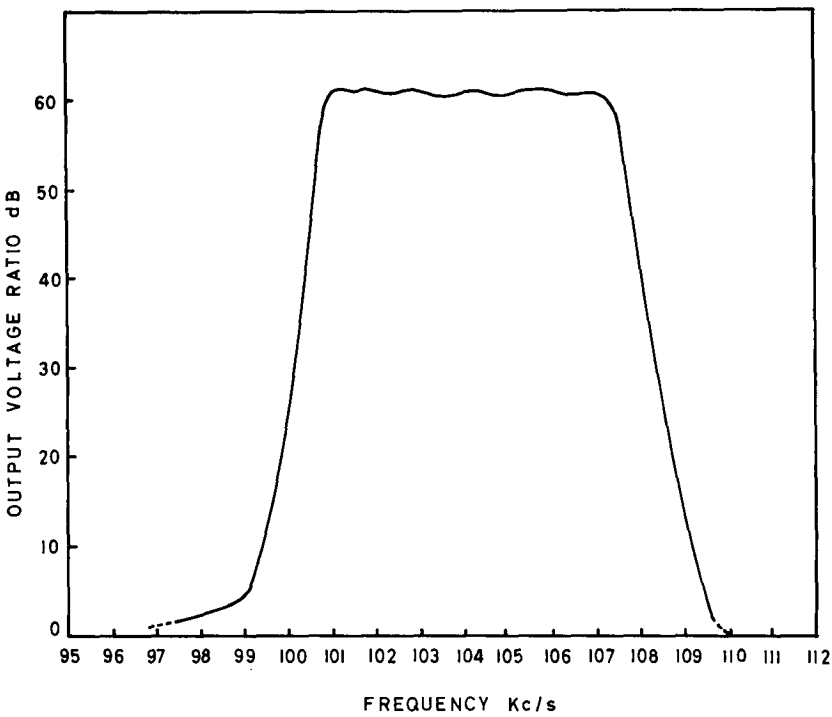

FIG. 4.18. Showing response curve for Filter No. 8. The response curve for Filter No. 9 was practically identical.

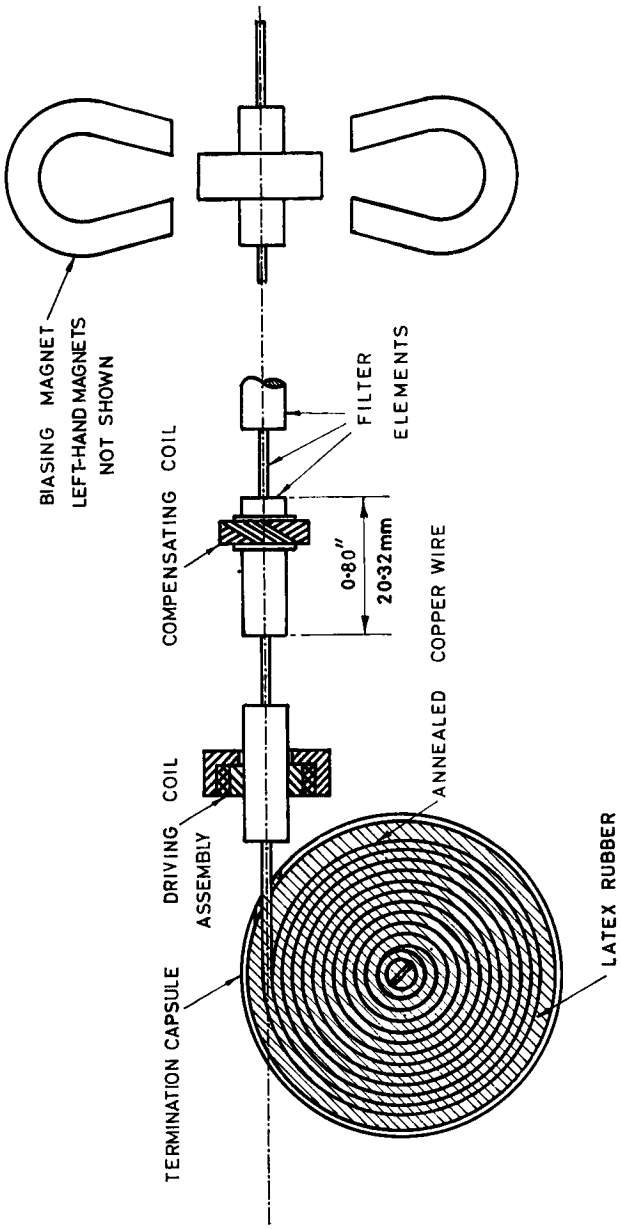

FIG. 4.19. Diagram of the filter arrangement used.

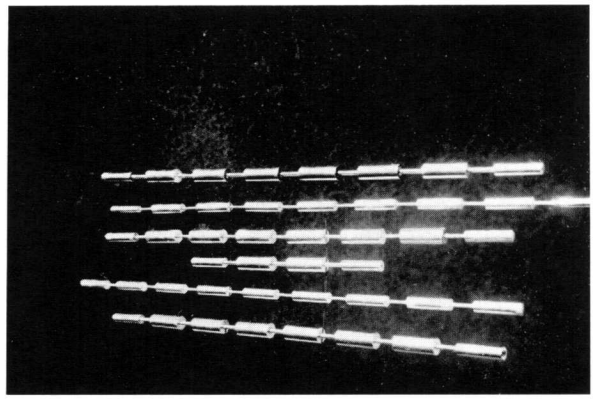

FIG. 4.20. Showing photograph of some of the filters which were made.

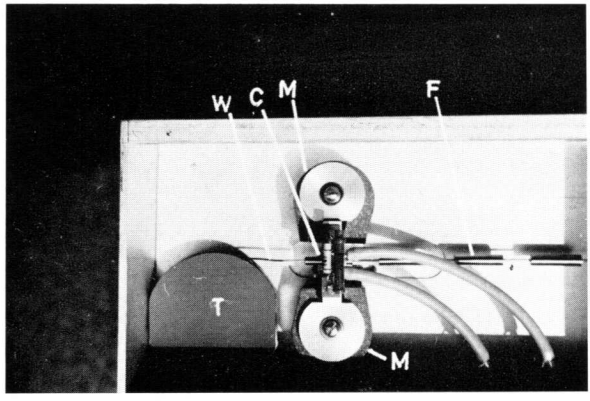

FIG. 4.21. Showing photograph of the driving end assembly.

C Driving coil
F Filter
M-M Biasing magnets
T Terminating unit
W Part of the copper wire termination

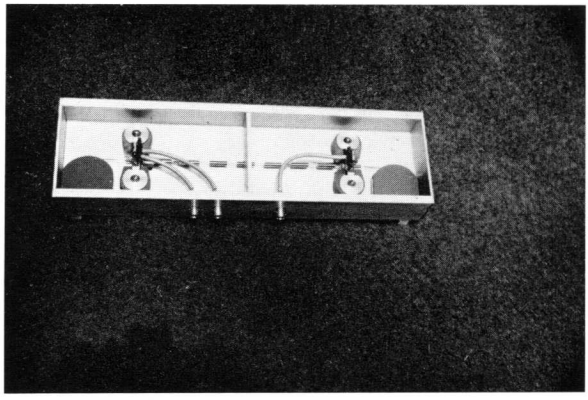

FIG. 4.22. Showing photograph of complete filter unit.

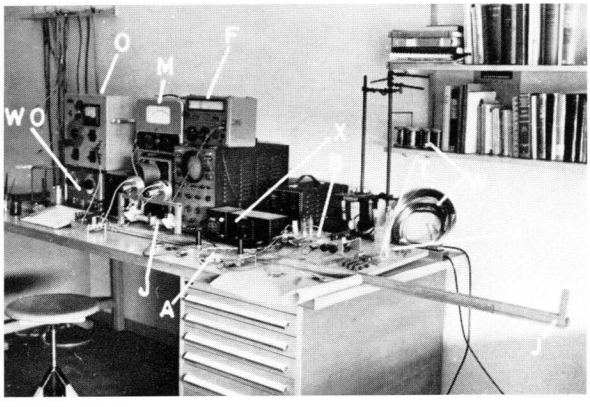

FIG. 4.23. Showing set-up for filter measurements.

A Bandpass amplifier
B Bridge for mechanical resonance with powerful magnet above.
F Interpolating oscillator
J-J Jig with amplifiers for filter tests.
M Output meter
O Signal generator
S Specimens of resonators
T Thermometer
WO Wobbulator
X Crystal-controlled frequency standard
W Annealed copper wire

4.2. Receiver

The synchronous receiver circuit is shown in Fig. 4.24. After the homodyne detectors (in-phase and quadrature) the signals are passed through maximally-flat low-pass filters to audio amplifiers. Both signals are then applied via asymmetrical to symmetrical transformers to the phase detector. This is a particularly convenient circuit for use in conjunction with a reactance tube, for, although it provides no amplification, its output voltage is zero for no input. The earth side of this phase detector is taken to a tapping-point on the cathode auto-bias resistor of the reactance tube, providing a fine-adjustment frequency control. A pentode is often used as a controlled reactance tube, but the heptode has several advantages for this application (24). The availability of separate grids for the feedback voltage and for the frequency control voltage enables the auto-bias to be adjusted to its optimum value without it being much affected by the voltage on g_3. With a pentode, of course, the cathode resistor constitutes feed-back which would reduce the change of reactance for a given change of applied voltage. In addition, the standing bias must be quite large in order to prevent grid current from flowing when the control voltage becomes positive. A pentode such as the 6AS6 which has a high mutual conductance for the suppressor grid could also be used in this manner, but the slope resistance is altered by varying the suppressor grid voltage.

Data concerning variation of mutual conductance with g_3 voltage are not normally published but as a rough guide, we may assume a value of 1 mA/V and expect it to fall to about half of this for a few volts negative on g_3. The values used in the phase-shifting network are 10 pF and 470 ohms, representing a step-down ratio of about 8:1 at the operating frequency of about 4·5 Mc/s. With the assumed value of 1 mA/V for the mutual conductance, this gives an electronic reactance of 4·7 pF while the equivalent damping resistance across the oscillator circuit works out at about 55 KΩ, which is negligibly high. If the two extreme values for mutual conductance are assumed to be 1 mA/V and 0·5 mA/V, and the tuning capacity is 56 pF, then the change in frequency produced is

$$\delta f = \frac{4{\cdot}5\ \text{Mc/s} \times (1 - 0{\cdot}5)\ \text{mA/V} \times 4{\cdot}7\ \text{pF per mA/V}}{2 \times 56\ \text{pF}} = 94\ \text{Kc/s}$$

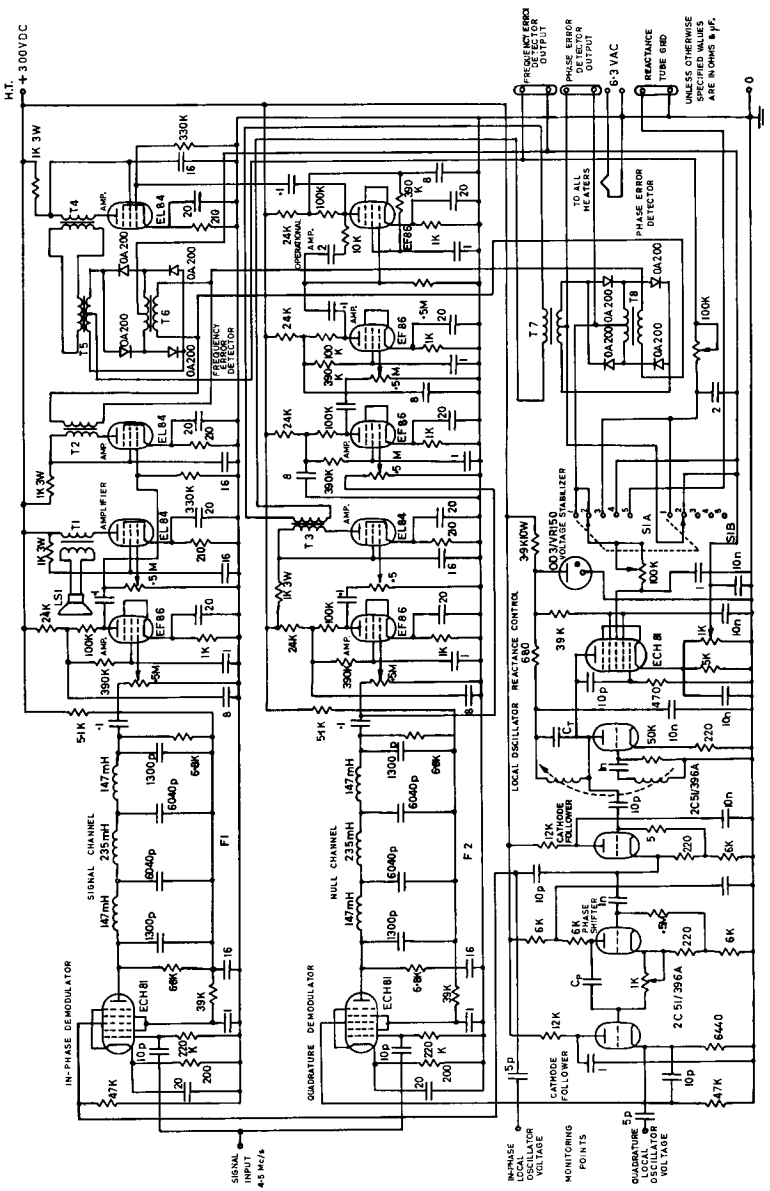

FIG. 4.24. Showing circuit diagram of the synchronous receiver with phase control and automatic frequency control.

The actual measured curve is shown in Fig. 4.25. When in the course of experiments the working frequency was varied, it was found useful to include a 50 ohm resistor in series with the oscillator grid to stabilize the amplitude of oscillation. In any case, the oscillator anode voltage is stabilized. The cathode follower and phase shifting circuits leading to the detectors are quite normal. Two loosely-coupled outlets are provided for monitoring the local oscillator voltage phase adjustment.

At the same time, the quadrature signal is passed through an operational amplifier to differentiate it and after amplification is applied via an asymmetrical to symmetrical transformer to a bridge-type phase detector. When the other terminals of the phase detector are supplied with a signal from the in-phase channel the output represents the frequency control voltage. A switch is included (**S1A** and **S1B**) to provide certain combinations. In **Position 1** (refer to the circuit diagram, Fig. 4.24) the phase control voltage source is connected in series with the frequency control voltage source between g_3 of the reactance tube and the cathode resistor tapping-point. This would be the normal position. In **Position 2,** the phase control is alone operative while **Position 3** provides for frequency control alone. **Position 4** connects the reactance tube grid to the auto-bias resistor while **Position 5** connects it to a terminal for measurement purposes. The method used in deriving the frequency control voltage is of course quite dissimilar to the normal discriminator method, and there are certain troublesome factors which make the operation also different. AC voltages are present in the output and as these must be filtered out a filter of variable time-constant is included. Dissimilarities in the diodes constituting the phase detector and asymmetry of the transformers also produce AC output terms. Balancing resistors were added in all branches to minimize this effect. Also, the variations of phase in the two channels feeding the frequency discriminator are different as one channel contains the operational amplifier and two more amplifiers, causing the output to vary as the applied frequency increases. As the mistuning increases, the audio frequencies involved cover a broader band. When a pure audio frequency is applied to the inputs of both channels simultaneously, the phase detector should ideally produce a DC output increasing steadily as the input frequency rises. The actual observed output is shown in Fig. 4.26, and shows the variations due to the causes

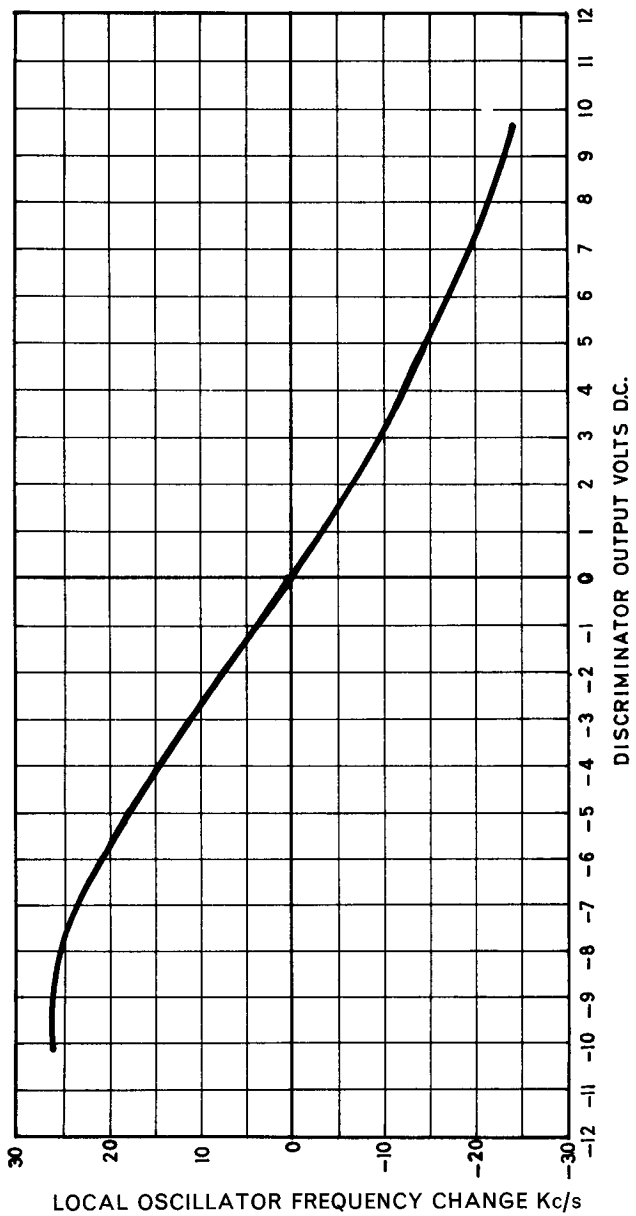

FIG. 4.25. Control characteristic of the local oscillator reactance tube control.

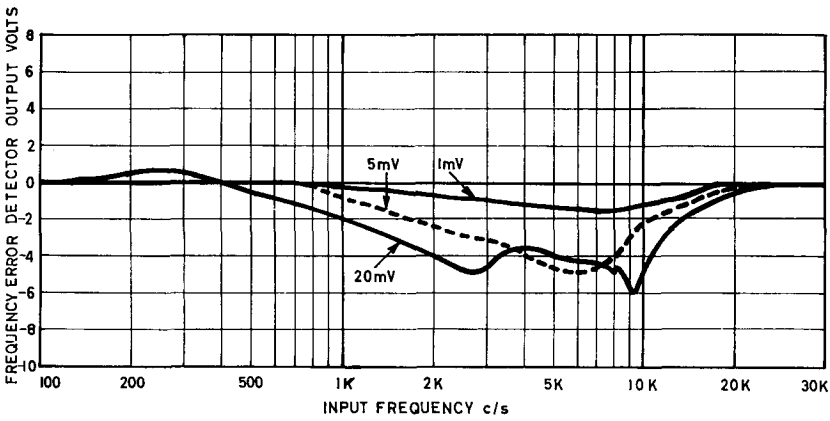

FIG. 4.26. Showing frequency error detector output as a function of audio input frequency to the receiver for different voltage inputs. Ideally the output should increase linearly with increasing frequency, but phase errors and inexact balance in the phase demodulator cause discrepancies.

mentioned above. The output voltage with double sideband suppressed carrier input is shown in Fig. 4.27. It can be seen that that part of the characteristic which is of interest corresponds excellently with what is required. However the curves reach their maxima earlier than can be accounted for by the low-pass filters, probably due to insufficient similarity with respect to phase in both channels and to spurious voltages due to unbalance in the detector. The straight portion is, however, adequately long and in any case, it would have been desirable to limit the characteristic so as to avoid the "blotting out" of a large channel adjacent to a strong signal.

The phase detector output also always contains an alternating component, except at the actual point of zero mistuning with symmetrical sidebands. In practice then, there will always be a component of modulation frequency and the large pull-in range discussed in the theoretical section is not practicable. Instead the low-pass filter cut-off is determined more by the modulation components. In addition, similar effects of unbalance and phase dissimilarity in the two channels add their quota of audio and DC components.

When the signal is already synchronized and its amplitude increases, the phase detector will become saturated at some point and synchronization will only be maintained until these spurious components are sufficiently large to disturb the process. We thus have a lower and an upper limit to the range of input voltage for which synchronization can be maintained. In practice, it would be quite easy to eliminate this upper limit by incorporating some form of quick-acting automatic gain control. In the experimental set-up, a limiter was used at the audio input to the transmitter. This proved to be quite sufficient to prevent the occurrence on peaks of speech and music, though of course at the expense of some additional distortion.

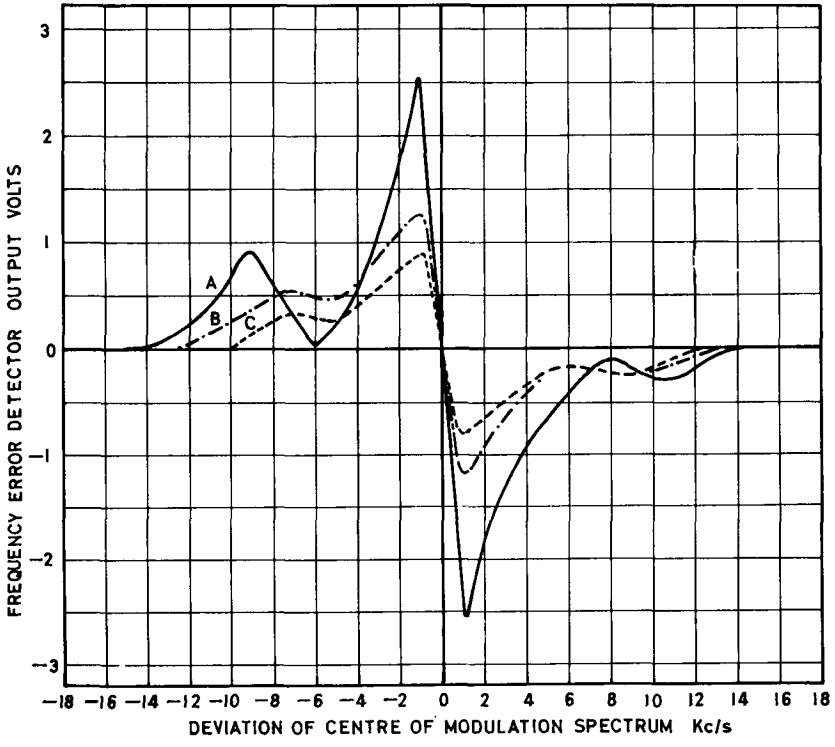

FIG. 4.27. Showing frequency error detector output as a function of frequency off-set of the centre of the modulation band of the applied signal. For the reasons mentioned under Fig. 4.26 the characteristic is not ideal. However, the centre portion was adequate for the purpose. Curves A, B and C are for progressively smaller signal input voltages.

Synchronization was confirmed by observing the Lissajous figure of transmitter oscillator voltage against receiver oscillator voltage. When the phase control was switched off, the figure rotated quite freely, even at separations of a few cycles/sec, indicating that there was no observable stray coupling causing frequency pulling. This was achieved by very careful shielding, through decoupling and the use of separate compartments for various parts of the receiver and transmitter. This absence of stray coupling may be seen from the slow beats shown in the oscillograms for non-synchronous cases.

It is not necessary here to go into the calculations for the signal levels throughout the system and the circuit design as these are of a routine nature. We shall consider the relevant parameters, using the notation and formulae of the theoretical section on the receiver (Chapter 2). The reactance tube constant S is 3000 c/s per volt (see Fig. 4.25) and may be assumed to be linear. Normal signal input (200 mV RF at the detector grids) gives a phase detector constant of 0·25 volts per radian. This gives a locking range of $\pm$ 750 c/s. In order to reduce the effects of audio frequency components in disturbing the synchronization process, the RC filter was set to have a cut-off frequency of 400 c/s.

Therefore we have for the natural frequency of the system

$$\omega_n = \sqrt{\frac{2K}{RC}} = 1950 \text{ radians/second.}$$

According to the empirical relationship

$$\frac{\textit{Pull-in range}}{\textit{Lock range}} = \sqrt{\frac{2}{KRC}} = 0{\cdot}41.$$

This is in fact a, and reference to the curve of Fig. 2.7 gives the more exact value of

$$\frac{\textit{Pull-in range}}{\textit{Lock range}} = 0{\cdot}5.$$

In the measurements made (Fig. 4.28), the observed points are somewhat dispersed and a straight line approximation for the pull-in

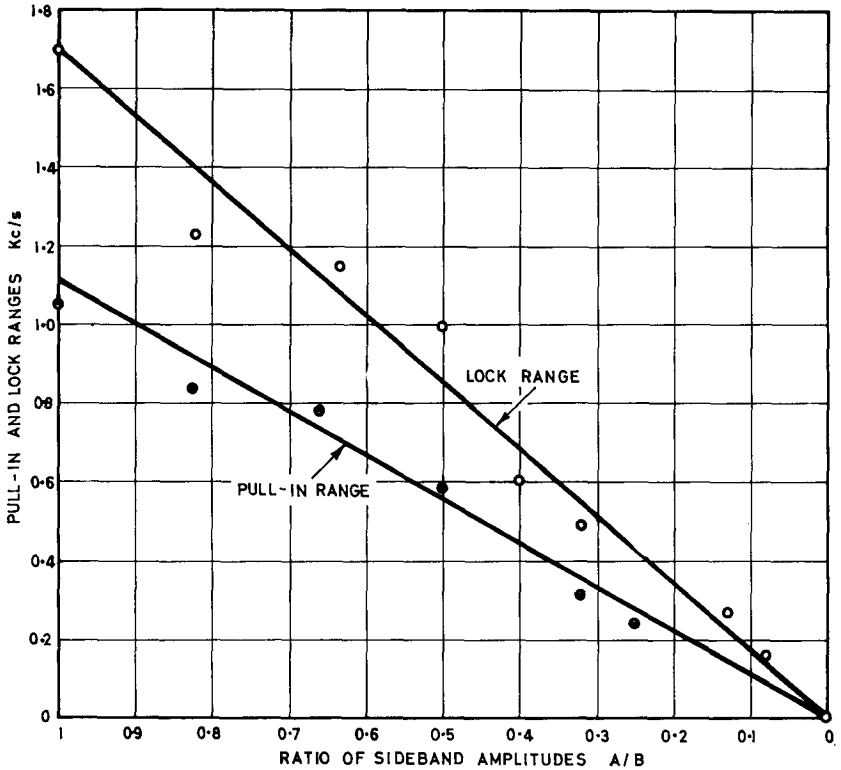

FIG. 4.28. Showing the change in lock and pull-in ranges measured as one sideband fades. The rather wide scattering of the observed points is due to insufficient stability of the receiver and transmitter oscillators. In theory, the pull-in range does not follow a straight line as here approximated.

range variation with fading has been drawn. The observed value for the ratio *Pull-in range / Lock range* or "Capture Ratio" of 0·6 is in reasonable agreement with the value calculated above. For the case shown in Fig. 4.31 the frequency off-set was about 500 c/s. The time required for synchronization is then

$$t = \frac{4(\triangle f)^2}{B^3} = 0{\cdot}375 \text{ milliseconds.}$$

The measured value is about 5 milliseconds. The main reason for this discrepancy is that the calculation takes no account of the interfering

terms of modulation products in the control loop or of the low-pass filters following the demodulators. In the period just before synchronization occurs these interference terms are of the same order of magnitude as the control voltage and their effect is appreciable.

The second set of measurements made with the independent sideband transmitter is shown in Fig. 4.29, showing the effect of selective fading on the signal and quadrature channels. The calculated curves have been given in Fig. 2.10 and the curve corresponding to zero detuning is repeated in Fig. 4.29. It can be seen that there is quite good agreement except for the region of high attenuation in the quadrature channel. In fact, the output voltage in that region, which was measured with a broadband valve-voltmeter consisted mainly of hum and other

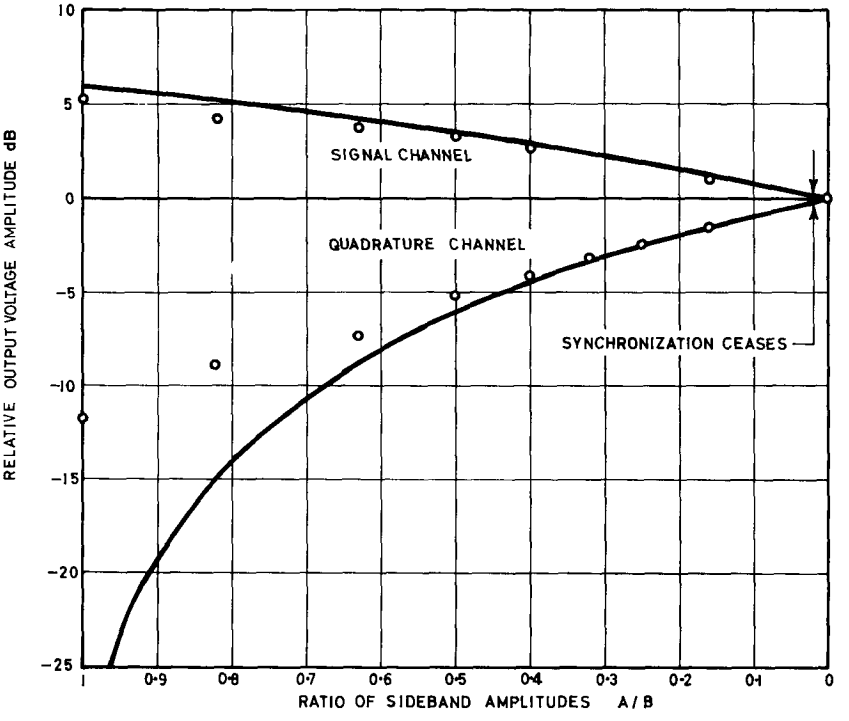

FIG. 4.29. Showing the in-phase and quadrature channel signals as one sideband fades, for a very small frequency off-set. Single sideband reception is represented by the zero ordinate. The output in the quadrature channel below about – 10 dB consisted mainly of hum.

undesired effects. The correspondence of the actual signal was therefore better than that suggested by the graph. The receiver remained satisfactorily synchronized until one sideband had faded to an amplitude of 0·02 of the other (−34 dB).

Next, an electronic gate was constructed. The audio frequency (1000 c/s) was applied through it to the transmitter while the gate switching was operated by the delayed sweep of an oscilloscope. The repetition rate was at about 10 times/sec. Since transmission through the gate was not quite constant during the sweep, the input voltage to the transmitter is shown for reference in Fig. 4.30.

The correct process of synchronization is shown in the oscillogram of Fig. 4.31. The upper trace shows the signal (in-phase) channel with the quadrature output on the lower. From the initial (pre-synchronization) voltages, it may be seen that the overall gains are about equal. Since the initial frequency off-set is quite small, the quadrature output is almost zero. The time required for synchronization is about 5 msec.

In Fig. 4.32 the local oscillator voltages used in the two demodulators are not quite 90° apart. Synchronization has taken longer to establish and the remaining quadrature voltage is fairly large.

The mistuning in the case of Fig. 4.33 is so large that synchronization has been lost. In such a case, the local oscillator frequency under-

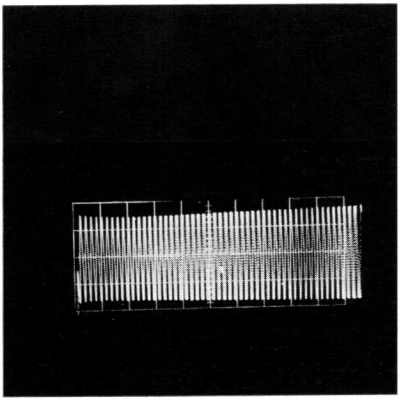

FIG. 4.30. Audio input to the transmitter from electronic switch.

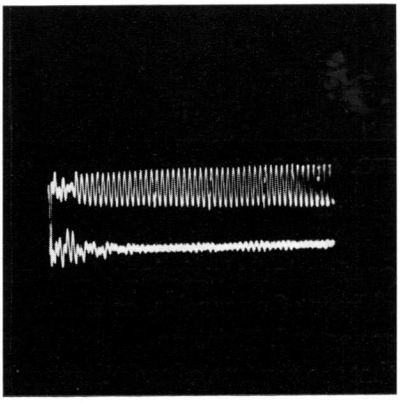

FIG. 4.31. Signal (upper trace) and quadrature channel outputs showing correct synchronization. (1000 c/s signal.)

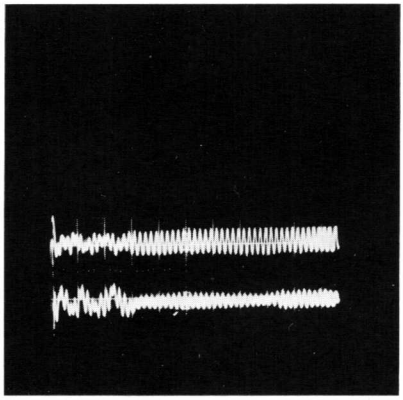

FIG. 4.32. Same as Fig. 4.31 but with phase error in local oscillator voltages.

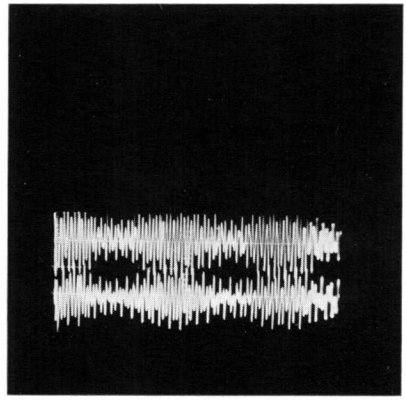

FIG. 4.33. Synchronization lost. Local oscillator frequency undergoing perturbations.

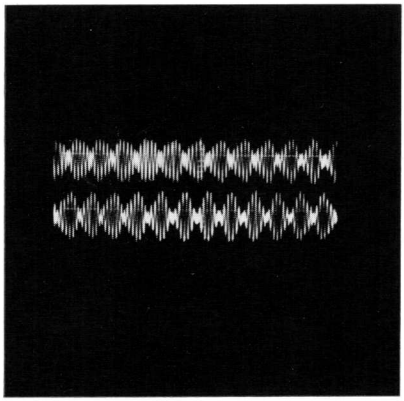

FIG. 4.34. Synchronization disconnected, frequency off-set large.

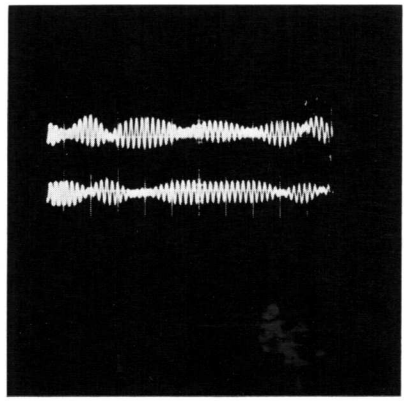

FIG. 4.35. Same as Fig. 4.34 but frequency off-set small.

goes periodic variations. The outputs are not simply the sums of two different frequencies, as is the case when the synchronization is disconnected. This condition is shown in Fig. 4.34. Here it may be seen that the maxima of each channel coincide with the minima of the other. When the frequency error is made very small with the synchronization still disconnected, as in Fig. 4.35, the phase drifts at random. This shows the absence of stray coupling and pulling between the oscillators.

A typical music signal is shown correctly synchronized in Fig. 4.36. The time for synchronization is again of the order of 5 msec. The same signal with synchronization lost is shown in Fig. 4.37.

Some carrier was deliberately introduced by unbalancing the transmitter and the receiver was induced to synchronize between it and one of the sidebands of the 1000 c/s modulated signal. The result is shown in Fig. 4.38. The main output signal should be at 500 c/s, but the furthest sideband acts as an interfering signal to produce an output component of 1500 c/s as well as to disturb synchronization.

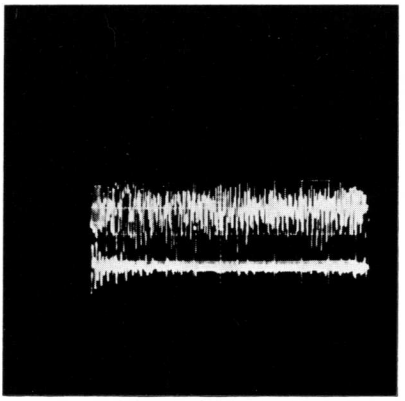

FIG. 4.36. Correct synchronization with music signal.

FIG. 4.37. Synchronization lost, music signal.

The electronic gate was then altered so that the audio input (1000 c/s) to the transmitter increased gradually to full amplitude over about 50 msec. The frequency was adjusted very carefully so that synchronization began almost immediately on application of a very small signal. The outputs of both channels are shown in Fig. 4.39 where the in-phase channel (upper trace) corresponds very closely to the input to the transmitter. However if the input level is too high, there is too much break-through of the audio output from the phase detector into the reactance tube circuit in spite of the low-pass filter. This effect may be seen clearly in Fig. 4.40, where synchronization is lost after a certain level of input signal is exceeded. Automatic gain control and possibly limiting are the remedy.

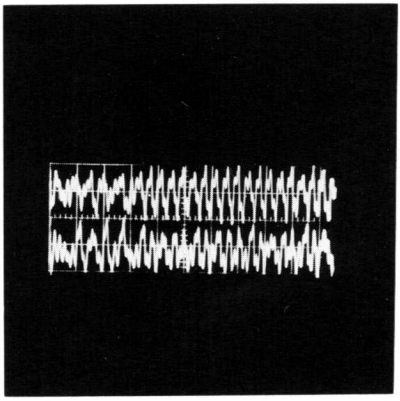

FIG. 4.38. Faulty synchronization between full-strength carrier and one sideband. Other sideband acts as 1500 c/s interference.

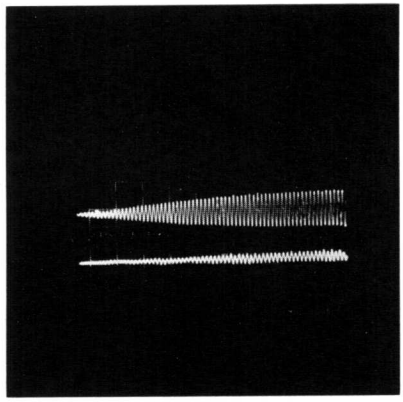

FIG. 4.39. Correct synchronization with input signal of gradually increasing amplitude.

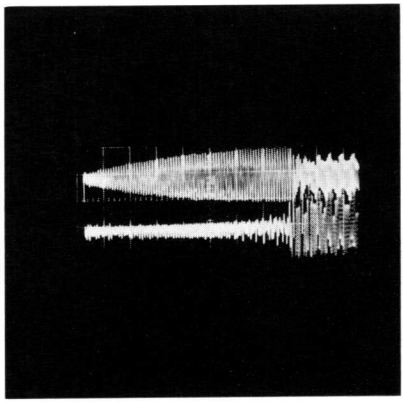

FIG. 4.40. Input signal (1000 c/s). Synchronization starts correctly but ceases when excessive signal breaks through into control circuit.

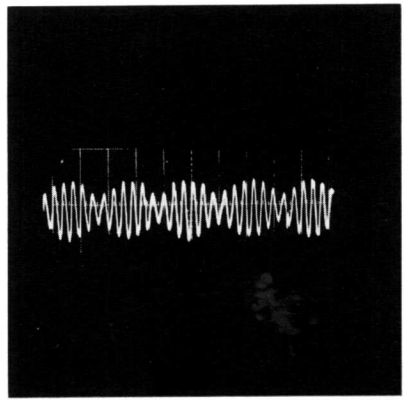

FIG. 4.41. (Asynchronous) Receiver output with interference cancellation. One sideband is incompletely cancelled causing beats. The synchronization has been disconnected so that the beats may be seen.

In conclusion, we may say that the receiver operated fairly satisfactorily on the whole. Signal quality (including transmission through the twin single-sideband transmitter) was moderate. If the frequency off-set was not too high, synchronization was sufficiently rapid not to

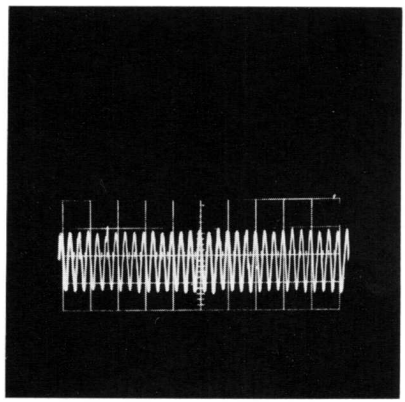

FIG. 4.42. (Asynchronous) Receiver output with better cancellation of one sideband. Only small beats are visible.

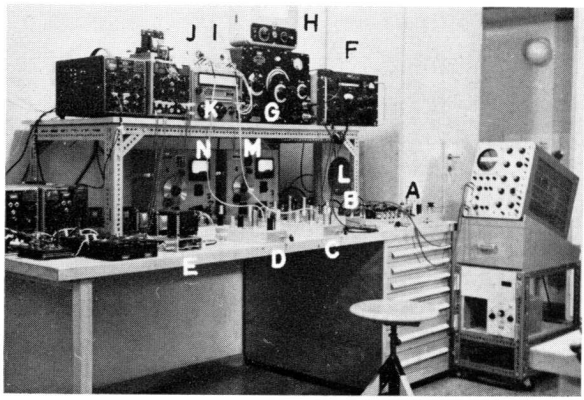

FIG. 4.43. Set-up for complete measurements. The filters are placed in between the phase shifters.

A Receiver
B Transmitter
C Phase shifter No. 1
D Phase shifter No. 2
E H. T. filterings units
F Monitor receiver
G Signal generator for transmitter
H Output meter
I Sideband attenuator
J Limiter
K Audio signal generator
L Loudspeaker
M Auxiliary carrier generator for Phase shifter No. 1.
N Auxiliary carrier generator for Phase shifter No. 2.

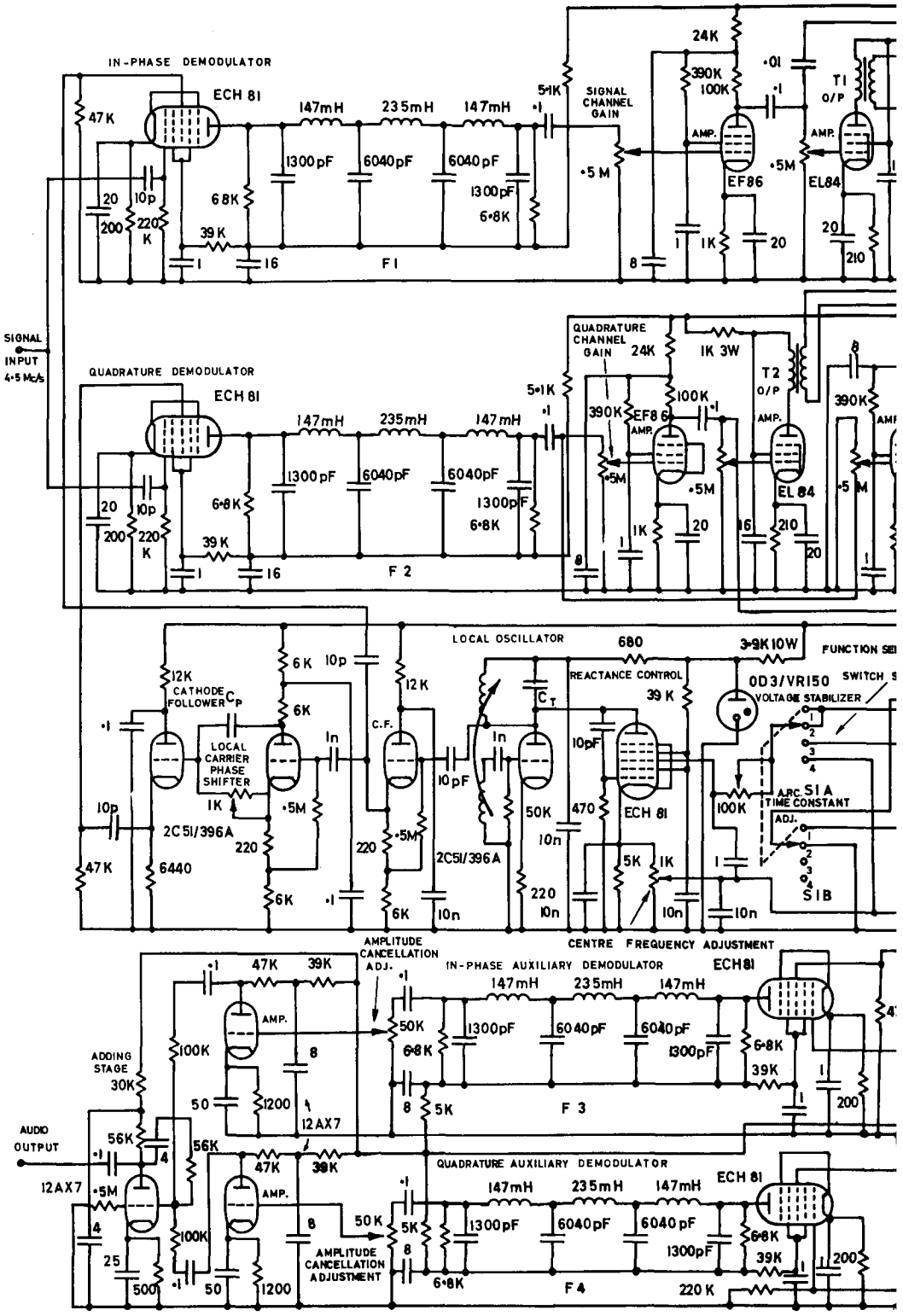

FIG.4.44. Circuit diagram of the interference-cancelling receiver. One sideband is cancelled, and in order to change

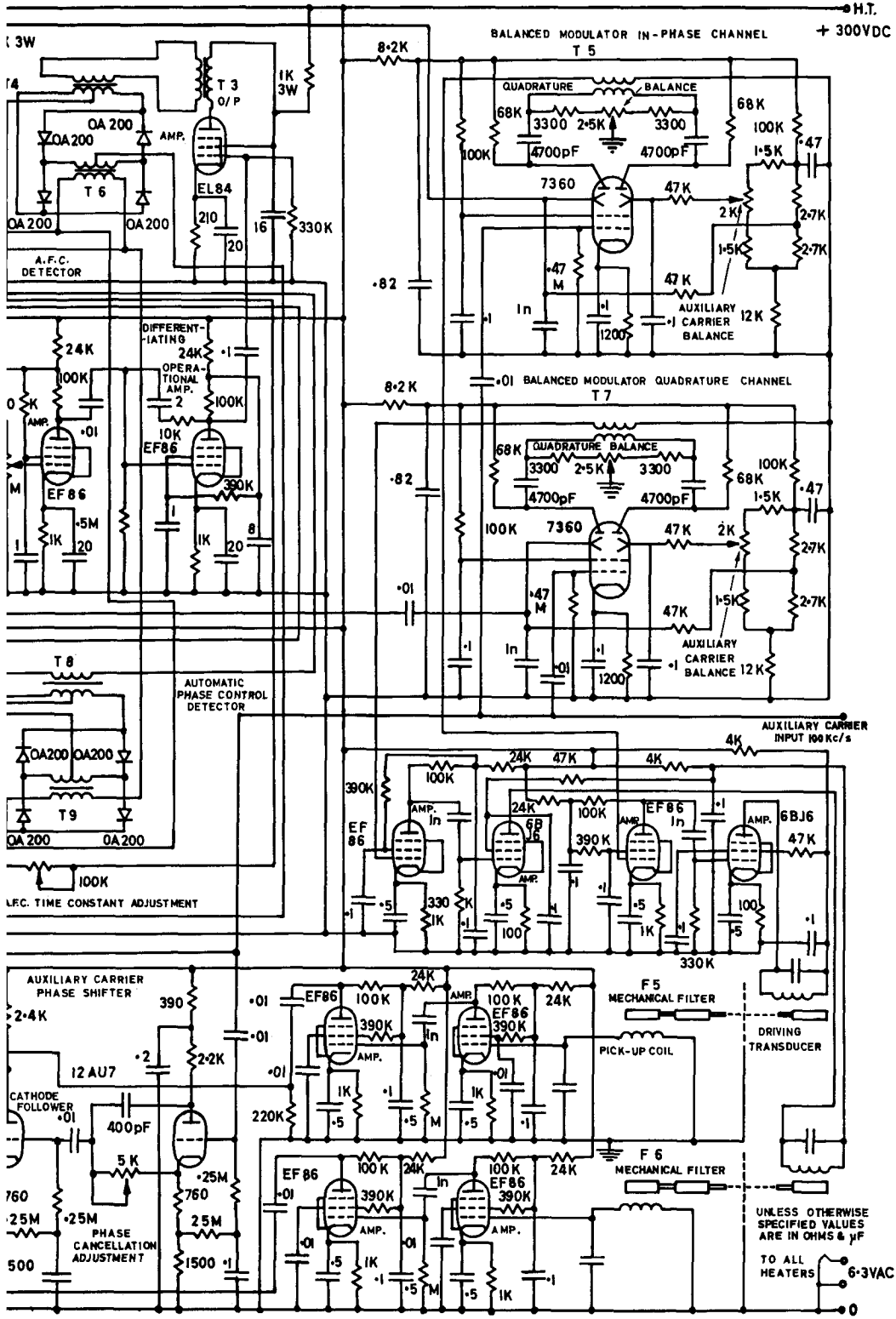

llation to the other sideband a 180° phase shift would have to be introduced in one of the inputs to the adding stage.

be noticeable on speech or even with percussion music, though with this last, the input to the transmitter was limited. The automatic frequency control was found to be particularly helpful on interrupted signals, such as speech.

The interference-cancelling synchronous receiver was a modification of the normal double sideband receiver. The circuit is shown in Fig. 4.44. After detection and amplification as before, the audio signals are shifted 90° relative to one another and added in a feed-back adding stage. Interference cancellation is the same whether synchronized or not though in the latter case, the audio output frequency is in error by the frequency off-set between transmitter and receiver oscillators. The automatic frequency control reduces this error to quite small values. The unwanted sideband suppression may be noted indirectly from the output. Complete absence of beats in a sine-wave modulation signal would indicate perfect suppression.

With the synchronization disconnected the outputs from the in-phase and quadrature channels are shown in Fig. 4.34. This shows a frequency off-set of about 200 c/s. The output from the adding stage is shown in Fig. 4.41. Here, the phase shifters are not yet correctly adjusted, and there is some output from the unwanted sideband. Fig. 4.42 shows the output with good adjustment of the phase shifts and amplitudes. Note that the time scales in the last two oscillograms have been expanded to show more detail.

CHAPTER 5

CONCLUSIONS

5.1. Transmitter

The transmitter was in principle quite satisfactory for the purpose and performed as expected. A drawback was the long warm-up period required until the operation became stable, referring to carrier and undesired sideband suppression. For the first two or three hours after switching on, frequent adjustment of the controls is required. The use of low impedance levels throughout minimized stray fields. Provision had been made for measurements of the effects of frequency dependent transmission path lengths and though an acoustic delay line was constructed it was not sufficiently developed to permit of this measurement being carried out.

5.1.1. Phase Shifters

The phase shifters were on the whole also satisfactory. Smaller tolerances on the stages and low-pass filters following the mechanical filters would further improve the accuracy of the phase shift. As the same type of deflection tube modulator as in the transmitter was used a long warm-up time was also required, with frequent adjustments of a multiplicity of controls being needed. A further trouble was the frequency drift of the mechanical filters with the ambient temperature. In an improved design either filters with a smaller temperature coefficient should be used, or else the auxiliary oscillator should be stabilized using, for example, a tuning fork made of the same material as the mechanical filters, so as to have the same temperature coefficient. Considerable heat was generated by the equipment during the long warm-up period which in turn caused the filters to drift further.

5.1.1.1. Mechanical Filters

The question of temperature coefficient has already been mentioned. Although the filters were not required to be identical, they were in fact so similar that the same oscillator could have been used for both. As it was not convenient to place them together, the drifts were not always identical and separate oscillators were sometimes employed. The construction used for the terminations was quite compact, though further experiment with finer gradations of wire diameter and with different damping materials would have probably led to improved performance. The long-term stability has of course not been determined and heat-treatment should be more elaborate in cases where this is to be relied on. The previous history of the material is important, since certain irreversible changes take place continuously, though these are very slow at room temperature. Certain new alloys apparently more suitable than nickel-iron for this purpose were not available in the time required, (25), (26) and (27).

5.2. Receiver

As may be seen from the oscillograms, the receiver performance was in the main as expected. Experiment showed the necessity for certain additions and refinements. A method of automatic gain control is an important adjunct. As an alternative the phase detector input could be limited in some manner, but this would probably not be as satisfactory. The need for such control is due to incorrect operation of the phase and frequency error detectors when a certain input amplitude is exceeded (Figs. 4.26 and 4.40). Instability in the feed-back loop can also occur with excessive gain. It is important, however, that any gain control used should not affect the overall phase shift or oscillator frequency.

The type of phase detector used is well-known in servo-mechanism work and was quite suitable except that performance would probably have been less sensitive to input amplitude if better unbalanced-to-balanced transformers had been used. The same applies to the frequency error detector.

The oscillator was quite sufficiently stable and isolated from the remainder of the circuit so as not to be affected by the signal levels. In a receiver covering a wide frequency range, the 90° phase shift would be a problem, unless the range were to be divided into bands sufficiently narrow over which the phase shift would hold accurately enough. Of course the superheterodyne principle could also be used. A very satisfactory but elaborate method is to employ a frequency synthesizer using the techniques described at the end of Sec. 3.2.

5.3. Complete System

Satisfactory measurements were made of general performance, pull-in time and the effects of selective fading on the signal and quadrature channels and on the pull-in and lock ranges. Synchronization was maintained until one sideband had faded to an amplitude of 0·02 of the other (−34 dB). Oscillograms are also given of the suppression of interference on one sideband and of the performance with typical speech and music signals.

Leer - Vide - Empty

APPENDIX 1

The non-linear differential equation

$$\frac{d^2\xi}{d\tau^2} + \alpha\frac{d\xi}{d\tau} + \sin\xi = \beta \qquad \text{(A.1.1)}$$

which represents the behaviour of the synchronous receiver treated in this work is also of interest in other fields. Thus the motion of a pendulum acted upon by a constant torque in a viscous fluid or the position of a synchronous machine rotor relative to the rotating field are governed by this same equation. The colour subcarrier oscillator in television affords a more recent example of such a phase-locked system (10). The behaviour of the system can be studied graphically using the *phase-space* concept, (see A. A. Andronow and C. E. Chaikin, "Theory of Oscillations," [29]). Thus the behaviour of a system with one degree of freedom can be depicted on a phase plane where the state of the system depends on a positional coordinate x and $\dot{x}$. As the time t varies then x and $y = \dot{x}$ will be functions of t. $x = f(t)$ and $y = g(t)$ are known as the parametric equations. The velocity of the point described by these coordinates is called the phase velocity and is not equal to the velocity of the system which is merely $\dot{x}$. The phase velocity is the plane vector with components x, y or $x, \dot{x}$. The particular path followed among all possible paths is fixed when a single point is known. (There is an analogy with the *world lines* of relativity.)

A graphical construction for obtaining a picture of the paths or a *phase portrait* of the system is the *method of isoclines*. An isocline is a locus of points where the paths have a given slope. The equation must first be transformed to an equation giving the slope as a function of position. Isoclines may then be plotted and a graphical averaging technique permits an approximate path to be drawn. Since there is one and only one path through any point on the phase plane, the phase portrait may be constructed. (For details of the method, see Andronow and Chaikin,

op. cit.) As the phase portrait and solutions to this equation describe exactly the behaviour of our receiver, some points from A. Giger's analytical treatment (7) are given here.

First the transformation

$$\xi = (\lambda + \pi - \sin^{-1}\beta) \text{ is performed on}$$

Equation A.1.1 giving

$$y\frac{dy}{d\lambda} + \alpha y - \sin(\lambda - \sin^{-1}\beta) = \beta \tag{A.1.2}$$

where $$y = \frac{d\lambda}{d\tau}.$$

In order to plot the isoclines, the equation

$$y = \frac{\beta + \sin(\lambda - \sin^{-1}\beta)}{c + \alpha}$$

where c = slope, is used.

Fig. A.1.1 (after Giger) shows how two types of solution are possible. A curve starting at A_z, for instance, ends up at a point of equilibrium Z after a time. For different initial conditions, a curve beginning at A_p eventually leads to the periodic solution y_p of the second type. This curve y_p may be represented by a Fourier series with the average value of

$$\frac{1}{2\pi}\int_{2\pi} y_p(\lambda)\, d\lambda = \frac{\beta}{\alpha} \tag{A.1.3}$$

As the value of α is increased, the curve y_p moves further towards the abscissa. In the limiting case, for $\alpha = \alpha_o$, y_p moves from one saddle point S to the next. For $\alpha > \alpha_o$ no periodic solution is any longer possible regardless of initial conditions. This corresponds to the case of guaranteed synchronization in the receiver.

α_o must then be determined. The limiting curve y_{po} has an average value given by Equation A.1.3 and may be represented by a power series y'_{po}, whereby the approximation must always go through the

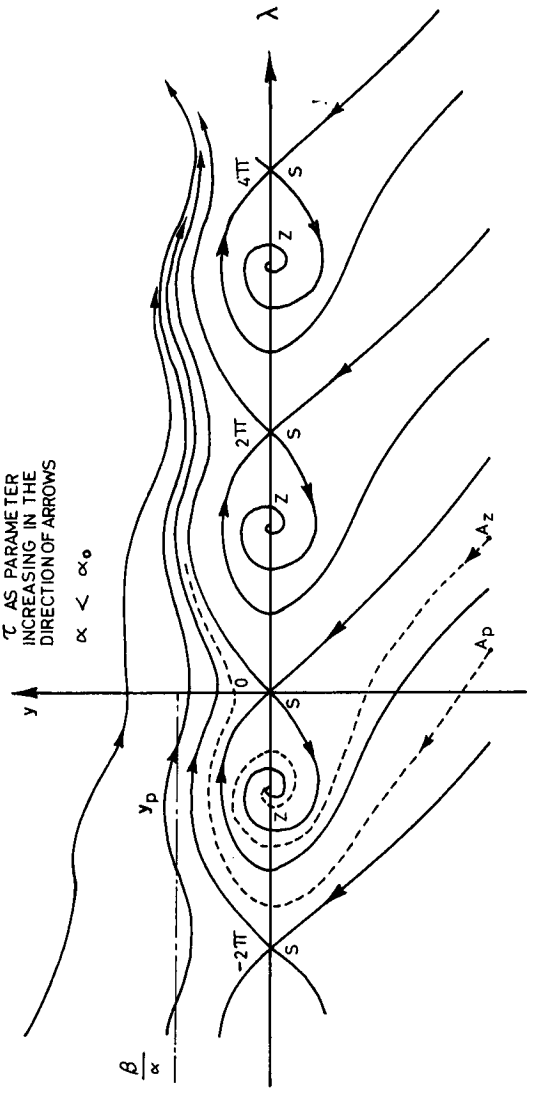

FIG. A. 1.1. Phase portrait of the system represented by the non-linear differential equation

$$\frac{d^2\xi}{d\tau^2} + \alpha\frac{d\xi}{d\tau} + \sin\xi = \beta.$$

The direction of the arrows is easily found if it be remembered that $y\,(=\dot{\lambda})$ is the system velocity, hence for y positive, for example, λ must increase with time.

points $\lambda = 0$, $\lambda = 2\pi$. The derivatives of y_{po} at the saddle points may be calculated from (A.1.2) and made to correspond with those of y'_{po} to n desired derivatives. With due attention to the question of convergence the values of a_o for various values of β are calculated from a set of equations obtained by comparing coefficients.

For a curve relating $|\beta|$ to a_o reference should be made to Fig. 2.7. For $a > 1{\cdot}1931$, synchronization is assured for $|\beta| < 1$, that is, for any frequency within the lock range of the receiver.

APPENDIX 2

Formulae for obtaining the minimum number of resonators and the smallest allowable unloaded resonator Q for various types of filter are given in a paper by Dishal (18). For convenience, the relevant expressions are given here, together with a short derivation, using material from M. E. Van Valkenburg, "Modern Network Synthesis," (30).

Using the inverse arm (constant-k) configuration, it has been shown that for a given number of resonators (n) and given passband ripple (V_p/V_v), the sharpest rate of cutoff between passband and reject band is that obtained by using a Chebyshev-type transfer function. This has the squared magnitude form

$$\left|G_{12}\right|^2 = \frac{1}{1 + \varepsilon^2 C_n^2(\omega)} \tag{A.2.1}$$

where $\varepsilon < 1$ is a real constant. (Fig. A.2.1)
The Chebyshev polynomial is defined as

$$T_n(\zeta) = \frac{1}{2^{n-1}} \cos(n \cos^{-1} \zeta)$$

A more convenient form here is

$$C_n(\zeta) = \cos(n \cos^{-1} \zeta)$$

as the amplitude of oscillatio ı is then unity.
When $|\zeta| > 1$, then $\cos^{-1} \zeta = j \cosh^{-1} \zeta$,
therefore $C_n(\zeta) = \cosh(n \cosh^{-1} \zeta)$, and equation (A.2.1) becomes

$$\left|G_{12}\right|^2 = \frac{1}{1 + \varepsilon^2 \cosh^2(n \cosh^{-1} \omega)} \tag{A.2.2}$$

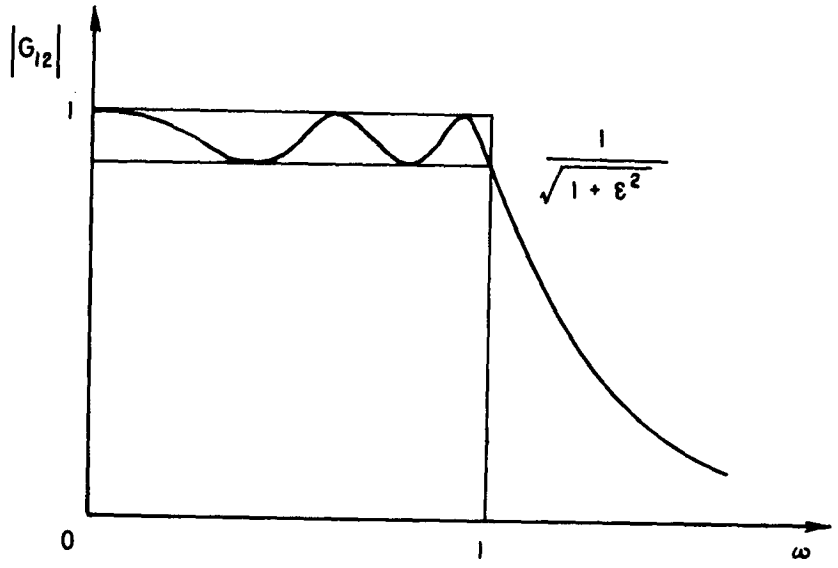

FIG. A.2.1. Chebyshev magnitude response.

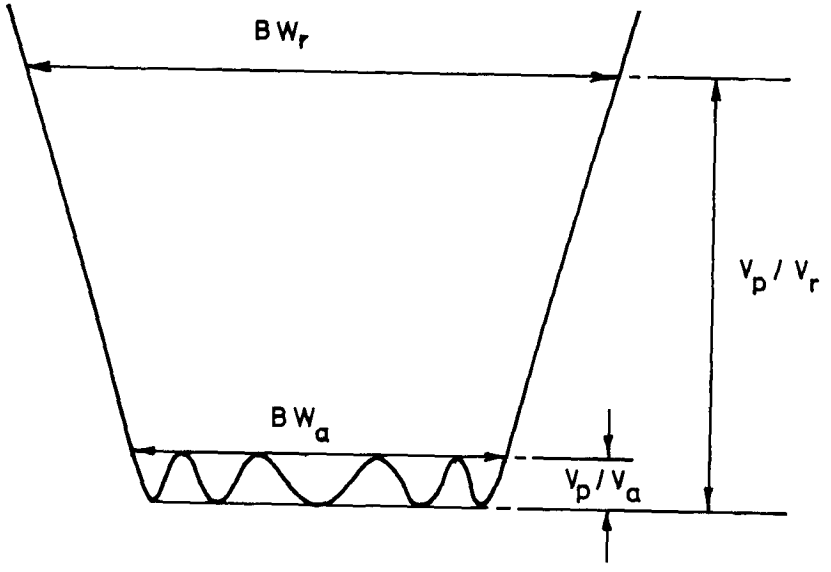

FIG. A.2.2. Quantities used in the filter specification.

In Dishal's notation this is written

$$n = \frac{\cosh^{-1}\sqrt{\dfrac{(V_p/V_r)^2 - 1}{(V_p/V_a)^2 - 1}}}{\cosh^{-1}\left(\dfrac{BW_r}{BW_a}\right)}$$

where the symbols are as defined in Fig. A.2.2. Since ε^2 is defined in the filter specification (where $1/\sqrt{1+\varepsilon^2}$ is the allowable ripple magnitude) and the transfer magnitude is specified for some ω where the attenuation must have some desired value, it is clearly possible to obtain n, the number of stages.

It has also been shown that if all the resonators have the same unloaded Q, and if the attenuation zeros of Equation A.2.6 are moved closer to the real frequency axis by an amount equal to the inverse of the unloaded Q of the resonators, then these newly positioned left half-plane zeros will define the reactances of the new network which will produce our desired attenuation shape when the reactance elements used have the assumed finite unloaded Q. Since the attenuation zeros of a physically realizable network cannot appear in the right half-plane, this fixes the lowest allowable resonator Q's. Thus, the smallest allowable resonator unloaded Q which can be used to produce our desired attenuation is equal to the inverse of the perpendicular distance between the $j\omega$ axis and that zero which is closest to this axis.

Writing $s = j\omega$ in Equation (A.2.1), we have

$$\left|G_{12}\right|^2 = \frac{1}{1 + \varepsilon^2 C_n^2(-js)}$$

For convenience, let $z = -js$. Poles of interest occur when

$$C_n(z) = \pm\frac{j}{\varepsilon} \tag{A.2.3}$$

If we now let $z = \cos w$ and $w = u + jv$, then Equation (A.2.3) becomes

$$C_n(z) = \cos nw = \cos nu \cosh nv - j\sin nu \sinh nv = \pm\frac{j}{\varepsilon},$$

which is satisfied when

$$\cos nu \cosh nv = 0 \tag{A.2.4}$$

and

$$\sin nu \sinh nv = \pm \frac{1}{\varepsilon} \tag{A.2.5}$$

Since $\cosh nv \neq 0$, then Equation (A.2.4) is satisfied only when $\cos nu = 0$ or when

$$u = \frac{1}{n}(2k-1)\frac{\pi}{2} \qquad k = 1,2,3,\ldots,2n$$

At these values of u, $\sin nu = \pm 1$ so that

$$nv = \sinh^{-1}\frac{1}{\varepsilon}$$

We define the value of v satisfying this equation to be a, so that

$$a = \frac{1}{n}\sinh^{-1}\frac{1}{\varepsilon}$$

We next determine the pole positions in the s-plane from the relationship

$$s = j\cos w = j\cos(u + jv) = j\cos\left[\frac{\pi}{2n}(2k-1) + ja\right]$$

Expanding, the pole locations are given by

$$\sigma_k = \pm \sinh a \sin\frac{2k-1}{n}\cdot\frac{\pi}{2} \tag{A.2.6}$$

where $k = 1,2,3,\ldots,2n$

and

$$\omega_k = \cosh a \cos\frac{2k-1}{n}\cdot\frac{\pi}{2}$$

These two equations give the positions of the attenuation zeros in the s-plane.

Thus the minimum unloaded resonator Q is given by

$$\frac{1}{\sigma_1} = \frac{1}{\sinh\left(\frac{1}{n}\sinh^{-1}\frac{1}{\varepsilon}\right)\sin\frac{\pi}{2n}}$$

(with $k = 1$), or in the notation of Dishal,

$$\frac{Q_{o\,min}}{f_o/BW_a} = \frac{1}{\sinh\left(\frac{1}{n}\sinh^{-1}\frac{1}{\sqrt{(V_p/V_a)^2 - 1}}\right)\sin\frac{90°}{n}}$$

where f_o is the centre frequency.

Leer - Vide - Empty

REFERENCES

1. *J. P. Costas*, "Synchronous Communications," Proc. IRE, vol. 44, pp. 1713–1718; December, 1956.

2. *L. R. Kahn,* "Compatible Single Sideband," Proc. IRE, vol. 49, pp. 1503–1527; October, 1961.

3. *H. Chestnut and R. W. Mayer,* "Servomechanisms and Regulating System Design," Volume 1, John Wiley and Sons, Inc., New York and Chapman and Hall, Ltd., London; 1959. *Textbook.*

4. *W. R. Bennett*, "Electrical Noise," McGraw-Hill Book Company, Inc., New York; 1960. *Textbook.*

5. *E. Labin*, "Théorie de la synchronisation par contrôle de phase," Philips Res. Rep., vol. 4, pp. 291–315; August, 1949.

6. *G. W. Preston and J. C. Tellier*, "The Lock-in Performance of an A.F.C. Circuit," Proc. IRE, vol. 41, pp. 249–251; February, 1953.

7. *A. Giger*, "Ein Grenzproblem einer technisch wichtigen nichtlinearen Differentialgleichung," Zeitschrift für angewandte Mathematik und Physik, vol. VII, Fasc. 2, pp. 121–129; March, 1956.

8. *W. J. Gruen*, "Theory of A.F.C. synchronization," Proc. IRE, vol. 41, pp. 1043–1049; August, 1953.

9. *H. T. McAleer*, "A new Look at the Phase-Locked Oscillator," Proc. IRE, vol. 47, pp. 1137–1143; June, 1959.

10. *D. Richman*, "Color-carrier reference phase synchronization accuracy in NTSC color television," Proc. IRE, vol. 42, pp. 106–133; January, 1954.

11. *G. Guanella et al*, U.S. Patent No. 2,522,371.

12. *D. G. Tucker*, "The Synchrodyne and Coherent Detectors," Wireless Engineer, vol. 29, pp. 184–188; July, 1952.

13. *E. I. Green*, U.S. Patent No. 2,020,409.

14. *R. B. Dome*, "Wideband Phase-shift Networks," Electronics, vol. 19, p. 112; December, 1946.

15. *H. J. Orchard*, "Synthesis of Wide-band Two-phase Networks," Wireless Engineer, vol. 27, p. 72; March, 1950.

16. *H. J. Orchard*, "Synthesis of Wide-band Two-phase Networks," Wireless Engineer, vol. 28, p. 30; January, 1951.

17. *A. A. Ahmed*, "A Wide Band Phase Shifter," Proc. IRE, vol. 48, p. 945; May, 1960.

18. *M. Dishal*, "Concerning the Minimum Number of Resonators and the Minimum Unloaded Q needed in a Filter," Transactions of the IRE Professional Group on Vehicular Communication, vol. PGVC-3, pp. 85–117; June, 1953: also, Electrical Communication, vol. 31, pp. 257–277; December, 1954.

19. *W. P. Mason*, "Electro-Mechanical Transducers and Wave Filters," D. Van Nostrand Company, Inc., New York; 1948. *Textbook.*

20. *W. Van B. Roberts and L. L. Burns, Jr.*, "Mechanical Filters for Radio Frequencies," RCA Review, vol. X, pp. 348–365; September, 1949.

21. *W. Strusz ynski*, "A Theoretical Analysis of the Torsional Electro-Mechanical Filters," The Marconi Review, vol. XXII, pp. 119–143; Third Quarter, 1959.

22. *V. Belevitch*, "Tchebyshev Filters and Amplifier Networks," Wireless Engineer, vol. 29, pp. 106–110; April, 1952.

23. *H. J. Orchard*, "Formulae for Ladder Filters," Wireless Engineer, vol. 30, pp. 3–5; January, 1953.

24. *K. R. Sturley*, "Radio Receiver Design," Part II, Chapman and Hall Ltd., London; 1954. *Textbook.*

25. H. A. Wilson Company Engineering Data Bulletin "Ni-Span C."

26. *M. E. Fine and W. C. Ellis*, "Thermal Variations of Young's Modulus in some Fe-Ni-Mo Alloys," Journal of Metals, vol. 3, pp. 761–764; September, 1951.

27. *M. E. Fine*, "Vibralloy—A new Ferromagnetic Alloy," Bell Lab. Record, vol. 30, pp. 345–348; September, 1952.

28. *F. E. Terman*, "Radio Engineers' Handbook," McGraw-Hill Publishing Company, Ltd., London; 1950. *Textbook.*

29. *A. A. Andronow and C. E. Chaikin*, "Theory of Oscillations," Princeton University Press, Princeton, N. J.; 1949. *Textbook.*

30. *M. E. Van Valkenburg*, "Modern Network Synthesis," John Wiley and Sons, Inc., New York and London; 1960. *Textbook.*

Leer - Vide - Empty

ZUSAMMENFASSUNG

In der vorliegenden Arbeit wird die Übertragung von amplitudenmodulierten Signalen mit unterdrücktem Träger behandelt. Dieses Verfahren unterscheidet sich von den Systemen mit reduziertem Träger dadurch, dass der Träger vom Empfänger erzeugt wird und seine Frequenz und Phase nur aus der Information, die in den Seitenbändern enthalten ist, gesteuert wird. Der Sender gibt dabei seine gesamte Leistung ausschliesslich in den Seitenbändern ab und ist in seinem Aufbau extrem einfach, was durch einen Gegentakt- oder Brückenmodulator erreicht werden kann.

Das Verfahren weist gleichzeitig eine Fading-Verminderung auf und arbeitet mit einem Homodyndetector. Dies ist von Vorteil bei frequenzabhängigem Fading und frequenzabhängigem Übertragungsweg. Ein gewisser Grad von Störungsunterdrückung ist möglich. Daneben sind Verstärkung und Selektivität gegenüber benachbarten Kanälen durch den Niederfrequenzteil der Anordnung gewährleistet. Da das Prinzip des Überlagerungsempfängers nicht verwendet wird, fallen eine Anzahl Störungsursachen weg.

Der Empfänger wird im Rahmen der Arbeit hinsichtlich seines Fang- und Haltebereichs und auf seine Eignung bei frequenzabhängigem Fading untersucht. Auch die Möglichkeit der Störungsunterdrückung wird diskutiert. Ein Verfahren der automatischen Frequenzsteuerung wird angegeben, das zusätzlich zu der bekannten, mittels Phasenkontrolle arbeitenden Frequenzregelung wirkt. Zur Überprüfung dieser Tatsachen wurden ein Versuchsempfänger und ein Sender gebaut, dessen beide Seitenbänder unabhängig voneinander moduliert werden konnten. Der hiezu erforderliche Breitband-Phasenschieber wurde neu entwickelt. Dabei benötigt man Filter mit steilen Flanken, deren Entwicklung als mechanische Filter ebenfalls beschrieben wird. Dieser Phasenschieber kann selbstverständlich auch anderweitig Verwendung finden.

Leer - Vide - Empty

CURRICULUM VITAE

I was born on the 25th September 1932 in Ein Shams, nr. Cairo. In 1939 I became a pupil of the English School, Heliopolis, nr. Cairo and obtained the London University Matriculation in 1948. After further preparation, I passed the Qualifying Examination for the Mechanical Sciences Tripos in 1950 and was accepted in that year as an engineering undergraduate at Jesus College, Cambridge University. On passing the Mechanical Sciences Tripos in 1953 I obtained the degree of B.A. (Hons.). Following this I attended a post-graduate course in Electrical Engineering for one academic year. In February 1955 I received the Certificate of Proficiency in Radio Engineering from Marconi College in Chelmsford, England, on completing a five-month course.

During the following six months, I worked on the development of low-noise input circuits for radio equipment in the Design Department of Murphy Radio, Ltd., Welwyn Garden City, England. Upon my return to Egypt, I was appointed to the post of Electronic Superintendent of the Scientific Instruments and Standards Centre at the National Council for Scientific Research, Dokki, Cairo. My work there included the design and maintainance of electronic equipment for use in other branches of science, particularly automatic spectrophotometry. I was also responsible for carrying out measurement and calibration work in the Standards Centre. For this period, I was in addition associated with the Meeco Electrical Engineering Co., Cairo as Engineering Consultant on development and production problems. In February 1957 I came to Switzerland and spent eight months in the research laboratories of Brown, Boveri & Co., Baden. I was first engaged on the development of steep cut-off electrical filters and then on the development of UHF circuits, both being for mobile communications sets working at 460 Mc/s.

Since January 1958 I have been persuing further studies at the Swiss Federal Institute of Technology, Zurich under the supervision of Prof. Dr. F. Tank. In the course of these studies I spent nearly a year working in the field of microwaves and in that period also prepared for the Examination for Admission to Doctoral Studies. I then began the work which forms the subject of this thesis.